

2001

Impact of Thymectomy on the Peripheral T Cell Pool in the Context of SIV Infection

Sarah Tuttleton Arron

Follow this and additional works at: http://digitalcommons.rockefeller.edu/student_theses_and_dissertations



Part of the [Life Sciences Commons](#)

Recommended Citation

Arron, Sarah Tuttleton, "Impact of Thymectomy on the Peripheral T Cell Pool in the Context of SIV Infection" (2001). *Student Theses and Dissertations*. 331.
http://digitalcommons.rockefeller.edu/student_theses_and_dissertations/331

This Thesis is brought to you for free and open access by Digital Commons @ RU. It has been accepted for inclusion in Student Theses and Dissertations by an authorized administrator of Digital Commons @ RU. For more information, please contact mcsweej@mail.rockefeller.edu.



THE LIBRARY

Rockefeller University Library
1230 York Avenue
New York, NY 10021-6399



Impact of Thymectomy on the Peripheral T Cell Pool in the Context of SIV Infection

A thesis presented to the faculty of
The Rockefeller University
in partial fulfillment of the requirements for
the degree of Doctor of Philosophy

by

Sarah Tuttleton Arron

For Joe,
My favorite collaborator.

“I spent four years prostrate to the higher mind,
got my paper, and I was free.”

-Emily Saliers, *Closer to Fine*

There are so many people I want to thank for their guidance and support over the past six years. First and foremost, my mother, who persuaded me to apply to the M.D./Ph.D. program and then tried to convince me that it was my idea. Mom is my role model, cheerleader, and my strongest ally. Thanks for all the late-night long-distance moral support.

Allen Clarkson, for giving me my start washing glassware and feeding the mice. He eventually let me graduate to 'real' science, and kept me around throughout high school and college. Georgios Pollakis, for teaching me that science is just another kind of arts and crafts. Joel Oppenheim, for suggesting I do the NYU summer recruitment program and getting me thinking about a joint degree.

My undergraduate advisors at Harvard: Fuzz Crompton, in whose lab I spent many nights grinding bone slides and patiently peering into the microscope, waiting for data to appear; and the late Richard Taylor, who agreed that it was much more important to spend the summer in Italy than in the lab.

Of course, everyone at ADARC who have participated in this undertaking, far too many to mention by name. All of our collaborators at the Tulane Regional Primate Research Center, where we keep our monkeys, especially Agegnehu Gettie (who likes to remind me that he's ADARC, not Tulane). Alan Perelson and Ruy Ribeiro out at Los Alamos, who continue to make sense out of my jumble of numbers. I especially want to thank my lab buddies (past and present) Jeremy Segal, Dan Bauer, Megan Sheehy, Michael Louie, Alex Kim, Susan Malenbaum, and Leslie Rowe. You kept me sane.

Xia Jin, for training me to be a cellular immunologist in a lab of virologists, for rigorous scientific discussions, for spirited political debate, for keeping up with American 'telly', and for sharing my love of single-malt whiskey.

Linqi Zhang has been my mentor for the last six years, and it is to him that I owe the majority of my training. He took me on as an undergraduate summer student, and patiently taught me as I cloned in circles and ran sequencing gels upside down. Although I did rotations in other labs, and worked on other projects in our lab, the road always leads back to Linqi's office. Linqi's cheerful spirit and keen insight have helped me through the highs and lows of this project, and I have consistently drawn from his expertise in molecular biology and in life. His projects are consistently the most exciting, the most cutting-edge, and the most successful, and I have learned as much from his example as from his direct lessons. Graduate school is sink or swim, Linqi has been my life preserver.

Finally, I want to express infinite gratitude to my mentor and advisor, David Ho. David entrusted me with a plum project and gave me the resources and support to see it through as well as the freedom to learn from my own experience. He taught me to be conservative in my interpretations of the data, but once certain, to stand behind my conclusions. I am also indebted to David for ongoing career advice (on a new career option each week), discussions of the stock market, intriguing tales about various biotech and drug companies, and, in exchange for a bit of lab gossip, the occasional ride home.

Table of Contents

1. Abstract	1
2. Introduction	
2.1. Thymic Function	2
2.1.1. Thymic Output in the Mouse	2
2.1.2. Thymic Output in the Sheep	2
2.1.3. Age-Related Changes in Thymic Mass	3
2.1.4. Age-Related Changes in Thymic Output	3
2.1.5. Age-Related Changes in the Peripheral T Cell Pool	4
2.1.6. RTE in Peripheral T Cell Homeostasis	4
2.2. Thymectomy and Thymic Deficiency	5
2.2.1. Adult Thymectomy	5
2.2.2. Neonatal Thymectomy	6
2.2.3. Congenital Thymic Deficiency	6
2.2.4. Children with HIV-1 Infection	6
2.2.5. Adults with HIV-1 Infection	7
2.3. Fetal Development of T Cells	7
2.4. Extrathymic Sources for T Cell Production	8
2.4.1. Intestinal Intraepithelial Lymphocytes	8
2.4.2. Liver	9
2.4.3. Bone Marrow	9
2.5. The Thymus and T Cell Dynamics in HIV-1 and SIV Infection	10
2.5.1. T Cell Dynamics in HIV-1 Infection	10
2.5.2. T Cell Dynamics in SIV Infection	11
2.5.3. HIV-1 Infection of the Thymus	11
2.5.4. SIV Infection of the Thymus	12
2.6. Role of the Thymus in Immune Reconstitution	12
2.6.1. Bone Marrow Transplant	13
2.6.2. Treatment of HIV-1 Infection with Antiretroviral Therapy	13
3. Methods for The Study of Thymic Function	
3.1. Morphology and Imaging Studies	16
3.2. CD45RA	16
3.3. Cht1	17
3.4. Fluorescence Labeling	17
3.5. T Cell Receptor Excisional Circles	18
4. Materials and Methods	
4.1. Rhesus Macaques (<i>Macaca mulatta</i>)	19
4.2. Surgical Thymectomy	19
4.3. Sample Collection	20
4.4. Flow Cytometry	20
4.5. Magnetic Cell Sorting	21
4.6. Quantifying Plasma SIV Viral Load by Real-Time PCR	21
4.6.1. Generation of RNA Standards for Real-Time PCR of RNA Species	22
4.7. Isolation of Intestinal Epithelial and Lamina Propria Lymphocytes	23
4.7.1. Intraepithelial Lymphocyte (IEL) Isolation	23

4.7.2.	Lamina Propria Lymphocyte (LPL) Isolation	24
4.7.3.	Lymphocyte Enrichment	24
4.8.	Real-Time PCR Detection of $\alpha 1$ TREC	25
4.8.1.	Generation of M13 Bacteriophage Standards for Real-Time PCR of DNA Species	26
4.9.	TCR β CDR3 Profile Analysis	27
4.10.	Statistical Analysis	28
5.	Results	
5.1.	Development of a Real-Time PCR/Molecular Beacon Assay to Quantify TREC as a Measure of Recent Thymic Emigrants in the Peripheral Blood	29
5.1.1.	TREC as a Marker for Recent Thymic Emigrants	29
5.1.2.	Development of a Real-Time PCR/Molecular Beacon Assay to Quantify $\alpha 1$ TREC in Humans	31
5.1.3.	Development of a Real-Time PCR/Molecular Beacon Assay to Quantify $\alpha 1$ TREC in Rhesus Macaques	32
5.1.4.	Generation of DNA Standards for Real-Time PCR Assays	36
5.1.5.	Age Distribution of $\alpha 1$ TREC in Normal Macaques	37
5.1.6.	$\alpha 1$ TREC in the Thymus of Juvenile and Neonatal Macaques	39
5.1.7.	Distribution of $\alpha 1$ TREC in Lymphoid Tissues of Two Normal Juvenile Macaques	41
5.2.	Thymectomy	42
5.2.1.	Surgical Removal of the Thymus	42
5.2.2.	Effect of Thymectomy on CD3, CD4, and CD8 T Cell Counts	42
5.2.3.	Effect of Thymectomy on Naïve T Cells	43
5.2.4.	T Cell Proliferation Post Surgery	54
5.2.5.	Thymectomy Results in a Decline in $\alpha 1$ TREC Bearing T cells	54
5.2.6.	Calculation of Thymic Export Rates in the Juvenile Rhesus Macaque	59
5.3.	Infection	61
5.3.1.	Viral Loads and Disease Progression	61
5.3.2.	Effect of Infection on CD4 ⁺ T Cell Counts	65
5.3.3.	Effect of Infection on CD8 ⁺ T Cell Counts	65
5.3.4.	CD4:CD8 Ratios After Infection	66
5.3.5.	Effect of Infection on Naïve T Cells	75
5.3.6.	Effect of Infection on T Cell Proliferation	82
5.3.7.	$\alpha 1$ TREC Decay Following Infection	84
5.4.	Tissues	90
5.4.1.	Distribution of $\alpha 1$ TREC in Lymphoid Tissues Post Thymectomy	90
5.4.2.	Impact of SIV Infection on $\alpha 1$ TREC in the Lymph Nodes	90
5.4.3.	Tissue Distribution of $\alpha 1$ TREC at Necropsy	92
5.4.4.	$\alpha 1$ TREC in the Tissues: Summary	94
5.5.	TCR β CDR3 Profile	97
5.5.1.	Thymectomy Results in Restriction of the TCR Repertoire	100
5.5.2.	Infection Results in Dramatic Restriction of the TCR Repertoire	100
6.	Discussion	

6.1. Development of an Assay to Detect $\alpha 1$ T Cell Receptor Excisional Circles in the Rhesus Macaque	101
6.2. $\alpha 1$ TREC in the Normal Macaque	103
6.3. Impact of Thymectomy on the Peripheral T Cell Pool	105
6.4. Impact of Thymectomy on $\alpha 1$ TREC Bearing Cells	107
6.5. $\alpha 1$ TREC in the Lymphoid Tissues After Thymectomy	109
6.6. TCR Repertoire Restriction After Thymectomy	110
6.7. Thymectomy in the Context of SIV Infection	111
6.8. $\alpha 1$ TREC in the Context of SIV Infection	114
6.9. $\alpha 1$ TREC in the Lymphoid Tissues After Infection	117
6.10. TCR Repertoire Restriction After Infection	119
7. Conclusion	121
8. Bibliography	122
Appendix 1. $\alpha 1$ TREC in PBMC, CD4, and CD8 post thymectomy	138
Appendix 2. $\alpha 1$ TREC in PBMC, CD4, and CD8 post infection	143

List of Figures

1. Recombination at the TCR α locus to delete the TCR δ locus
2. Threshold cycle is inversely proportional to the log of the input copy number
3. Comparison of $\alpha 1$ TREC sequences from human and rhesus macaque
4. $\alpha 1$ TREC beacon binding specificity
5. M13 phage external standard curves for real-time PCR of $\alpha 1$ TREC and CCR5
6. Age distribution of $\alpha 1$ TREC in normal rhesus macaques
7. $\alpha 1$ TREC concentrations in the thymus
- 7b. % of $\alpha 1$ TREC bearing cells among thymocyte subsets
8. Tissue distribution of $\alpha 1$ TREC in two normal juvenile rhesus macaques
9. Absolute CD3 $^{+}$, CD4 $^{+}$, and CD8 $^{+}$ counts post thymectomy
10. % of CD3 $^{+}$, CD4 $^{+}$, and CD8 $^{+}$ cells post thymectomy
11. % of CD45RA $^{+}$ cells among CD3 $^{+}$, CD3 $^{+}$ CD4 $^{+}$, and CD3 $^{+}$ CD8 $^{+}$ T cells post thymectomy
12. Absolute naïve CD3 $^{+}$, CD4 $^{+}$, and CD8 $^{+}$ counts post thymectomy
13. %Ki67 $^{+}$ CD3 $^{+}$ CD4 $^{+}$, and CD3 $^{+}$ CD8 $^{+}$ T cells post thymectomy
14. $\alpha 1$ TREC/ 10^6 PBMC at baseline and 10 months post surgery
15. $\alpha 1$ TREC/ 10^6 PBMC, CD4, and CD8 post surgery
16. Calculation of an absolute thymic export rate
17. SIV viral loads
18. Boxplots of peak viral load and viral setpoint
19. Absolute CD3 $^{+}$, CD4 $^{+}$, and CD8 $^{+}$ counts post infection
20. % of CD3 $^{+}$, CD4 $^{+}$, and CD8 $^{+}$ cells post infection
21. CD4:CD8 ratios post infection
22. % of CD45RA $^{+}$ cells among CD3 $^{+}$, CD3 $^{+}$ CD4 $^{+}$, and CD3 $^{+}$ CD8 $^{+}$ T cells post infection
23. Absolute naïve CD3 $^{+}$, CD4 $^{+}$, and CD8 $^{+}$ counts post infection
24. Ki67 $^{+}$ CD3 $^{+}$ CD4 $^{+}$ and CD3 $^{+}$ CD8 $^{+}$ T cells post infection
25. $\alpha 1$ TREC decay in PBMC following thymectomy and infection
26. $\alpha 1$ TREC decay in CD4 following thymectomy and infection
27. $\alpha 1$ TREC decay in CD8 following thymectomy and infection
28. Tissue distribution of $\alpha 1$ TREC eight months post thymectomy
29. $\alpha 1$ TREC in lymph nodes pre and post infection
30. Tissue distribution of $\alpha 1$ TREC at necropsy
31. Thymic histopathology of SIV, hematoxylin and eosin stain
32. TCR V β length polymorphism profiles
33. Model of peripheral T cell homeostasis
34. Model of $\alpha 1$ TREC homeostasis

List of Tables

1. TCR V β PCR primers
2. Absolute T cell decay slopes post thymectomy
3. Absolute naïve T cell decay slopes post thymectomy
4. α 1 TREC decay slopes post thymectomy
5. α 1 TREC decay post thymectomy
6. Necropsy findings
7. Absolute T cell decay slopes pre vs. post infection
8. Absolute T cell decay slopes post infection, thymectomy vs. sham
9. Absolute naïve T cell decay slopes, pre vs. post infection
10. Absolute naïve T cell decay slopes, thymectomy vs. sham
11. α 1 TREC decay slopes, pre vs. post infection
12. Adjusted α 1 TREC decay slopes, post infection
13. Percentage of α 1 TREC bearing cells in lymphoid tissues
14. Number of species in each V β family

Abbreviations Used in this Paper

APC	Allophycocyanin
AID ₅₀	Animal infectious dose (50 th percentile)
BMT	Bone marrow transplant
BrdU	Bromodeoxyuridine
CDR	Complementarity determining region
CFDA/CFSE	5-(and 6-)carboxyfluorescein diacetate, succinimidyl ester
CT	Computed tomography
DABCYL	Dimethylaminophenylazo benzoic acid
DMSO	Dimethylsulfoxide
DN	Double negative
DP	Double positive
EDTA	Ethylenediamine tetraacetic acid
FAM	6-carboxyfluorescein
FCS	Fetal calf serum
FITC	Fluorescein isothiocyanate
HAART	Highly active antiretroviral therapy
HBSS	Hanks' balanced salt solution
HIV	Human immunodeficiency virus
IEL	Intraepithelial lymphocytes
IM	Intramuscular
LPL	Lamina propria lymphocytes
MHC	Major histocompatibility complex
MRI	Magnetic resonance imaging
NK	Natural killer
PBMC	Peripheral blood mononuclear cells
PCR	Polymerase chain reaction
PE	Phycoerythrin
PerCP	Peridinin chlorophyll protein
QC-PCR	Quantitative competitive polymerase chain reaction
RAG	Recombinase activating gene
RSS	Recombination signal sequence
RTE	Recent thymic emigrants
SAIDS	Simian acquired immunodeficiency virus syndrome
SCID	Severe combined immunodeficiency
SHIV	Simian/human immunodeficiency virus
SIV	Simian immunodeficiency virus
SRV	Simian retrovirus
TCR	T cell receptor
TET	Tetramethylrhodamine
TREC	T cell receptor excisional circle
TUNEL	TdT-mediated dUTP nick-end labeling

ABSTRACT

The thymus is the primary lymphoid organ responsible for T cell production. It is of particular interest in the context of human immunodeficiency virus (HIV)-1 infection, in which the progressive loss of CD4⁺ T cells leads to immunodeficiency and opportunistic infection. CD4⁺ T cell loss is thought to result from direct and indirect killing of CD4 cells in the periphery as well as from pathogenic effects of the virus on the thymus. However, it is not fully understood which is the greater factor in viral-induced CD4⁺ T cell decay.

The development of an assay to detect T cell receptor excisional circles (TREC) as a marker for recent T cell receptor (TCR) recombination in the thymus has proved to be an invaluable tool for the study of recent thymic emigrants. Here we describe the development of this technique in the rhesus macaque model and use this method in combination with other techniques to study the role of the thymus in maintenance of the peripheral T cell pool.

This study has two major goals: to define the role of the thymus in peripheral T cell homeostasis in the juvenile rhesus macaque (*Macaca mulatta*) and to assess the significance of thymic output in the context of simian immunodeficiency virus (SIV) infection. To this end, we have studied the impact of surgical thymectomy on the peripheral T cell pool in a cohort of macaques. We present evidence that thymic output in the juvenile macaque is measurable but quantitatively insignificant in the context of the total T cell pool. While SIV infection does have pathogenic effects on the thymus, these effects play a minimal role in the overall destruction of the peripheral T cell pool.

2. Introduction

2.1 Thymic Function

2.1.1 Thymic Output in the Mouse In order to understand the capacity of the thymus to reconstitute the T cell pool after injury, it is crucial to determine normal thymic export rates. Data from a number of thymocyte labeling experiments using fluorescein isothiocyanate (FITC) and 5-(and 6-)-carboxyfluorescein diacetate, succinimidyl ester (CFDA, CFSE) to track recent thymic emigrants (RTE) in the periphery agree that only a small population of thymocytes leave the thymus each day, the remainder presumably dying by apoptosis during selection. Among the first such labeling studies using FITC to label thymocytes in mice demonstrated that 1% of thymocytes are exported each day, approximately 2×10^6 cells per day(1). 1% of thymocytes exported per day has been observed using FITC labeling in pigs as well(2).

Comparisons of bromodeoxyuridine (BrdU) uptake in dividing cells of thymectomized and euthymic mice reveal that BrdU labeling is of lower intensity in the thymus than in the spleen and lymph nodes. Thymectomized mice lacked the BrdU^{lo} subset seen in sham thymectomized mice, while both groups had the BrdU^{hi} subset(3). These BrdU^{lo} cells were found to accumulate in the spleen and lymph nodes of sham thymectomized mice at a rate of approximately 0.9×10^6 cells per day, similar to the results observed using FITC labeling.

2.1.2 Thymic Output in the Sheep CFSE has the advantage of remaining stable in cells for up to two months, allowing longer studies of RTE. Intrathymic injection of CFSE in 2 week old lambs confirmed an export rate of 1% of thymocytes per day. It was also observed that 74% of the CFSE-labeled RTE localized to the spleen within the first 24 hours, with equal proportions of the remainder in the blood and lymph nodes. After 15 days, 51% of RTE were found in the lymph node. The percentage of RTE in the blood was fairly constant during this period(4). Similar export rates and distribution of RTE were found using FITC injection in fetal sheep(5). In this experiment, it was observed that nearly 60% of CD8⁺ RTE localized to the spleen in the first 24 hours

postlabeling, while 60% of CD4⁺ RTE localized to the lymph nodes. Approximately 30% of CD4⁺ and CD8⁺ RTE were found in the blood. These studies make no mention of the absolute number of thymic emigrants in the periphery, although it is expected that this number must be quite small.

Intrathymic FITC injection in fetal sheep and 3 month old lambs demonstrated 0.34% and 0.36% of thymocytes exported daily, respectively. This constant export rate translated to a total number of thymic emigrants per day increasing from 8.5×10^7 in the 120 day fetus to 4×10^8 in the 3 month lamb. Interestingly, the smaller number of emigrants in the fetal sheep represented a higher concentration of cells, presumably as the thymus was seeding the peripheral pool(6).

2.1.3 Age-Related Changes in Thymic Mass The progressive involution and atrophy of the thymus that occur with age were first documented by Galen. In the 1920s this phenomenon was studied by Hammar and others using data from autopsy (reviewed in(7)). At that time it was believed that the thymus grows until puberty before beginning this progressive involution. In the 1980s, Steinmann reviewed the data collected for earlier papers as well as a large number of healthy thymuses and concluded that in fact the thymus shows no evidence of growth beyond the first year of life, and maintains a constant size and weight(7). Thymic mass remains fairly constant due to the fact that as the thymus atrophies, lymphoid tissue is replaced by fat, a change evident both on autopsy as well as in computed tomography (CT) scans(7-10).

2.1.4 Age-Related Changes in Thymic Output A corresponding age-related reduction in thymic function is currently under debate. Multiple lines of evidence indicate that thymic function persists with age, although the degree of output is uncertain. Thymopoiesis, as measured by the production of lymphocytes bearing the naïve phenotype (CD45RA⁺CD62L⁺) is most active during childhood and declines in the later years of life(11, 12). However, small numbers of immature T cell precursors and mature thymocytes are found in the thymic tissue of normal individuals over the age of 60, and the distribution of thymocyte subsets is similar to that in childhood(7, 11, 13). The same distribution of thymic subsets is also observed in neonatal and aged sheep(14). Thymic

diversity, as measured by TCR V β family usage, does not differ significantly between fetal and adult thymuses(15). TREC have been measured in the peripheral blood of normal individuals up to the age of 95, and there is an age-related decrease in TREC concentrations. Despite this decrease, significant TREC numbers are detected in individuals over the age of 70(16-18).

A more comprehensive study of age-related thymic export rates was done in sheep using FITC and CFSE injection. The total number of RTE recovered from the blood, spleen, and pooled lymph nodes 24 hours after labeling increased from 2.4×10^8 in the fetal sheep to 15.3×10^8 in the 2 week old lamb. This number decreased to 9.8×10^8 in the 3-4 year old sheep. These numbers represented roughly 1% of thymocytes exported daily at all ages, indicating that the age-related changes in thymic output are determined by the relative size of the thymus rather than export rates. The relative contributions of RTE to the peripheral T cell pool fell dramatically with age, resulting from the decreased size of the thymus and increased size of the peripheral T cell pool, rather than any reduction in thymic export rates(14).

2.1.5 Age-Related Changes in the Peripheral T Cell Pool Along with age-related changes in thymic output, there are alterations in the composition of the peripheral T cell pool. The elderly have decreased naïve T cells (both CD45RA⁺ and CD62L⁺) and increased memory (CD45RO⁺) and activated (HLA-DR⁺) T cells compared to younger people. The elderly also have higher numbers of CD16⁺ natural killer (NK) cells, as well as CD3⁺CD56⁺ NK cells and CD3⁺CD56⁺ T cells(19-21).

The intensity expression of various T cell markers is also altered with age. CD3 antigen expression is downregulated on total T lymphocytes as well as on memory T cells, but is upregulated on CD56⁺ T cells. Despite the greater numbers of activated T cells, the intensity of HLA-DR on those cells is decreased. Likewise, the expression of CD62L is increased although the numbers of those cells are decreased(19, 20).

2.1.6 RTE in Peripheral T Cell Homeostasis A steady-state T cell pool requires balancing rates of input and loss. Naïve and memory T cell subpopulations are believed to occupy separate niches, with long-lived naïve cells dividing slowly and antigen-driven

memory cells turning over at a higher rate(3, 22). Thymic output functions to maintain diversity within the naïve population, which would be lost if the pool was maintained by peripheral expansion only(23).

Despite this, there appears to be no homeostatic mechanism regulating thymic export. When additional thymic lobes were grafted into athymic and euthymic mice, 0.7% of thymocytes, approximately 10^6 cells, were exported daily from both the natural and engrafted thymuses, regardless of the presence or absence of the other. This indicates that the thymic export rate is determined by the amount of thymic tissue present, and not the size of the peripheral pool(24). Although initial studies conflicted, it now appears that thymus grafting increases the T cell pool size in proportion to the number of grafted lobes(25). Thymic export also seems to be unaffected by peripheral T cell depletion induced by anti-CD4 or anti-Thy-1 antibodies(26).

The fate of RTE within the naïve T cell pool is debated. There is some evidence that RTE are transiently favored for survival over existing naïve T cells(24, 25), while other studies demonstrate random deletion of RTE and other naïve cells(27).

The diversity created by thymic production of new T cells is particularly crucial following lymphocyte depletion. Although peripheral expansion also aids in the replenishment of the T cell pool, it cannot regenerate the quality of T cells produced by the thymus. T cells generated via peripheral expansion have the CD45RO⁺ phenotype and tend to display an oligoclonal TCR repertoire, while T cells produced in the thymus have the naïve CD45RA⁺CD62L⁺ phenotype and a polyclonal TCR repertoire(23, 28, 29).

2.2 Thymectomy and Thymic Deficiency

2.2.1 Adult Thymectomy The frequency of thymoma in patients with myasthenia gravis led to the observation that thymectomy in that context is associated with an increase in muscle strength. Patients thymectomized for myasthenia gravis do not appear to have any decrease in peripheral T cell populations or humoral and cellular immune responses(30-32), and the mechanism for thymectomy's palliative effect remains unknown.

2.2.2. Neonatal Thymectomy Neonatal thymectomy, in contrast, results in significant depletion of T cells in the periphery. Neonatal mice, when thymectomized, fail to mount an immune response to skin grafts(33, 34). Fetal sheep thymectomized in utero have at term only 10-20% of the recirculating pool of euthymic newborns, and lymphopenia in blood, spleen, and lymph nodes, as well as decreased cellular immunity (35, 36). Human neonates thymectomized during surgical repair of congenital heart defects had a decrease in T cell levels, but showed no evidence of immune compromise within the first year(37). However, human infants thymectomized before three months had evidence of impaired immunity in later childhood (38).

2.2.3 Congenital Thymic Deficiency In congenital thymic deficiency such as complete DiGeorge syndrome in humans and the *nude* mutation in mice, the thymus fails to form and few T cells are generated(39-47). DiGeorge syndrome results from the maldevelopment of anatomic structures derived from the third and fourth pharyngeal pouches. The syndrome includes congenital heart defects, hypocalcemic tetany resulting from failed parathyroid development, multiple facial abnormalities, and maldevelopment of the thymic epithelium. Though patients with DiGeorge display a spectrum of thymic deficiency from mild to complete T cell deficiency, B cell levels are typically normal(48).

2.2.4 Children with HIV-1 Infection Thymic function is thought to be a critical determinant of disease progression in HIV-1 infected children. HIV-1 infected children display two distinct modes of disease progression: exceedingly fast, with death occurring within two to three years of infection, and relatively slow with a pattern of progression similar to that found in adults, with death occurring five to ten years after infection(49-52). In infants, rapid disease progression has been associated with low levels of CD4⁺ and CD8⁺ T lymphocytes, as opposed to low levels of CD4⁺ T lymphocytes and high levels of CD8⁺ T lymphocytes, and is thought to be related to thymic insufficiency resulting from infection early in life(52).

2.2.5 Adults with HIV-1 Infection CT scans detect abundant thymic tissue in approximately 50% of HIV-1-infected individuals with ages ranging from 20 to 59(13). The presence of thymic tissue was significantly associated with both a higher CD4⁺ T cell count and a higher percentage and absolute number of circulating naïve (CD45RA⁺CD62L⁺) CD4⁺ T cells(13). Autopsy samples from individuals who died of complications of HIV-1 reveal that most patients do not have detectable thymic tissue, and when present, the thymus does not prevent prolonged lymphopenia(11, 53). Limited case reports of HIV-1 infection in athymic adults suggest that disease progression is not altered by the absence of thymic tissue, and that thymectomy before HIV-1 infection did not prevent a clinical response to treatment or the regeneration of the peripheral T cell pool(53).

2.3. Fetal Development of T Cells

The thymus develops from the ectoderm of the third branchial cleft and the endoderm of the third pharyngeal pouch. Studies in embryonic mice suggest that the ectodermal layers give rise to the epithelium of the cortex, while the epithelium of the medulla arises from the endoderm(54). The rudimentary thymus, or thymic anlage, is colonized late in gestation in mice, but in humans the thymus is colonized in the first trimester, between weeks 7 and 9 of gestation in humans. CD7⁺ T cell precursors are present in the thorax, neck, yolk sac, and fetal liver before week 7, and by week 9.5 of gestation have colonized the thymus and are scattered throughout the fetal liver(55).

The human fetal gut develops during week 4 of gestation. It is divided into the foregut, midgut, and hindgut by the arterial blood supply: the celiac, superior mesenteric, and inferior mesenteric arteries. Early on in week 4, branches of the celiac artery vascularize the liver, which is an outgrowth of the foregut. This provides a common blood supply and link between the developing gut and liver(56).

$\gamma\delta$ T cell receptors generated during human fetal development have been identified in the fetal liver during weeks 6-8 of gestation, before colonization of the

thymus. These cells are biased towards V γ 9/V δ 2 use and are of limited diversity(57). Rearranged TCR δ genes are also expressed in the developing gut between 6 and 9 weeks of gestation, and have a repertoire distinguishable from that observed in the liver and thymus(58).

2.4. Extrathymic Sources for T Cell Production

Extrathymic T cell development in the fetus and the presence of T cells in athymic mice and mice with genetic defects preventing T cell development via the thymic pathway have led to an examination of extrathymic sites of T cell differentiation(59-63). However, T cells originating outside of the thymus are different from thymic-derived T cells in phenotype and functional behavior. These cells are rarely found in peripheral lymphoid organs but are abundant in the gut epithelium, and may play a role in local immune response (reviewed in (64, 65)).

The majority of extrathymic T cells appear to be NK1.1⁺ T cells. TCR diversity appears to be skewed in these cells(66-68), and there is evidence that dominant recombination between V α 14-J α 281 marks extrathymic selection of the TCR repertoire, and TREC generated from this recombination event are detected in intestinal intraepithelial lymphocytes (IEL), bone marrow, liver, spleen, and Peyer's patches.(66). This skewed repertoire is positively selected by the MHC class I-like CD1d molecule, in association with β_2 -microglobulin (β_2m)(69).

Overall, the picture of extrathymic T cell production is both localized and limited, and it is doubtful if it would be able to restore complete T cell function following depletion, in the absence of the thymic function.

2.4.1 Intestinal Intraepithelial Lymphocytes The most abundant T cell population outside of the thymus is located in the intestinal mucosa. All gut intraepithelial lymphocytes (IEL) bear the $\alpha E\beta 7$ integrin (CD103), which binds the gut epithelial E-cadherin(70). IEL are comprised of cells with heterogeneous phenotypes,

and this heterogeneity provided the first clues that T cells can differentiate outside of the thymus.

In the normal mouse, a major subset of IEL are phenotypically identical to thymus-derived peripheral blood T cells and display TCR $\alpha\beta$ and CD8 $\alpha\beta$ or CD4, and are Thy1⁺, CD5⁺, CD28⁺, and CD69⁺. These cells are also depleted of potentially autoreactive V β subgroups, evidence of repertoire selection in the thymus.

A second subset of IEL is characterized by TCR $\alpha\beta$ or TCR $\gamma\delta$, CD8 $\alpha\alpha$ homodimers, and are Thy1⁺, CD5⁻, and CD28⁻. These cells are not deleted of potentially autoreactive V β subgroups, indicating that they do not undergo thymic selection(71).

A third and minor subset of IEL are CD3⁻ cells, which express recombinase activating gene (RAG)-1 mRNA and are thought to be progenitors of thymus-independent IEL(72, 73). These cells are increased in *nude* mice and are the only IEL population observed in *scid* and RAG^{-/-} mice(65).

2.4.2 Liver There is also evidence in mice for the liver as a site of extrathymic T cell production. The liver contains double negative (DN) CD4⁻CD8⁻ T cells that are TCR $\alpha\beta$ ^{int}, NK1.1⁺, and IL-2R β ⁺ (reviewed in(74)). c-kit⁺ stem cells in the liver have the potential to differentiate into lymphoid cells as well as granulocytes and erythrocytes(75-77).

Evidence that liver TCR^{int} cells are of extrathymic origin comes from athymic *nude* mice, whose T cells are entirely TCR^{int}(78, 79). These cells have skewed V β subgroup use and have not undergone negative selection(68, 80, 81).

2.4.3 Bone Marrow A third reported source for extrathymic T cells is the bone marrow. While the classical pathway for T cell development requires the migration of T cell precursors from the bone marrow to the thymus for maturation, there has been evidence that the bone marrow can also support the differentiation of these precursors into T cells(82). Like the extrathymic T cells reported in the liver, extrathymic T cells in the bone marrow are NK1.1⁺, and can be double negative as well as single positive(83).

2.5. The Thymus and T Cell Dynamics in HIV-1 and SIV Infection

2.5.1 T Cell Dynamics in HIV-1 Infection The central hallmark of HIV-1 and SIV infection is the progressive loss of CD4⁺ T cells. The mechanism for this remains unclear, but is likely to involve a combination of accelerated destruction and impaired regeneration. Highly active antiretroviral therapy (HAART) leads to a rapid decline in plasma viremia and concurrent rise in CD4⁺ T cells(84, 85). This led to the hypothesis that high levels of viral induced T cell destruction and demand on CD4⁺ T cell proliferation resulted in immune collapse(84-88). An alternate view suggests that the rise in CD4⁺ T cells after HAART reflects a redistribution of T cells trapped in peripheral sites by antigen, cytokine, or chemokine signals(89).

Different methods to quantify T cell turnover in HIV-1 infected patients have reached conflicting conclusions. One approach, using telomere shortening as an indicator of replicative history, failed to detect telomere shortening in CD4⁺ T cells of HIV-1 infected patients, suggesting normal or reduced CD4⁺ T cell turnover(90, 91). However, this method does not account for cells that have been destroyed and is biased towards non-dividing cells. Another approach is the measurement of nuclear antigen Ki67, specific for cell proliferation. Increased turnover of CD4⁺ and CD8⁺ T cells in HIV-1 infected patients was demonstrated with this technique, in both the periphery and germinal centers of lymph nodes(92, 93). Thirdly, using the stable isotope-labeled metabolite ²H-glucose to measure T cell kinetics *in vivo*, it was demonstrated that the half-lives of both CD4⁺ and CD8⁺ T cells is decreased in late-stage HIV-1 disease(94).

An initial study using deuterium-labeled glucose (D-glucose) as an *in vivo* label demonstrated higher levels of CD4⁺ and CD8⁺ T cell turnover in infection. However, these rates were even higher in patients treated with HAART, which led to the interpretation that a block in production is the basis for peripheral CD4 decline(94). A more recent study using D-glucose labeling also demonstrated increased levels of CD4⁺ and CD8⁺ T cell turnover in infection. However, in this study both proliferation and death decreased following HAART, contradicting the concept of a lymphocyte

regenerative defect (95). These observations were supported by Ki67 as well as TdT-mediated dUTP nick-end labeling (TUNEL), used as an indicator of apoptosis.

2.5.2 T Cell Dynamics in SIV Infection A more direct measure of T cell proliferation *in vivo* has been obtained by studying SIV-infected rhesus macaques following the ingestion of BrdU, which is incorporated into the DNA of proliferating cells(96, 97). These studies demonstrated an increased turnover of CD4⁺ and CD8⁺ T cells as well as natural killer (NK) cells, suggesting generalized immune activation in SIV infection.

2.5.3 HIV-1 Infection of the Thymus There is evidence that HIV-1 can infect the thymus and disrupt thymopoiesis. Thymuses from HIV-1-infected individuals demonstrate a wide range of morphologic abnormalities(49, 50, 53, 98-107). This is most pronounced in fetal and neonatal subjects. The HIV-1-infected thymus displays precocious involution associated with loss of lymphoid cells and profound stromal damage(49). These abnormalities have been associated with the presence of HIV-1 antigen and HIV-1 RNA within thymocytes(108, 109). In some HIV-1-infected individuals there is enlargement of the perivascular space with CD8⁺ T cell infiltration(11, 53).

Further support comes from studies using *in vitro* thymocyte organ culture. Freshly isolated thymic tissue supports active HIV-1 replication *in vitro* and both immature and mature thymocytes are infected(101, 106, 110-113). Using thymic organ culture, it was observed that CD4⁺ T cells in the cortex are infected by HIV-1 and by day 8 postinfection there is a significant depletion in CD3⁺CD4⁺CD8⁺ and CD3⁺CD4⁺CD8⁻ subsets(49, 100, 114).

In addition, following inoculation of the SCID-hu mouse model with primary isolates of HIV-1, multiple thymocyte subsets are infected, including CD3⁺CD4⁺CD8⁻ intrathymic T-progenitor cells, CD3⁺CD4⁺CD8⁺ cortical thymocytes, and CD3⁺CD4⁺ or CD3⁺CD8⁺ medullary thymocytes(98, 102, 115-126). Thymocyte depletion proceeds with disruption and loss of the cortical architecture and inversion of the normal CD4:CD8 ratio in the medulla(106, 114, 116, 118, 121, 124, 127).

2.5.4 SIV Infection of the Thymus Studies of SIV-infected neonatal and juvenile rhesus macaques have demonstrated a variety of thymic abnormalities following primary SIV infection(51, 128-134). In pig-tailed and cynomolgus macaques, infection with a chimeric HIV-1 and SIV virus (SHIV) or SIV has resulted in a marked depletion of thymocytes and disruption of thymic architecture(131, 135). Infectious virus has also been isolated from thymic samples from infected macaques(128).

In a longitudinal study of the SIV-infected thymus, a dramatic increase in thymocyte apoptosis was observed seven to fourteen days after infection. This was followed by a depletion of thymic progenitors by day 21. By day 50, there was a rebound in thymocyte progenitors with some thickening of the thymic cortex, accompanied by increased proliferation of immature thymocytes. This increase in thymocyte progenitor activity may suggest an increased thymic output early in infection, before peripheral loss of CD4⁺ T cells is observed(129). However, it is not clear whether these observations correspond to an actual increased T cell output from the thymus. Moreover, it is not known how long the thymus can sustain this rebound.

2.6. Role of the Thymus in Immune Reconstitution

Regeneration of T cell numbers following lymphocyte depletion can occur via two mechanisms: thymopoiesis and peripheral expansion. T cells generated via thymopoiesis can be identified by the expression of CD45RA, whereas T cells generated via peripheral expansion tend to express CD45RO. In the presence of thymopoiesis, peripheral expansion is suppressed, but when thymopoietic pathways are limited, peripheral expansion is enhanced(136). While thymopoiesis engenders a diverse TCR repertoire and immune panel, the diversity of the TCR repertoire resulting from peripheral expansion is limited to the existing population and thus results in a suboptimal response to new antigens(23, 28, 29).

2.6.1 Bone Marrow Transplant In the mouse, thymic-competent hosts were able to rapidly restore normal T cell number and function after receiving lethal irradiation and subsequent bone marrow transplantation (BMT), while thymic-deficient hosts had prolonged T cell depletion(22, 136, 137). The thymus is also necessary for developing skin graft rejection and response to viral challenge following BMT(23, 138).

There is evidence for an age-related reduction in thymic regenerative capacity, impacting on the balance between thymopoiesis and peripheral expansion. T cell regeneration following bone marrow transplant in patients under the age of 15 was rapid and involved CD4⁺CD45RA⁺ T cells, whereas in patients over 18, reconstitution was slower and levels of CD4⁺CD45RA⁺ T cells were low(139). Prolonged CD4 depletion after bone marrow transplant is related to age-associated thymic impairment, even when peripheral blood progenitor cells are supplied(139-142).

Infants with severe combined immunodeficiency (SCID) have vestigial amounts of thymic tissue and low numbers of circulating T cells, mainly CD45RO⁺ maternal cells. Restoration of normal peripheral T cell number and function was observed following treatment with haplotype-identical BMT(40, 143). After BMT, thymus-derived CD45RA⁺ cells appear, as do TREC, indicating that even a small amount of thymic tissue can produce T cells(144).

While CD4⁺ cells require a functional thymus for regeneration, CD8⁺ cells seem to be under different regulatory requirements. Despite an age-associated CD4 depletion following intensive chemotherapy, CD8⁺ T cells regenerate rapidly regardless of age or thymic enlargement(29). In one case of a thymectomized patient undergoing bone marrow transplant for mediastinal sarcoma, it was determined that CD8⁺CD45RA⁺ cells were able to regenerate as effectively as in thymus-bearing patients, but that CD4⁺CD45RA⁺ cells were unable to regenerate during 24 months following BMT(145).

2.6.2 Treatment of HIV-1 Infection with Antiretroviral Therapy Treatment of HIV-1-infected individuals with HAART results in a dramatic decline in viral load and a significant increase in circulating CD4⁺ T lymphocytes(84, 85, 89, 146-149). These changes provide an opportunity to study the processes regulating T cell turnover, including the role of the thymus.

Like chemotherapy, it appears that the efficacy of HAART on CD4⁺ T cell reconstitution is age-dependent. In studies of HIV-1 infected children, there is a more significant early recovery of naïve, memory, and total CD4⁺ T lymphocytes in those below three years of age than older children(150). In addition, the recovery rate of naïve CD4⁺ T lymphocytes in patients below three years of age was 10- to 40-fold higher than previously reported in HIV-1-infected adults following HAART(150). This suggests that the contribution of the thymus to CD4⁺ T lymphocyte regeneration following HAART may be of great significance in children.

In vertically infected infants, smaller thymic volume on magnetic resonance imaging (MRI) is correlated with lower CD4⁺ and naïve CD4⁺ T cells and higher viral loads(107). With treatment, vertically infected infants had a decrease in viral load, an increase in CD4⁺ and naïve CD4⁺ T cells, and reconstitution of the TCR V β repertoire. These were all shown to correlate to thymic volume, providing evidence for thymus-mediated reconstitution of the T cell pool following HAART(151).

A different pattern of regeneration is seen in HIV-1-infected adults following HAART. The initial rise in T lymphocytes within the weeks following therapy is primarily restricted to the memory (CD45RO⁺) population, whereas an increase in naïve (CD45RA⁺CD62L⁺) T lymphocytes becomes more significant after six months of therapy(89, 146-148, 152). The mechanisms responsible for the early and late rise in T lymphocytes remain controversial. Some argue that the early increase in memory T lymphocytes is caused by T cell redistribution from lymphoid tissues to the periphery(89). Others believe that T cell proliferation in the periphery and/or increased thymic output after therapy may play the dominant role in T cell recovery(146-148, 152).

Functional recovery of the T cell compartment is not complete unless the TCR repertoire is restored. Studies of the TCR repertoire changes by studying the varying lengths of the β chain CDR3 hypervariable region before and after HAART have yielded mixed results(147, 148, 152). The T cell repertoire is markedly disrupted through HIV-1 infection and may be difficult to restore after HAART(147, 148). However, there are some reports implying that the T cell repertoire is not only restored but also can be expanded in diversity following HAART, suggesting an increase in naïve T cells via a thymus-dependent regenerative pathway(89, 146, 152). Recent studies monitoring

changes in the number of TREC after HAART support the latter notion(16). It was found that in 10 adult patients treated with HAART, there was a rapid and sustained increase in TREC in almost all cases(16). In studies involving more patients, HAART had no appreciable effect on TREC numbers in patients whose baseline levels are already within the normal range, while significant increases were seen in patients with a preexisting impairment(17). However, these TREC increases were not sufficient to account for the rise in naïve (CD45RA⁺CD62L⁺) CD4⁺ and CD8⁺ T lymphocytes. This suggests that the rise in naïve T cells following HAART may not be a direct reflection of thymic output(17). It must be remembered that TREC concentrations reflect cell proliferation and death as well as thymic output, and conclusions regarding thymic output cannot be made from these studies without the more detailed investigation of TREC dynamics discussed in this work.

3. Methods for the Study of Thymic Function

A phenotypic marker for recent thymic emigrants in humans has yet to be identified. While there are candidate markers such as the α E integrin (CD103)(153), no consensus has been reached as to their suitability. Various alternative methods for the study of thymic function have been developed, and the combination of these various approaches has yielded significant information about the role of the thymus in postnatal T cell homeostasis and regeneration following injury.

One of the goals of this study is to describe the use of the α 1 TREC, a recently developed molecular marker for RTE. We have adapted the α 1 TREC assay system to rhesus macaques in an effort to better understand the frequency and distribution of these episomes in the blood and lymphoid tissues, and to assess the role of thymic output and peripheral processes on recent thymic emigrants bearing this marker.

3.1 Morphology and Imaging Studies In the first half of the twentieth century, studies of the thymus were limited to morphology and extensive autopsy studies of thymic mass, volume, and histology. Modern imaging studies of the mediastinum, such as CT scan and MRI, provide an estimate of thymic volume, and are a noninvasive means of studying the thymus in age and response to disease(7, 10, 154). While these techniques have the advantages of being noninvasive and feasible for use in humans, critics argue that lymphoid mass provides only a rough estimate of thymic function, and that as the adult thymus involutes, infiltrating fat makes imaging of lymphoid tissue difficult.

3.2 CD45RA Differential expression of the CD45 isoforms have been used to distinguish naïve from memory CD3⁺ T cells in humans(136, 139, 155-157). Coexpression of CD62L (L-selectin) with CD45RA further increases the specificity of naïve T cell identification(158). The availability of cross-reactive antibody clones allow the identification of CD45RA⁺ naïve T cells in the rhesus macaque as well.

The dynamics of the naïve and memory T cell subpopulations complicate their use as indicators of thymic output. CD45RA⁺ naïve T cells have a long lifespan, and may persist in a resting state for years, while CD45RO⁺ memory T cells have a much shorter lifespan(159, 160). A major shortcoming of this technique is that in some cases CD45RO⁺ memory cells can revert to a CD45RA⁺ phenotype(161, 162). Therefore while RTE are expected to exist within the CD45RA⁺ T cell population, CD45RA alone does not mark recent thymic emigration.

3.3 ChT1 The avian model of thymic function is unique in that there is a phenotypic surface marker for recent thymic emigrants. This marker, chT1, is probably the best existing marker for recent thymic emigrants. The percentage of cells bearing chT1 declines rapidly following thymectomy in the chicken. In partial thymectomy, the percentage of chT1 cells is directly proportional to the number of thymic lobes remaining(163). Unfortunately, this marker is only useful in the chicken model, as the human homologue of chT1 is not a marker for recent thymic emigrants. A similar phenotypic marker for RTE in humans has not yet been described.

3.4 Fluorescence Labeling Other studies of thymic function have relied on indirect methods for the detection of recent thymic emigrants in the periphery. *In vivo* thymic injection of fluorescent dyes such as FITC and CFDA have enabled researchers to track the movement of labeled thymocytes into the blood and peripheral lymphoid organs(4-6, 14, 164). The advantage of *in vivo* injection of fluorescent dyes is that it provides a means of readily identifying RTE by flow cytometry; however, injection is a technically difficult surgical procedure, and recovery of fluorescent RTE often necessitates sacrificing the animal. Obviously, this technique is not appropriate for humans.

Uptake of BrdU, a DNA precursor, enables the identification of dividing cells. In mice, cells of thymic origin have a lower intensity of BrdU labeling than cells in the spleen and lymph node, allowing discrimination between the two(3, 165, 166). BrdU can be given in the drinking water, and thus has the advantage of being noninvasive, but it labels all dividing cells and thus has limited utility in thymic studies apart from those described. Use in humans is limited due to potential cytotoxicity.

3.5 T Cell Receptor Excisional Circles A recent addition to these methods is the use of T cell receptor excisional circles to detect recent rearrangement of the T cell receptor in newly developed T cells. Progenitor cells in the thymus destined to become $\alpha\beta$ T cells must first delete the δ locus from the α locus on the chromosome(167, 168). One such recombination event is found to occur in 70% of human $\alpha\beta$ T cells, and produces an 89.1kb TREC ($\alpha 1$ circle)(169). Other detectable TREC result from TCR β chain rearrangement(18). TREC are stable within the cell, but are diluted by cell division and lost with cell death. TREC in the blood can serve as a marker for RTE, although 'recent' refers to the number of cell divisions since leaving the site of rearrangement rather than the time elapsed. Further support for TREC as a marker for RTE comes from the chicken model, as TREC have been shown to correlate with chT1⁺ T cells in the chicken(163, 170). TREC measurements can be performed on peripheral blood, which makes it ideal for use in humans and primates, and TREC concentrations can be followed for long periods of time, enabling longitudinal assessment of thymic output in various disease and recovery states.

4. Materials and Methods

4.1 Rhesus Macaques (*Macaca mulatta*) All rhesus macaques used in this study were of Indian origin and were housed at the Tulane Regional Primate Research Center, Covington, LA. All animals were screened for simian retrovirus (SRV) before being assigned to the study and were subsequently moved to single animal cages. All animals were maintained in accordance with NIH guidelines and approval of the Institutional Animal Care and Use Committee.

For blood draws, anesthesia was induced with ketamine hydrochloride (10mg/kg, IM) and analgesia was provided via butorphanol (0.013mg/kg, IM). The standard method of euthanasia for nonhuman primates was used, anesthesia with ketamine HCl, 10mg/kg, followed by an overdose with sodium pentobarbital. This method is consistent with the recommendation of the American Veterinary Medical Association's Panel on Euthanasia.

4.2 Surgical Thymectomy Surgery was performed by Drs. James Blanchard and Rudolph Bohm at the Tulane Regional Primate Research Center. Before surgery, each animal was pre-anesthetized with acepromazine (0.1mg/kg), buprenorphine (0.01 mg/kg), and glycopyrrolate (0.01 mg/kg) half an hour before the procedure. The animals were then anesthetized with ketamine HCl, 10mg/kg, intubated and placed on isofluorane gas, 1.5-2.5% to effect and oxygen through inhalation during surgery. Intermittent positive pressure ventilation is used to maintain respiration at a rate of 10-15 breaths per minute.

The approach was via a ventral sternotomy using an oscillating bone saw and scissors. The initial skin incision began at the level of mandibular ramus in the ventral cervical region and extended caudally, 2/3 the distance of the sternum. The sternotomy likewise extended from the manubrium 2/3 the distance of the sternum, leaving the caudal 1/3 of the sternbrae intact. The thymus was freed from the pericardium using blunt dissection. The dissection was continued cranially over the cranial thoracic vessels and into the cervical region. The limits of dissection in the ventral cervical area are: the internal jugular veins laterally, and the thyroid glands cranially. After removal of the largest part of the gland, dissection was completed by removing small remnants of fat and

thymus in piecemeal fashion. Saline was used to lavage the surgical site after dissection was completed. A thoracotomy tube was placed through the thoracic inlet period to closure. Air and fluid were aspirated as the tube was withdrawn. The rate of assisted ventilation was decreased to 6 breaths per minute at the time of closure. Closure was completed using simple interrupted 2.0 vicryl suture in the sternbrae and 3.0 vicryl in a simple continuous pattern in the musculature. Subcutaneous closure was performed using 3.0 vicryl in a simple continuous pattern and the skin was closed using 3.0 nylon in a simple interrupted pattern. Assisted ventilation was discontinued at the end of procedure. Postoperative thoracic radiography was performed to verify reduction of pneumothorax. Postsurgery, buprenorphine (0.1mg/kg) was given for three days for pain. Sham animals underwent the same surgery without removal of the thymus.

4.3 Sample Collection Blood samples were drawn into vacutainers containing EDTA as an anticoagulant and shipped overnight on ice. Upon receipt of the samples, whole blood was removed as needed for TruCount and antibody staining before centrifugation. Plasma was removed and banked at -70°C, and peripheral blood mononuclear cells (PBMC) were isolated by gradient centrifugation with Ficoll-Paque (Pharmacia, Peapack, NJ) or Cellgro Lymphocyte Separation Medium (Mediatech, Herndon, VA). PBMC were pelleted and frozen at -70°C for DNA and RNA extraction or frozen viably at 150°C in 90% fetal calf serum (FCS) with 10% dimethyl sulfoxide (DMSO).

4.4 Flow Cytometry Absolute CD4 and CD8 counts were obtained from 50µl of whole blood using TruCount tubes (BD PharMingen, San Diego, CA (BD)) and the following monoclonal antibodies: anti-CD3-PE (BD), anti-CD8-PerCP (BD), and anti-CD4-APC (Exalpa, Boston, MA).

Quantitation of CD3⁺, CD4⁺, CD8⁺, CD20⁺ and CD45RA⁺ subpopulations was done by four-color flow cytometry using the following monoclonal antibodies: anti-CD3-FITC clone FN18 (Biosource International, Camarillo, CA), anti-CD3-biotin (Biosource), streptavidin-PerCP (BD), anti-CD20-PE (BD), anti-CD8-PerCP (BD), anti-CD8-APC (BD), anti-CD4-APC (Exalpa), and anti-CD45RA-FITC (BD).

For intracellular Ki67 staining, 100µl of whole blood was incubated with anti-CD3-biotin (Biosource), anti-CD8-PerCP (BD), and anti-CD4-APC (Exalpha). After 30 minutes, erythrocytes were lysed and cells were permeabilized for 15 minutes at room temperature with FACS Lysing Solution (BD). Samples were washed three times with PBS and incubated for 30 minutes with anti-Ki67-FITC (DAKO, Carpinteria, CA) and streptavidin-PE (BD). After two more washes the samples were resuspended in 2% formaldehyde (Tousimis Research Corp., Rockville, MD) For each sample, an isotype control incubated with a mouse immunoglobulin G1 (IgG1)-FITC antibody (Caltag Laboratories, Burlingame, CA) instead of anti-Ki67-FITC was processed in parallel.

All analyses were performed with a FACScalibur flow cytometer and Cellquest software (BD).

For fluorescence activated cell sorting of double positive and single positive thymocytes, cells were stained with anti-CD3-FITC (Biosource), anti-CD4-PE (Exalpha), and anti-CD8-APC (BD). Cells were gated on CD3 and sorted into CD4⁺CD8⁺ double positive and CD4⁺ and CD8⁺ single positive cells.

4.5 Magnetic Cell Sorting CD4⁺ cells were obtained from PBMC using positive selection with anti-CD4 MACS microbeads according to the manufacturer's instructions (Miltenyi Biotec). The negative fraction was collected and used for a second round of positive selection with anti-CD8 MACS microbeads. Both CD4⁺ and CD8⁺ cells were pelleted and frozen at -70°C for DNA extraction and TREC analysis.

4.6 Quantifying Plasma SIV Viral Load by Real-Time PCR This system of quantifying plasma SIV viral load by real-time PCR with molecular beacon has been described previously (171). To measure the viral load of infected monkeys, plasma was separated from whole blood collected in EDTA-containing tubes. Plasma samples were initially spun at 5,000 rpm for 10 min to remove any cells. Viral RNA was purified from 140µl of plasma using the QIAamp viral RNA kit (Qiagen Inc., Hilden, Germany).

Reverse transcription of viral RNA was performed in 96-well plates. Each 30µl reaction contained the following: 10µl of viral RNA, 1X Taqman Buffer A (Perkin-Elmer, Boston, MA (PE)), 5 mM MgCl₂, 2.5µM random hexamers (PE), 0.5mM each of

dATP, dCTP, dGTP, and dTTP (Roche), 20 U RNAsin (Promega, Madison, WI), and 20 U Moloney murine leukemia virus reverse transcriptase (Superscript; Gibco BRL, Carlsbad, CA). One round of reverse transcription (25°C for 15 min, 42°C for 40 min, 75°C for 5 min) was performed.

To quantify the copy number of viral RNA, a molecular beacon was used in combination with real-time PCR. This method of detection using molecular beacons (172, 173) and a fluorescence detector system (174) has been described previously. Each 50µl reaction contained the entire 30µl of cDNA from the reverse transcription reaction, and the final concentration of each component was as follows: 1X Taqman buffer A, 3.5 mM MgCl₂, 0.4 pmol/µl of molecular beacon, 0.4 pmol/µl of each primer, 1.25 U of AmpliTaq Gold DNA polymerase (PE).

The primers used were SL03 (5'-AGGGAAGAAAGCAGATGAATTA-3') and SL04 (5'-GTTTCACTTTCTCTTCTGCGT-3'). The molecular beacon was designed to recognize a region within SIV gag (5'-FAM-CGCTGGAGAACAAAGAAGGATGTCACAGCG-DABCYL-3') where FAM (6-carboxyfluorescein) serves as the reporter fluorochrome and DABCYL (4' dimethylaminophenylazo benzoic acid) the quencher. One cycle of denaturation (95°C for 10 min) was performed, followed by 45 cycles of amplification (95°C for 15 s, 55°C for 30 s, 72°C for 30 s). The PCR reaction was carried out in an ABI 7700 PRISM spectrofluorometric thermal cycler (Applied Biosystems, Inc., Foster City, CA) that monitors changes in the fluorescence spectrum of each reaction tube, while simultaneously carrying out programmed temperature cycles.

Each test specimen was reverse transcribed and amplified in duplicate. A third reaction was processed and amplified without the addition of reverse transcriptase to control for potential DNA contamination. Copy numbers were calculated by interpolation of the experimentally determined threshold cycle as described previously (174). The mean of duplicate samples was reported.

4.6.1 Generation of RNA Standards for Real-Time PCR of RNA Species This method of quantifying viral load was adapted from a previous report (174) with some modifications. For each run, a standard curve was generated from duplicate samples of purified RNA transcripts ranging from 10⁶ copies to 10 copy equivalents per reaction. To

generate RNA standards, the SIV-gag amplicon was generated with a 5' T7 promoter by extension PCR using primer SL03 T7 (5' TAATAACGACTCACTATAGGGAGGAGGGAAGAAAGCAGATGAATTA-3') and SL04. RNA was generated by *in vitro* transcription using the Megascript T7 High Yield Transcription Kit (Ambion, Austin, TX) according to the manufacturer's instructions. RNA was treated twice with RNase-free DNase I (Boehringer Mannheim, Ingelheim, Germany). Copy number was determined using optical density and the molecular weight of the RNA species, and serial dilutions were made in RNase-free water. Standards were stored at a concentration of 1×10^7 copies/ μ l in single-use tubes, and serial dilutions were made from 10^6 copies to 10 copies with each run.

4.7 Isolation of Intestinal Epithelial and Lamina Propria Lymphocytes This method of isolating viable intestinal epithelial and lamina propria lymphocytes has been described previously (175, 176). Tissue was removed from the animal during surgical biopsy or within 30 minutes of euthanasia. For necropsy, 6-10 cm lengths of intestine were taken from ileum, jejunum, and colon. For biopsy, smaller sections were taken from terminal ileum and cecum. Fat, mesenteries, and visible blood vessels were carefully removed. The intestine was cut open with sharp scissors to expose mucosa, washed with PBS until all visible chyme was removed, and placed into 50ml tubes with PBS for transport to lab. Pieces remained moist throughout procedure.

4.7.1 Intraepithelial Lymphocyte (IEL) Isolation Tissue was cut into 0.5-1.0 cm square pieces with a razor blade and placed into 25cm² plastic tissue culture flasks with 25-30ml of IEL separation media consisting of Complete Hanks balanced salt solution (HBSS) containing 100 IU/ml penicillin/streptomycin, 2mM glutamine, 25mM Hepes buffer, 5% fetal calf serum (FCS), 1 mM EDTA (anhydrous, MW 280) adjusted to pH 7.2-7.4. Flasks were incubated for 30 minutes at 37°C with rapid shaking. Supernatant was collected into 50 ml tubes using a stainless steel screen cup (Sigma) which allows cell rich supernatant to pass through but blocks mucus and debris. Cells were washed and resuspended in 30ml RPMI-1640 containing 100 IU/ml penicillin/streptomycin, 2mM glutamine, and 10% FCS (R-10) after each incubation and

stored on ice during the procedure. The incubation was repeated two more times in fresh IEL separation media and pooled cells were resuspended in R-10 on ice.

4.7.2 Lamina Propria Lymphocyte (LPL) Isolation After IEL removal, remaining intestinal segments were minced with scissors into 2-3mm pieces and transferred into a clean 25cm² flask with 25-30ml of LPL separation media consisting of RPMI-1640 containing 100 IU/ml penicillin/streptomycin, 2mM glutamine, 25mM Hepes buffer, 5% FCS, and 50 U/ml collagenase type II (Sigma). Flasks were incubated for 30 minutes at 37°C with rapid shaking. Supernatant was collected into 50ml tubes using a stainless steel screen cup, and cells were washed and resuspended in 30ml (R-10) after each incubation and stored on ice during the procedure. The incubation was repeated two more times in fresh LPL separation media and pooled cells were resuspended in R-10 on ice.

4.7.3 Lymphocyte Enrichment Lymphocytes were isolated from the pooled supernatants with Percoll bilayer density gradient centrifugation. Isotonic Percoll (one part 10x PBS with 9 parts Percoll (Sigma)) to prepare 35% and 60% Percoll solutions with R-10. 2ml 60% Percoll was overlaid with 2ml 35% Percoll in 15ml polypropylene centrifuge tubes. The gradients were refrigerated for at least 1 hour before use. 2-3 gradient tubes were used for each pooled sample. 10ml of the pooled cell suspension was overlaid onto each gradient and centrifuged at 1000g for 20 minutes with no brake. Lymphocytes were removed from the 35%/60% interface and washed with R-10. Cells were counted with Trypan blue to assess viability and frozen at -150°C in 90% FCS with 10% DMSO or pelleted at -70°C for DNA extraction.

4.8 Real-Time PCR Detection of $\alpha 1$ TREC The method of detection using molecular beacons (172, 173) and a fluorescence detector system (174, 177, 178) has been described previously. Genomic DNA was extracted using the QIAmp DNA extraction kit (Qiagen) according to the manufacturer's instructions. To detect $\alpha 1$ TREC, molecular beacon was used in combination with real-time PCR.

Each 50 μ l reaction contained 5 μ l of genomic DNA, and the final concentration of each reagent was as follows: 1X Taqman buffer A (PE), 3.5 mM MgCl₂, 0.2mM each of dATP, dCTP, dATP, dTTP (Roche, Basel, Switzerland), 0.4 pmol/ μ l of molecular beacon, 0.4 pmol/ μ l of each primer, and 1.25 U of AmpliTaq Gold DNA Polymerase (PE).

The primers used were ST3 (5'-GGATGGAAAACACAGTGTGACATGG-3') and ST4 (5'-CAACCATGCTGACGCCTCTGG-3'). These primers amplified a 182-bp product. The molecular beacon, ST2, was designed to recognize a region upstream from the signal joint. (5'-FAM-CGGCGTCTGCTCTTCATTACCATTTCTCACGCCG-DABCYL-3') where FAM (6-carboxyfluorescein) serves as the reporter fluorochrome and DABCYL (4' dimethylaminophenylazo benzoic acid) the quencher. One cycle of denaturation (95°C for 10 min) was performed, followed by 45 cycles of amplification (95°C for 30 s, 60°C for 30 s, 72°C for 30 s). The PCR reaction was carried out in an ABI 7700 PRISM spectrofluorometric thermal cycler (Applied Biosystems, Inc.) that monitors changes in the fluorescence spectrum of each reaction tube, while simultaneously carrying out programmed temperature cycles.

To normalize for cell equivalents in the input DNA, we used a separate real-time PCR/molecular beacon assay to quantify the CCR5 coding sequence, as it is known that this gene is present at exactly two copies per cell, with no pseudogenes (L. Kostrikis, personal communication).

For the CCR5 assay, each 50 μ l reaction contained 5 μ l of genomic DNA, and the final concentration of each reagent was as follows: 1X Taqman buffer A (PE), 3.5 mM MgCl₂, 0.2mM each of dATP, dCTP, dATP, dTTP (Roche), 0.4 pmol/ μ l of molecular beacon, 0.4 pmol/ μ l of each primer, and 1.25 U of AmpliTaq Gold DNA Polymerase (PE).

The primers used were CCR1 (5'-GCTGTGTTTGCCTCTCTCCCAGGA-3') and LK47 (5'-CTCACAGCCCTGTGCCTCTTCTTC-3'). These primers amplified a 182-bp product. The molecular beacon was LK155, (5' TET GCGCCTATGACAAGCAGCGGCAGGAGGCGC)-DABCYL-3') where TET (tetramethylrhodamine) serves as the reporter fluorochrome and DABCYL (4' dimethylaminophenylazo benzoic acid) the quencher. One cycle of denaturation (95°C for 10 min) was performed, followed by 45 cycles of amplification (95°C for 30 s, 60°C for 30 s, 72°C for 30 s).

4.8.1 Generation of M13 Bacteriophage Standards for Real-Time PCR of DNA species M13 bacteriophage DNA standards were made as follows: The amplicon of interest was generated using the appropriate primers for the assay and a Pfu polymerase to generate a blunt ended product. The product was purified on a 1% agarose gel and ligated into M13mp 18 RF DNA (Gibco) according to manufacturer's instructions. The ligation product was used to transform DH5aF'competent cells (Gibco). Plaques generated from phage containing inserts were identified using blue/white selection for the absence of β -galactosidase activity. Positive plaques were screened by PCR using primers M13/pUC-f (5'-CCCAGTCACGACGTTGTAAAACG-3') and M13/pUC-b (5'-AGCGGATAACAATTTCACACAGG-3') in a 30 cycle PCR (95°C for 30 s, 55°C for 30 s, 72°C for 1 m). Fragments of the correct size were further screened by sequence analysis. Bacteriophage was titered and serial dilutions were made in RNase-free water. Bacteriophage was put directly into the PCR reaction, as the 10 minute 95° denaturation step was sufficient to expose the phage DNA.

An external standard curve was generated for each real-time PCR assay using a minimum of 6 replicates ranging from 2.5×10^6 to 2.5×10^1 . As the phage is single stranded, one particle corresponds to 0.5 double-stranded DNA copies in the real-time PCR assay. Each PCR plate also contained duplicate internal standards in the same range, and these were compared to the external standard curve to validate the run and check for standard degradation. Phage standards were stable at 4°C, although stocks were maintained at -20°C.

4.9 TCR β CDR3 Profile Analysis RNA was isolated from PBMC using the Qiagen RNeasy RNA Extraction Kit (Qiagen) according to the manufacturer's instructions. cDNA was generated by a reverse transcription reaction as follows: RNA was denatured at 70°C for 10 minutes, then placed on ice and combined with a mixture containing final concentrations of 1X First Strand Buffer (Gibco), 0.01M DTT (Gibco), 0.5mM each of dATP, dCTP, dGTP, and dTTP (Roche), and 5 μ M random hexamers (Perkin-Elmer). RNA was allowed to prime at 25°C for 10 minutes followed by 42°C for 2 minutes. 20 U Moloney murine leukemia virus reverse transcriptase (Superscript; Gibco) was added and reverse transcription took place at 42°C for 50 minutes followed by 70°C for 15 minutes.

cDNA was PCR amplified for 24 V β families by using individual V β -specific primers and a C β -specific primer as described previously(179) (Table 1). The entire RT reaction mixture was divided equally among 25 50 μ l first round PCR reactions containing final concentrations of 1X PCR buffer II (PE), 3.5mM MgCl₂, 0.2mM each of dATP, dCTP, dTTP, and dGTP (Roche), 0.4pmol/ μ l of primer 3CB and of the appropriate V β family primer 1-25, and 1.25 U of AmpliTaq Gold DNA Polymerase (PE). Reaction conditions were 95°C for 1 m 30 s, 35 cycles of 95°C for 30 s, 52°C for 30 s, 72°C for 30s, and a final extension of 72°C for 9 m 30 s.

5 μ l of first round PCR product was placed into a second round of heminested PCR performed with the same V β primers and an inner C β primer labeled at its 5' end with the FAM fluorophore. All other reagents and reaction conditions were the same as above. The PCR products were purified using the QIAquick PCR Purification Kit (Qiagen) and eluted into 50 μ l of RNase-free water.

CDR3 profiles were analyzed by Genescan-based spectratyping(180). 0.2 μ l of each PCR reaction was mixed with deionized formamide (Amresco, Solon, OH) and a ROX-500 size standard (Applied Biosystems, Warrington, England) and electrophoresed on a 5% acrylamide gel on an ABI 377 DNA sequencer (Applied Biosystems, Foster City, CA). Components of the gel were Long Ranger Gel Solution (BioWhittaker Molecular Applications, Rockland, MD), TBE (Promega, Madison, WI), urea (Fisher Scientific, Fair Lawn, NJ), ammonium persulfate (Promega), TEMED (Promega), and H₂O. Data were analyzed for size and fluorescence intensity with the Genescan software (Applied Biosystems).

4.10 Statistical Analysis Absolute T cell decay slopes and $\alpha 1$ TREC decay slopes were calculated based on the natural log of the number of cells. The nonparametric Mann-Whitney U test was used to compare sets of slopes. Statistical analysis was performed using StatView software. p values < 0.05 were considered statistically significant.

Table 1. TCR V β PCR primers (after ref. 179)

Primer	5'→3' Sequence	Tm
VB1	GCA CAA CAG TTC CCT GAC TTG CAC	66.28
VB2	CAT CAA CCA TCC AAA CCT GAC CT	62.77
VB3	GTC TCT AGA GAG AAG AAG GAG CGC	66.28
VB4	ACA TAT GAG AGT GGA TTT GTC ATT	57.73
VB5	TGA GCT CCT TGG AGC TGG G	64.48
VB6	AGG ACT GAG GGA TCC GTC TC	64.50
VB7	CCT GAA TGC TCC AAG AGC TCT C	64.54
VB8	ATT TAC TTT AAC AAC AAG TCT CCG	57.73
VB9	TCT CCA GAC AAA GCT CAT TT	56.30
VB10	CCC AAA ACT CAT CCT GTA CC	60.40
VB11	TCA ACA GTC TCC AGA ATA AGG A	58.95
VB12	AAA GGA GAA GTC TCA GAT	53.07
VB13.1	ACC CAG GCA TGG GGC TGA	64.46
VB13.2	ACG TGT CAC CAG ACT TGG A	60.16
VB14	GTC TCT CGA AAA GAG AAG AGG AA	60.99
VB15	GGG TAC AGT GTC TCT AGA GA	60.40
VB16	CAG GAT GAG TCC GGT ATG CC	64.50
VB17	GAT GAG TCA GGA ATG CCA AAG GAA	62.86
VB18	AGC TCT GAG GTG CCC CAG AAT CTC	67.98
VB19	CAG ATA GTA AAT GAC ATT CA	52.20
VB20	CAA TGC CCC AAG AAC CTA CC	62.45
VB21	GAG AGG CTC AAA GGA GTA	57.62
VB22	GGA AGC ATC CCT GAT CGA TT	60.40
VB23	AGT CTG AAA TAT TTG AAG ATC	52.80
VB24	AAC ACT TCT TTC TGC TTT C	53.69
3CB	GTG CTG ACC CCA CTG TGC ACC TC	69.90
3CBFAM	FAM- GGC ACA CCA GCG TGG CCT TTT GG	69.90

5. Results

5.1 Development of a Real-Time PCR/Molecular Beacon Assay to Quantify TREC as a Measure of Recent Thymic Emigrants in the Peripheral Blood.

5.1.1 TREC as a Marker for Recent Thymic Emigrants The variability among T cell receptors is generated by site-specific recombination within the chromosomal DNA. Multiple variable (V), diversity (D), and joining (J) regions are encoded within the TCR loci. These recombine at the DNA level to form the genes for the TCR α , β , γ , and δ chains.

Somatic recombination occurs at conserved recombination signal sequences (RSS) that flank the multiple V, D, and J segments. Each RSS contains a conserved heptamer and nonamer sequence, separated by a nonconserved spacer of 11/12 or 22/23 base pairs. The “12-23” rule governing recombination dictates that an RSS with a 12 nucleotide spacer combines with an RSS containing a 23 nucleotide spacer, ensuring that gene segments recombine in the functional order of V(D)J (181).

Recombination at the TCR loci mainly occurs via deletion of the DNA separating the RSSs of the V, D, or J segments. Two joints are formed by the recombination event. The “coding joint” is formed within the chromosomal DNA between the recombining elements. This joint often contains base pair insertions or deletions, increasing variability among T cell receptors. The “signal joint” is formed by the conserved joining of the two heptamer sequences of the RSSs. This joining serves to link the ends of the excised chromosomal DNA, forming an episomal byproduct of TCR rearrangement(182-184). These deletion circles are termed T-cell receptor excisional circles (TREC).

V(D)J recombination is mediated by the recombinase activating genes, RAG-1 and RAG-2. RAG-1 and RAG-2 are encoded within the same locus on chromosome 11p in humans (chromosome 2 in the mouse)(185-189). Expression of RAG-1 and RAG-2 occurs at two points in thymocyte development. The first occurrence is in the double negative (DN) stage, and corresponds to TCR β , γ , and δ mRNA expression. The second is in the double positive (DP) stage, and corresponds to TCR α mRNA expression(190).

Somatic rearrangement of the TCR loci precedes surface expression of the TCR. V(D)J recombination at the various TCR loci occurs in a sequential manner. A small percentage of T cells express a TCR $\gamma:\delta$ heterodimer, and these T cells arise from the same progenitor as $\alpha:\beta$ T cells. β , γ , and δ genes rearrange simultaneously; successful rearrangement of the γ and δ genes leads to expression of a $\gamma:\delta$ TCR. However, in some cases successful β gene rearrangement occurs first, and β chain protein expression with the invariant partner chain pre-T α blocks further γ and δ rearrangement. Expression of this pre-T receptor signals for proliferation and induces the expression of CD4 and CD8. During this proliferation phase, RAG-1 and RAG-2 are repressed, and no recombination takes place. Once many DP thymocytes expressing the same β chain are present, proliferation ceases and RAG-1 and RAG-2 are expressed and function in the recombination of the α chain gene. Thus a single β chain heterodimerizes with multiple α chains in different cells, increasing the range of antigen specificity(54).

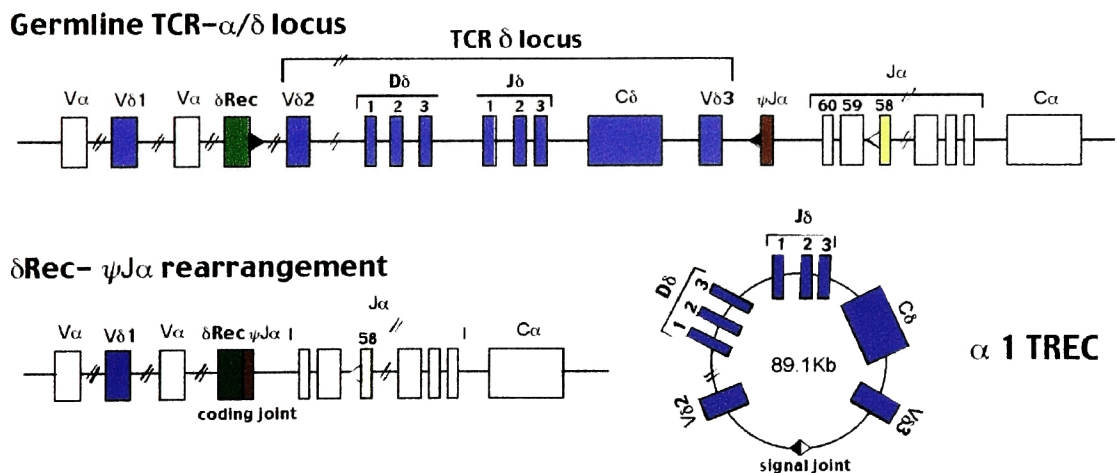


Figure 1. Recombination at the TCR α locus to delete the TCR δ locus. Recombination between δ Rec (in green) and ψ J α (in red) forms the TCR α coding joint as well the 89.1 Kb α 1 TREC containing the signal joint.

The TCR α chain locus encompasses the δ locus, and in the majority of cases, the initial recombination of the α locus occurs between two regions termed δ Rec and ψ J α in

such a way as to delete out the entire δ locus, forming an 89.1 episome termed the $\alpha 1$ TREC. (Fig. 1). Douek *et al.* used QC-PCR to quantify this particular TREC(16). In a study of 25 normal individuals, they found that the number of $\alpha 1$ TREC in the blood decreased by 1-1.5 log between birth and age 73, and that low $\alpha 1$ TREC numbers in 10 HIV-1 infected patients were increased after treatment with HAART.

5.1.2 Development of a Real-Time PCR/Molecular Beacon Assay to Quantify $\alpha 1$ TREC in Humans. We developed a real-time PCR/molecular beacon assay to quantify this $\alpha 1$ TREC as a measure of recent thymic emigrants (RTE) in peripheral blood(17). We designed an assay to amplify a 209-nucleotide fragment spanning the signal joint of the excised $\alpha 1$ TREC using PCR. A molecular beacon was included in the reaction mixture throughout PCR to serve as a real-time detector for the amplified product. The beacon is specifically designed to have a hairpin structure, with a 6-bp stem and a 26-nucleotide target recognition loop, plus a fluorophore and a quencher in close proximity at the two ends of the oligonucleotide. During the annealing phase of PCR, the molecular beacon binds to its target. This event strips open the stem, physically separating the fluorophore from the quencher and allowing fluorescence to be emitted. Fluorescence emission is detected in real time using a spectrofluorometric thermocycler. As the PCR fragment is amplified, increased fluorescence is detected. The cycle number that yields a fluorescence intensity significantly above background levels is designated as the threshold cycle (C_T). C_T is inversely proportional to the logarithmic of the copy number of the target sequence in the input DNA. (Fig. 2). To normalize for cell equivalents in the input DNA, we used a separate real-time PCR/molecular beacon assay to quantify the CCR5 coding sequence, since it is known that this gene is present at exactly two copies per cell, with no pseudogenes (L. Kostrikis, personal communication).

Human $\alpha 1$ TREC were detected in great abundance ($\sim 10^5$ copies/ 10^6 cells) in fetal thymic tissue, but were undetectable in non-lymphoid tissue or immortalized cell lines. $\alpha 1$ TREC were enriched in naïve ($CD45RA^+CD62L^+$) subpopulations of peripheral CD4 and CD8 cells compared to memory ($CD45RO^+$) subpopulations. In a study of 532 normal persons, we found that $\alpha 1$ TREC are high in the first 10-15 years of life, followed by a sharp drop between the ages of 15 and 20, and a gradual decline thereafter.

Compared with age-matched uninfected controls, most HIV-1 infected patients had normal $\alpha 1$ TREC numbers, while a subset had reduced numbers. Interestingly, after receiving HAART, patients with a pre-existing impairment in $\alpha 1$ TREC numbers exhibited a significant increase, whereas those with normal baseline $\alpha 1$ TREC showed no change with treatment(17).

5.1.3 Development of a Real-Time PCR/Molecular Beacon Assay to Quantify $\alpha 1$ TREC in Rhesus Macaques In order to use TREC as a marker for RTE in further studies, the corresponding region of the $\alpha 1$ TREC was amplified and sequenced in rhesus macaques. (Fig. 3). As the primer sequences designed to detect the $\alpha 1$ TREC in humans did not demonstrate 100% homology with those of macaques, new primers were designed to amplify a 183 base pair region. Thermal profiles of the human $\alpha 1$ TREC beacon revealed that a single base pair change in the macaque target sequence resulted in a 10% decrease in binding at the assay annealing temperature. A new beacon was designed for the macaque target sequence. (Fig. 4).

No sequence variation was observed in the beacon target site for the CCR5 gene between humans and macaques. The appropriate base pair substitutions were made in the CCR5 primer sequences to adapt the primers for macaques.

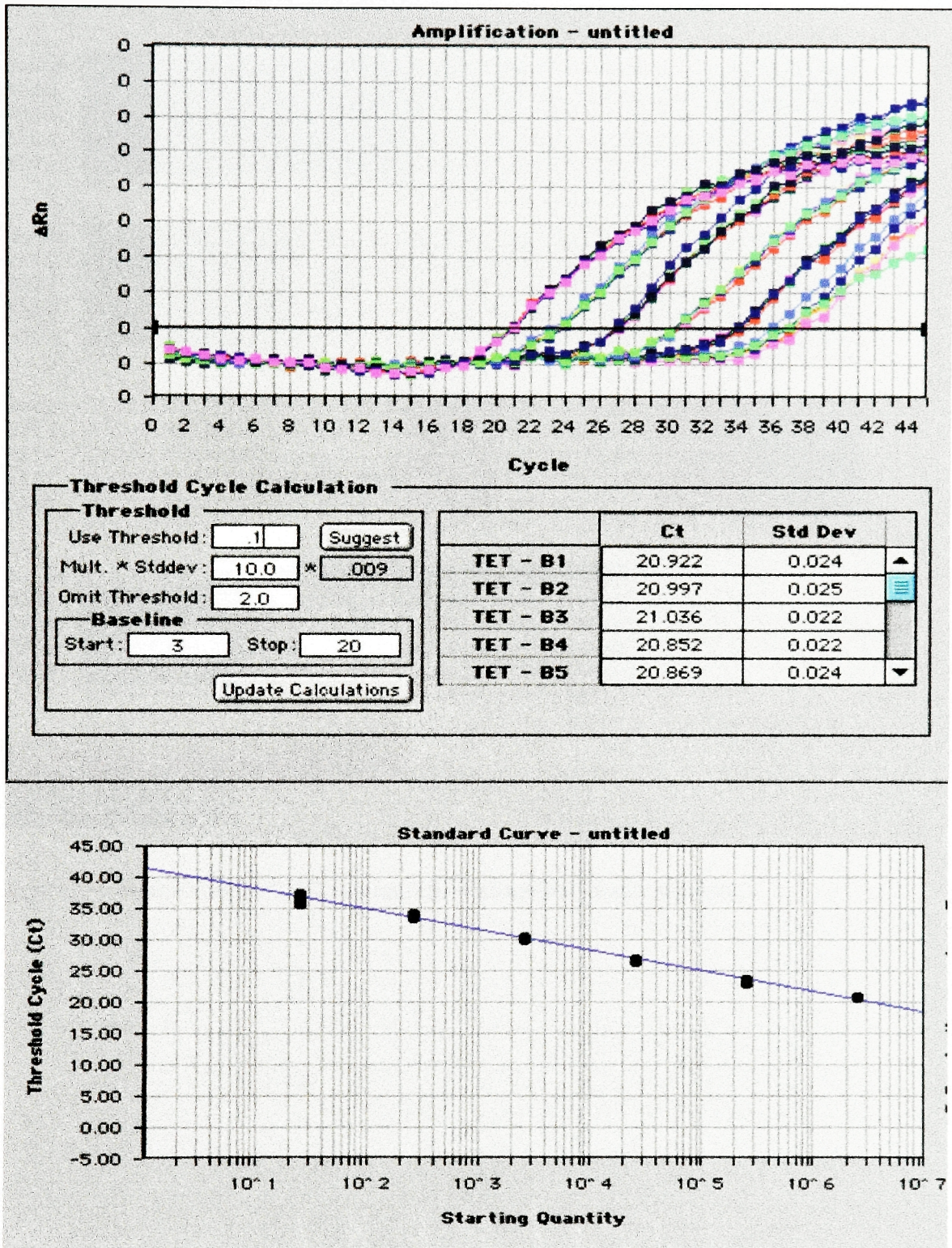


Figure 2. Threshold cycle is inversely proportional to the log of the input copy number.

Human GGATGGAAAACACAGTGTGACATGGAGGGCTGAACTT---ATTCAACTCTGAGAAACGG
R209 GGATGCAAAAACAGAGTGTGACATGGAGGGCTGAACTTTCATTCAACTCTGAGAAATGG
R258 GGATGGAAAACACAGTGTGACATGGAGGGCTGAACTTTCATTCAACTCTGAGAAATGG
R104 GGATGGAAAACACAGTGTGACATGGAGGGCTGAACTTTCATTCAACTCTGAGAAATGG
R105 GGATGGAAAACACAGTGTGACATGGAGGGCTGAACTTGTTCATTCAACTCTGAGAAATGG

Human TGAATGAAGAGCAGACAGGGCCCCGTGCCAGCTGCAGGGTTTAGGCACGGGGTGCAGGTGC
R209 TGAATGAAGAGCAGACAGGGCCCCGTGCCAGCTGCAGGGTTTAGGCACGGGGTGCAGGTGC
R258 TGAATGAAGAGCAGACAGGGCCCCGTGCCAGCTGCAGGGTTTAGGCACGGGGTGCAGGTGC
R104 TGAATGAAGAGCAGACAGGGCCCCGTGCCAGCTGCAGGGTTTAGGCACGGGGTGCAGGTGC
R105 TGAATGAAGAGCAGACAGGGCCCCGTGCCAGCTGCAGGGTTTAGGCACGGGGTGCAGGTGC

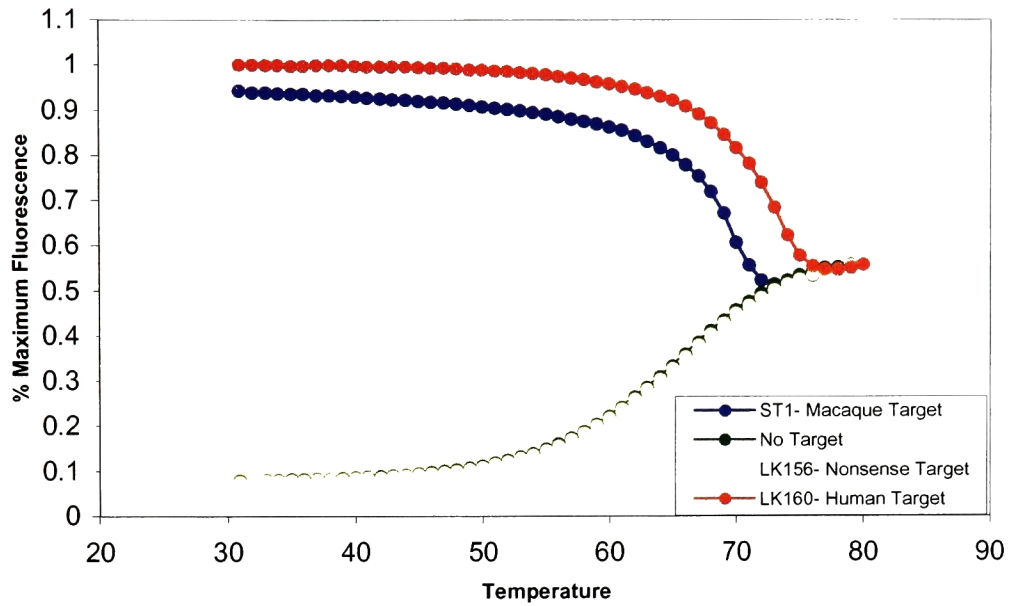
Human CTATGCATCACCGTG-----CACAGGAGTGGGCACCTTTACAAAAACAGAGGTG
R209 CTGTGCATCACCGTG-----CACAGGAGTGGGCACCTTTACAAAAACAGAGGCG
R258 CTGTGCATCACCGTG-----CACAGGAGTGGGCACCTTTACAAAAACAGAGGCG
R104 CTGTGCATCACCGTGGGG---GTC-CACAGGAGTGGGCACCTTTACAAAAACAGAGGTG
R105 CTGTGCATCACCGTG-----CACAGGAGTGGGCACCTTTACAAAAACAGAGGCG
** * *****

Human TCAGCATGGTTGAAAGCCATGTGGCATCACCTTTGTTGACAG
R209 TCAGCATGGTTGAAAGGGATGTGGCATCACCTTTGTTGACAG
R258 TCAGCATGGTTGAAAGGGATGTGGCATCACCTTTGTTGACAG
R104 TCAGCATGGTTGAAAGGGATGTGGCATCACCTTTGTTGACAG
R105 TCAGCATGGTTGAAAGGGATGTGGCATCACCTTTGTTGACAG

Recombination Signal Sequence 1
Recombination Signal Sequence 2
Recombination Target Site
Primer Target Site

Figure 3. Comparison of $\alpha 1$ TREC sequences from human and rhesus macaque

Human $\alpha 1$ TREC Beacon Thermal Profile



Macaque $\alpha 1$ TREC Beacon Thermal Profile

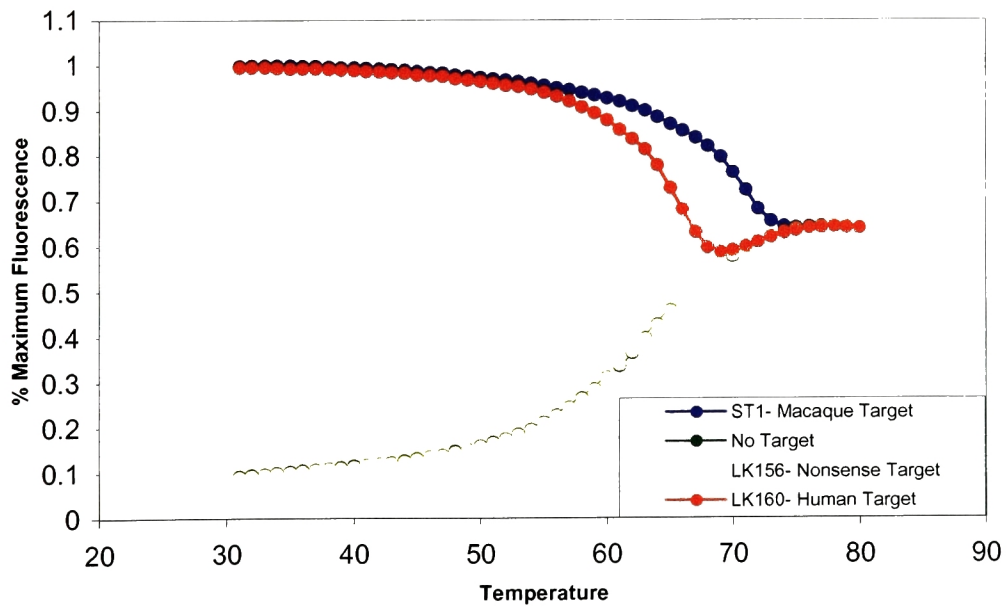


Figure 4. $\alpha 1$ TREC beacon binding specificity

5.1.4 Generation of DNA Standards for Real-Time PCR Assays An internal standard is used on all runs of real-time PCR, ranging from 1×10^7 to 10 copies. Internal standards can be compared to an external standard curve resulting from a minimum of 6 replicates to validate individual runs. Initially these assays were developed with optical-density quantified PCR product standards, however these standards demonstrated an inherent instability and were abandoned in favor of plasmid standards containing the PCR amplicon of interest cloned into a T/A cloning vector (Invitrogen, Carlsbad, CA). Competent cells (Invitrogen) were transformed with this plasmid and grown to large quantities. Plasmid was purified using the Wizard Miniprep kit (Promega) and quantified by O.D. Amplicons were confirmed by sequence analysis.

Plasmid standards were more stable than PCR product; however, the means of quantifying plasmid and calculating copy number using the molecular weight of the plasmid was not as accurate as was desirable, and the plasmid standards were found to be sensitive to multiple rounds of freeze-thaw. We turned to M13 bacteriophage as the optimal strategy for generating a stable and accurately quantified DNA standard.

The PCR product of interest was generated and cloned into M13 bacteriophage by blunt-ended ligation. Standards were confirmed by sequence analysis. Viral titers were calculated from plaque generation and copy number was calculated. Phage standards were found to be stable under a variety of conditions, and copy numbers were deemed sufficiently accurate for this assay system.

External standard curves were generated for each assay using a minimum of six replicates ranging from 2.5×10^6 to 2.5×10^1 . These curves are shown in Figure 5. As the phage is single stranded, one particle corresponds to 0.5 double-stranded DNA copies in the real-time PCR assay. Each PCR plate contained duplicate internal standards in the same range, and these were compared to the external standard curve to validate the run and check for standard degradation. Phage standards were stable at 4°C , although stocks were maintained at -20°C .

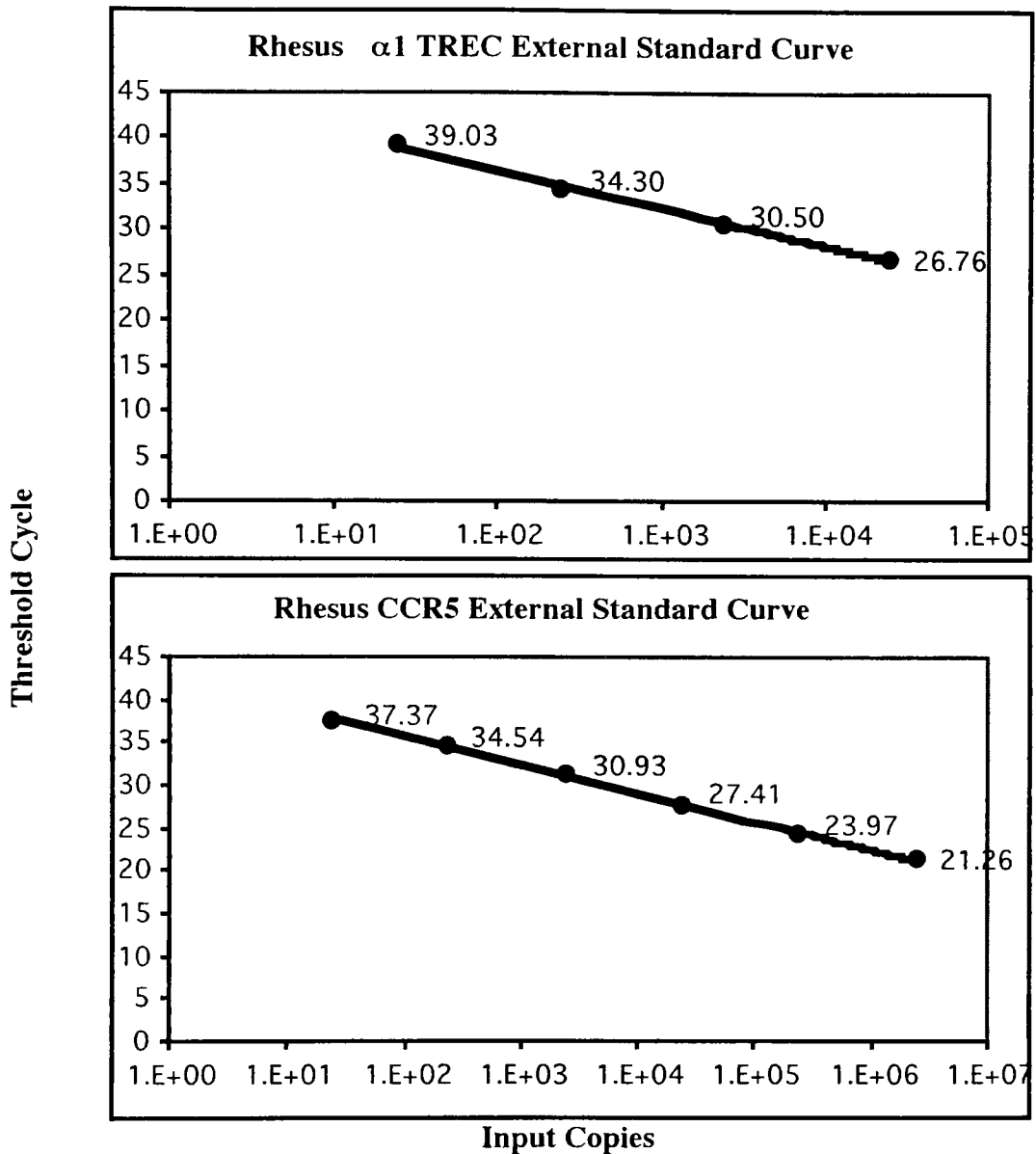


Figure 5. M13 phage external standard curves for real-time PCR of $\alpha 1$ TREC and CCR5. Standard curve equation for $\alpha 1$ TREC: $y = -1.7637\ln(x) + 44.414$, $R^2 = 0.9966$. Standard curve equation for CCR5: $y = -1.4372\ln(x) + 42.146$, $R^2 = 0.9982$.

5.1.5 Age Distribution of $\alpha 1$ TREC in Normal Macaques $\alpha 1$ TREC values were measured in PBMC of 96 normal rhesus macaques ranging in age from 1.4 to 5.6 years (Fig. 6). The average $\alpha 1$ TREC value for rhesus macaques of ages 1-4 was

$1.98 \times 10^4 / 10^6$ PBMC. The median $\alpha 1$ TREC value was $6.18 \times 10^3 / 10^6$ PBMC. There was an individual variation of up to two logs between animals within any age category.

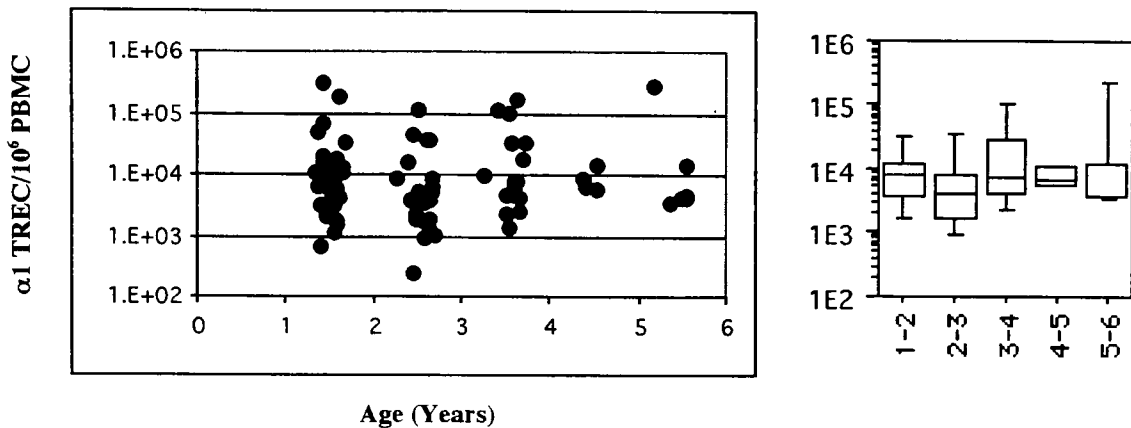


Figure 6. Age distribution of $\alpha 1$ TREC in normal rhesus macaques. (n=96)

Age 1-2 n=44, 2-3 n=25, 2-4 n=16, 4-5 n=4, 5-6 n=7. Mean of ages 1-4 = 1.98×10^4 , median of ages 1-4 = 6.18×10^3 .

A small number of animals (n=6) had concentrations of greater than 10% $\alpha 1$ TREC bearing PBMC. These values seem quite high, particularly as the average concentration of $\alpha 1$ TREC bearing cells in the thymus is slightly less than 10% (discussed below). We believe TREC concentrations in the periphery to be lower than concentrations in the thymus, however we do not have thymic tissue from these animals to compare to the PBMC. Longitudinal studies of individual animals, rather than a single 'snapshot' sample, would give more valuable information in terms of inter-animal variation.

These values may also be overestimated due to processes occurring in PBMC that alter the T cell to non-T cell ratio. These six animals may have unusually high percentages of T cells among their PBMC at this time point, creating an artificially high concentration of $\alpha 1$ TREC bearing cells. This is one of the flaws of using PBMC as a denominator of $\alpha 1$ TREC calculations; more valuable data would be obtained from studying sorted T cells. While initial studies in this area used PBMC as a readily

obtainable population to examine, future studies will need to focus on sorted T cell populations.

5.1.6 $\alpha 1$ TREC in the Thymus of Juvenile and Neonatal Macaques Figure 7 shows the concentration of $\alpha 1$ TREC in the thymocytes of ten juvenile macaques (age 2) and three neonatal macaques (ages 6-8 weeks). Tissue was obtained from two normal juvenile macaques at necropsy, the other samples were collected from surgical thymectomy at the start of this study. The mean concentration of $\alpha 1$ TREC in the thymus of juvenile macaques was $9.1 \times 10^4 / 10^6$ thymocytes, or 9.1%. Values ranged from 5.5×10^4 to $2.01 \times 10^5 / 10^6$ thymocytes. The mean concentration of $\alpha 1$ TREC in the thymus of neonatal macaques was $6.28 \times 10^4 / 10^6$ thymocytes, or 6.28%, with values ranging from 4.88×10^4 to $7.51 \times 10^4 / 10^6$ thymocytes.

To better define the concentration of $\alpha 1$ TREC bearing cells at various stages of thymocyte development, juvenile macaque thymuses were stained and sorted for $CD3^+CD4^+CD8^+$ (double positive, DP), $CD3^+CD4^+$ (single positive CD4), and $CD3^+CD8^+$ (single positive, CD8) subsets (Fig. 7b). The mean concentrations in single positive CD4 and CD8 were 11.14% and 11.12% thymocytes bearing $\alpha 1$ TREC, respectively. These values are similar to the reported concentration of 10% of $\alpha 1$ TREC bearing cells in sorted $CD45RA^+CD62L^+$ naïve cells in humans(198). These values will also be crucial to the thymic output calculations discussed below, as they will serve as a means of calculating the absolute thymic output from the measured output of $\alpha 1$ TREC bearing cells.

The percentage of $\alpha 1$ TREC bearing cells might be expected to be higher in the double positive stage of thymocyte development, where $TCR\alpha$ recombination takes place. In fact, the mean concentration in double positive thymocytes was 10.19%. This value is reasonable when one takes into account the fact that the majority of cells in the double positive stage of development have already undergone recombination followed by one or more rounds of division, and that those having divided greatly outnumber those recombining. If the $\alpha 1$ recombination event occurs in 70% of $TCR\delta$ deletion recombination events, as reported previously(169), we can estimate that 70% of actively recombining DP thymocytes contain the $\alpha 1$ TREC before division, 35% contain the $\alpha 1$

TREC after 1 round of division, 17.5% after two rounds, 8.75% after 3, and so on. Assuming cell death occurs randomly at each round of division, the weighted average of the cells in various stages of the double positive subset would yield an overall average of 18.6% with 3 rounds of replication, 11.3% with four rounds, and 6.6% with five rounds of replication. Our data would thus support an average of 4 divisions between TCR α recombination and thymic export.

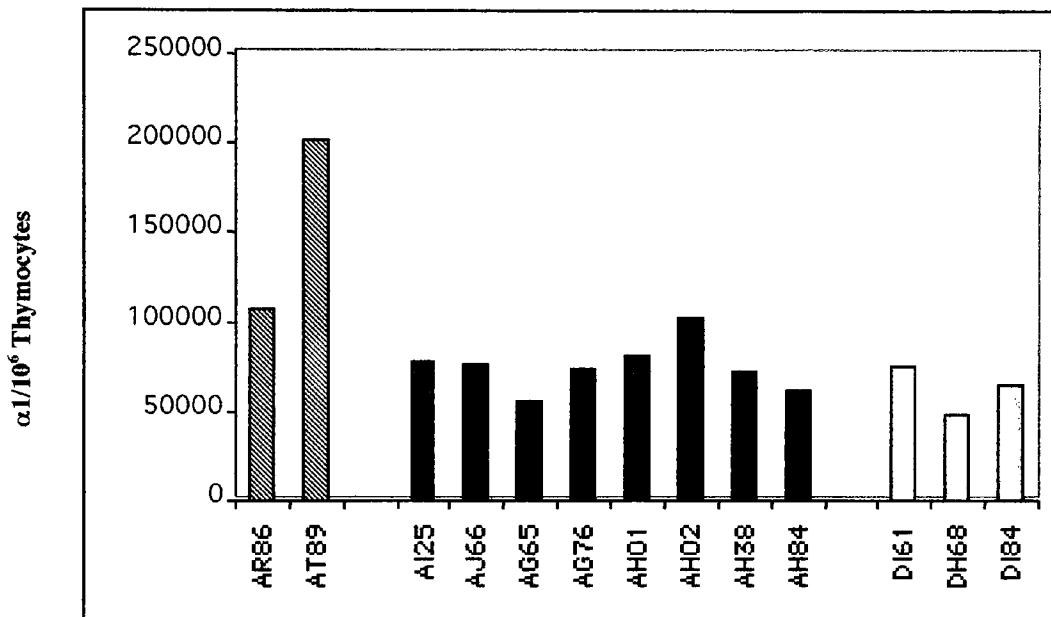


Figure 7. $\alpha 1$ TREC concentrations in the thymus. Hatched bars indicate juvenile macaques at necropsy, dark bars indicate juvenile macaques at thymectomy, and light bars indicate neonatal macaques at thymectomy. Mean for juvenile macaques: 9.1×10^4 , mean for neonatal macaques: 6.28×10^4 .

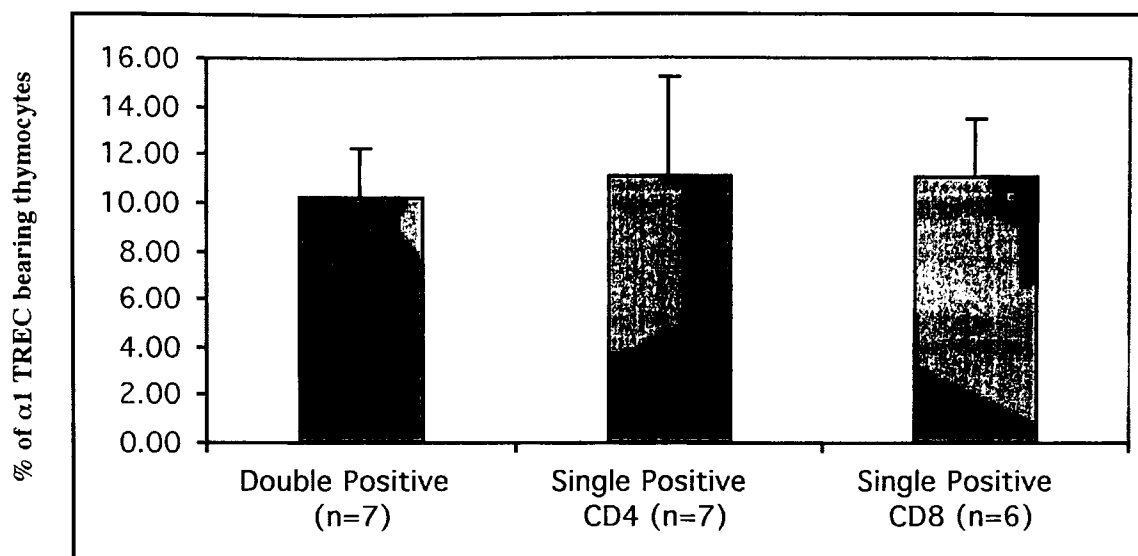


Figure 7b. % of $\alpha 1$ TREC bearing cells among thymocyte subsets. Mean for double positive: 10.93%, mean for single positive CD4: 11.14%, mean for single positive CD8: 11.12%.

5.1.7 Distribution of $\alpha 1$ TREC in Lymphoid Tissues of Two Normal Juvenile

Macaques $\alpha 1$ TREC values were measured in multiple lymphoid tissues of two juvenile macaques at necropsy (Fig. 8). $\alpha 1$ TREC were measured to be approximately $1 \times 10^4/10^6$ PBMC in these animals, well within the normal range for juveniles of the same age. The $\alpha 1$ TREC concentration was tenfold higher in the thymus of animal AR86 and twentyfold higher in the thymus of AT89, corresponding to 10 and 20% of thymocytes, respectively (also shown in Fig. 7).

$\alpha 1$ TREC concentrations in the lymph nodes ranged from values similar to those measured in PBMC up to values fourfold higher. There was a considerable variety in TREC concentrations among different lymph nodes in the same animal. Intestinal intraepithelial lymphocytes and lamina propria lymphocytes from the ileum, jejunum, and colon contained fewer than 0.5% $\alpha 1$ TREC positive cells in both animals.

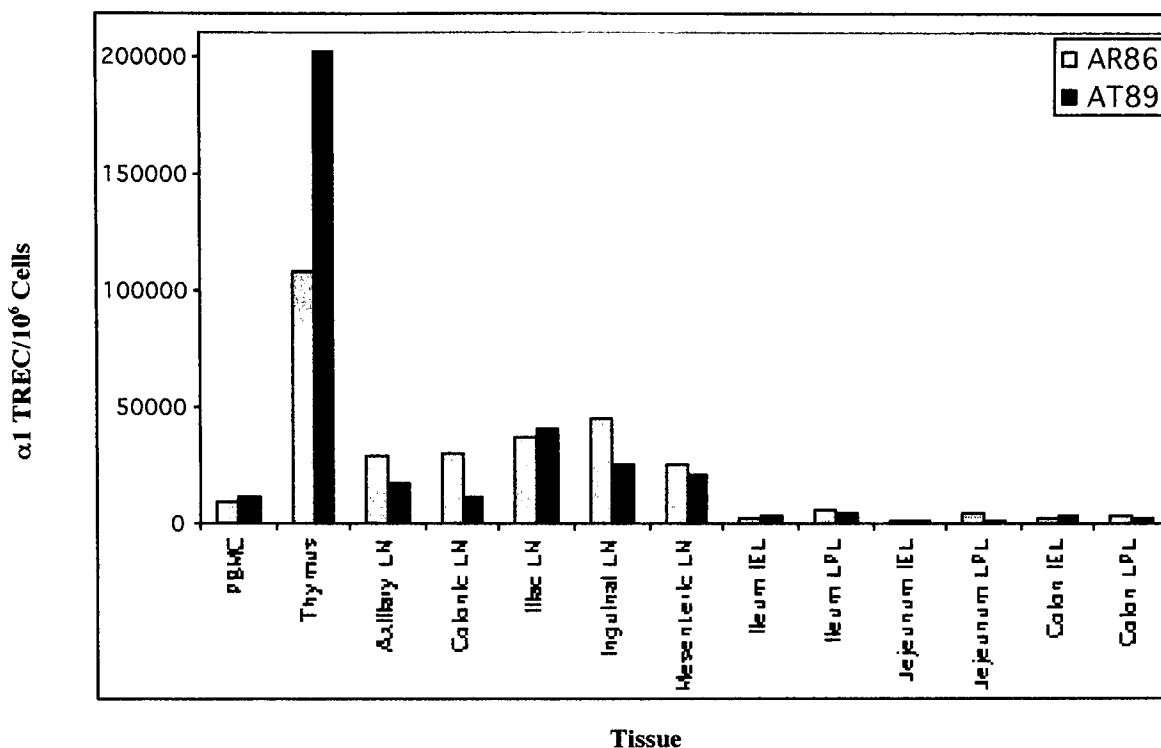


Figure 8. Tissue distribution of $\alpha 1$ TREC in two normal juvenile rhesus macaques.

5.2 Thymectomy

5.2.1 Surgical Removal of the Thymus Nine animals were selected for thymectomy and eight for sham surgery. Animals were anesthetized and surgery performed as described above. The thymus of the juvenile macaque has a thoracic portion which is easily identified, and a cervical portion which extends up into the neck. The organ is readily distinguished from surrounding fat and is encapsulated, which allows for ease of removal. Visual inspection at the time of surgery indicated that thymectomy was complete, and this was later confirmed on necropsy in the animals which were sacrificed.

5.2.2 Effect of Thymectomy on CD3, CD4, and CD8 T Cell Counts Absolute T lymphocyte counts were measured at multiple time points for three hundred days following thymectomy (Fig. 9a) and sham surgery (Fig. 9b). Thymectomy had no observable effect on absolute T cell counts, a result which is expected from analogy to clinical scenarios involving thymectomy in children. Slopes were calculated for CD3⁺,

CD4⁺, and CD8⁺ T cells in each animal and are shown in Table 2. A comparison of these slopes demonstrated no statistically significant difference in T cell decay between the two groups (p value for CD3⁺= 0.3865, CD4⁺= 0.1489, CD8⁺= >.9999, obtained by Mann-Whitney U test). Similarly, there were no observable changes in the percentages of CD3⁺, CD4⁺, or CD8⁺ lymphocytes after thymectomy, despite minor fluctuations in both groups (Fig. 10a-10b).

5.2.3 Effect of Thymectomy on Naïve T Cells There were no overall changes in the percentages of CD45RA⁺ cells within CD3⁺, CD3⁺CD4⁺, and CD3⁺CD8⁺ lymphocytes following surgery (Fig. 11a-11b), although some animals of both groups show considerable fluctuation in naïve cell percentages from month to month.

Because absolute CD45RA⁺ naïve T cell counts were obtained by multiplying the percentage of CD45RA⁺ cells within any T cell subset and the absolute count of that subset, absolute naïve T cell counts largely reflect the patterns seen in the absolute CD3⁺, CD4⁺, and CD8⁺ T cells counts. Despite any transient fluctuation in naïve cell percentages, there was no significant decline in total CD45RA⁺ naïve T cell counts (Fig. 12a-12b).

Slopes were calculated for CD3⁺CD45RA⁺, CD4⁺CD45RA⁺, and CD8⁺CD45RA⁺ and are shown in Table 3. There was no statistically significant difference in naïve T cell decay slopes between the two groups (p value for CD3⁺CD45RA⁺= 0.5006, CD4⁺CD45RA⁺= 0.5006, CD8⁺CD45RA⁺= >.9999 obtained by Mann-Whitney U test).

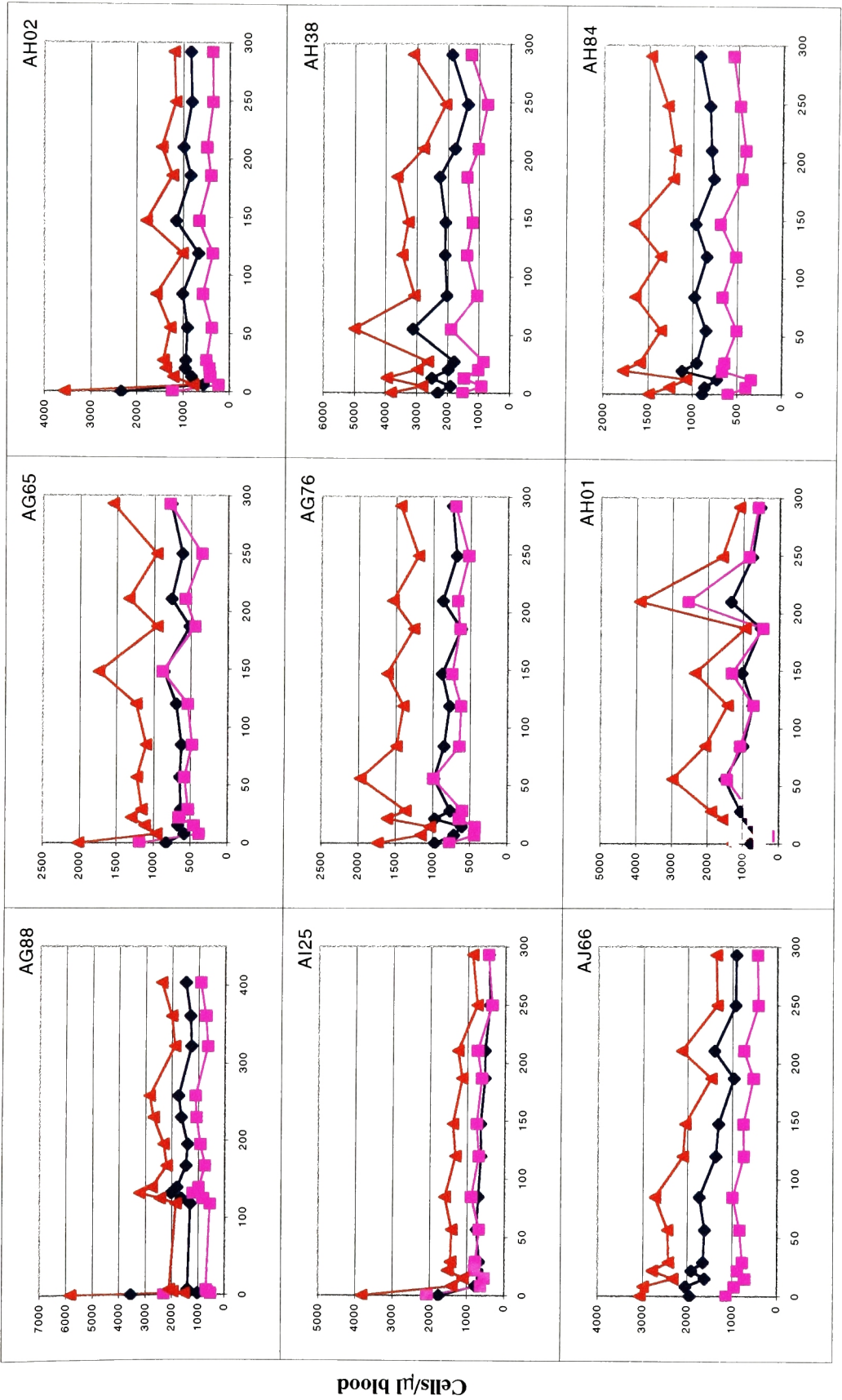


Figure 9a. Absolute CD3, CD4, and CD8 counts post thymectomy: thymectomized macaques.
Red triangles represent CD3⁺ cells, blue diamonds represent CD4⁺ cells, and purple squares represent CD8⁺ cells.

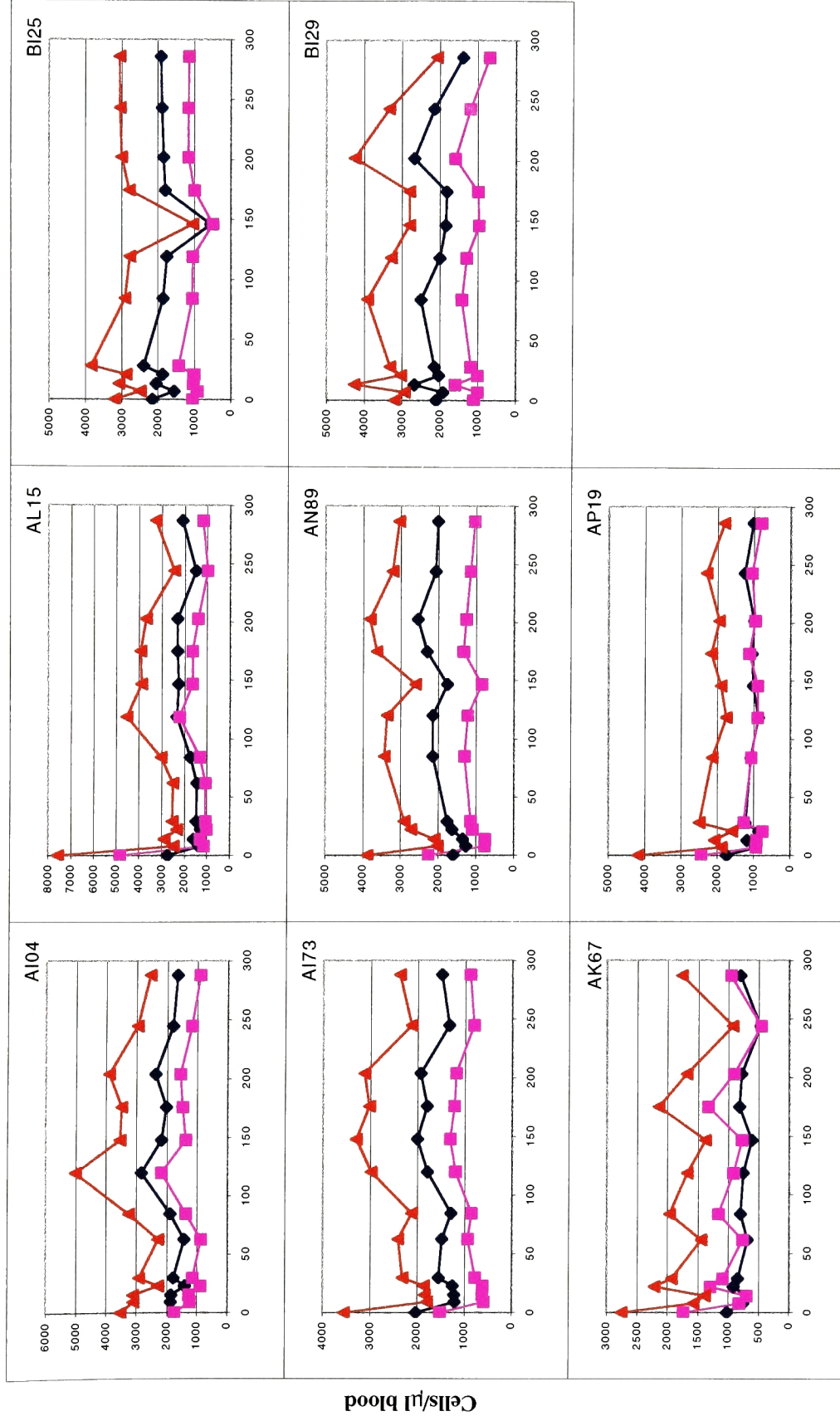


Figure 9b. Absolute CD3, CD4, and CD8 counts post thymectomy: sham macaques. Red triangles represent CD3⁺ cells, blue diamonds represent CD4⁺ cells, and purple squares represent CD8⁺ cells.

Table 2. Absolute T cell decay slopes post thymectomy

		Slope (Day ⁻¹)		
		CD3 ⁺	CD4 ⁺	CD8 ⁺
Thymectomized	AG88	-0.0003	-0.0004	-0.0001
	AI25	-0.0025	-0.0026	-0.0024
	AJ66	-0.0026	-0.0026	-0.0025
	AG76	-0.0001	-0.0004	0.0003
	AH38	-0.0008	-0.0010	-0.0005
	AH84	-0.0002	-0.0002	-0.0002
	AG65	0.0000	0.0002	-0.0003
	AH01	0.0008	-0.0002	0.0018
	AH02	-0.0006	-0.0006	-0.0007
	Average	-0.0007	-0.0009	-0.0005
Sham	AI04	0.0003	0.0005	-0.0001
	AI73	0.0007	0.0005	0.0010
	AK67	-0.0011	-0.0009	-0.0013
	AL15	0.0001	0.0009	-0.0009
	AN89	0.0009	0.0015	0.0000
	AP19	-0.0007	-0.0004	-0.0010
	BI25	-0.0004	-0.0006	0.0000
	BI29	-0.0007	-0.0007	-0.0007
	Average	-0.0001	0.0001	-0.0004
p value		0.3865	0.1489	>.9999

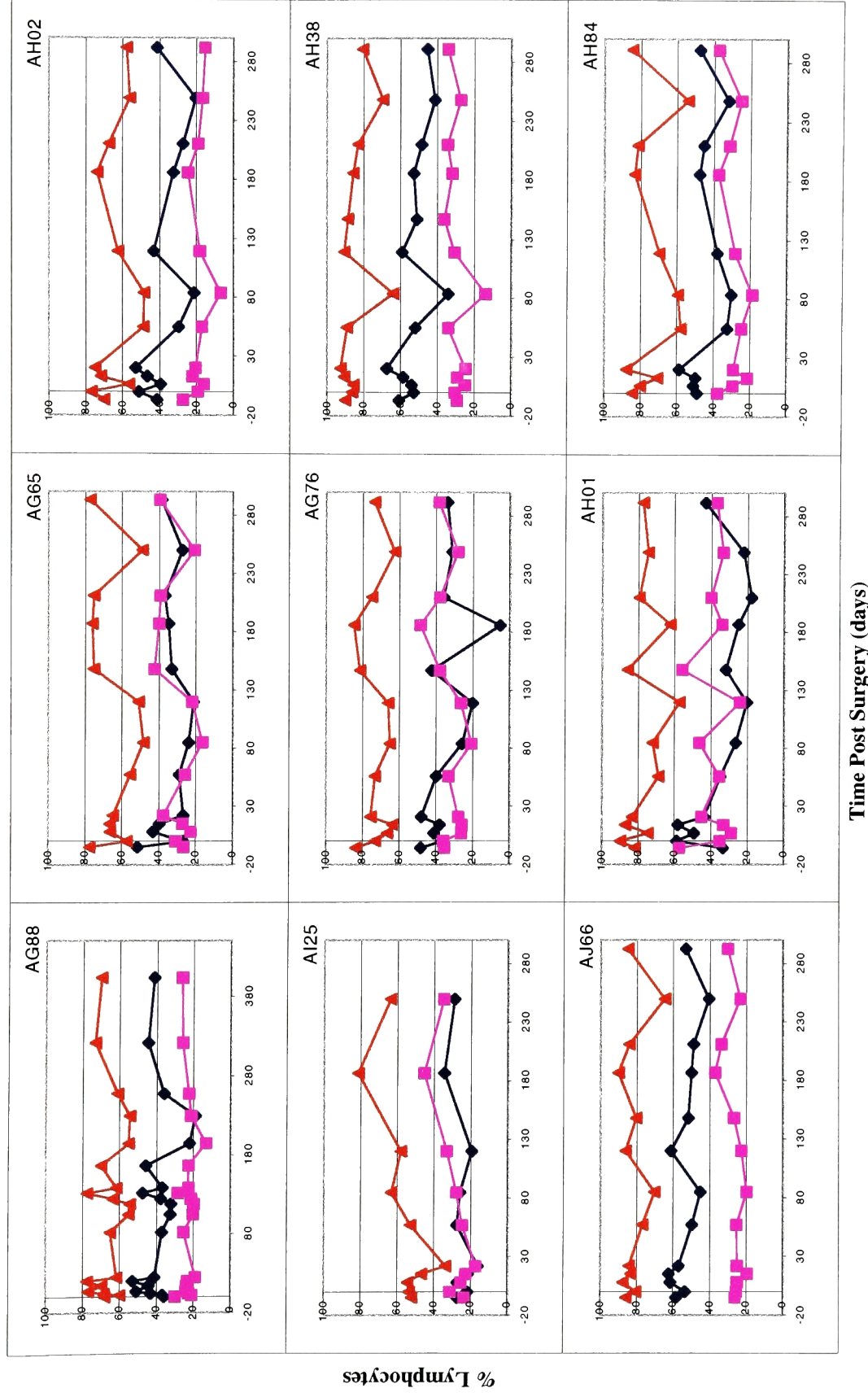


Figure 10a. % of CD3⁺, CD3⁺CD4⁺, and CD3⁺CD8⁺ T cells post thymectomy: thymectomized macaques. Red triangles represent CD3⁺ cells, blue diamonds represent CD3⁺CD4⁺ cells, and purple squares represent CD3⁺CD8⁺ cells.

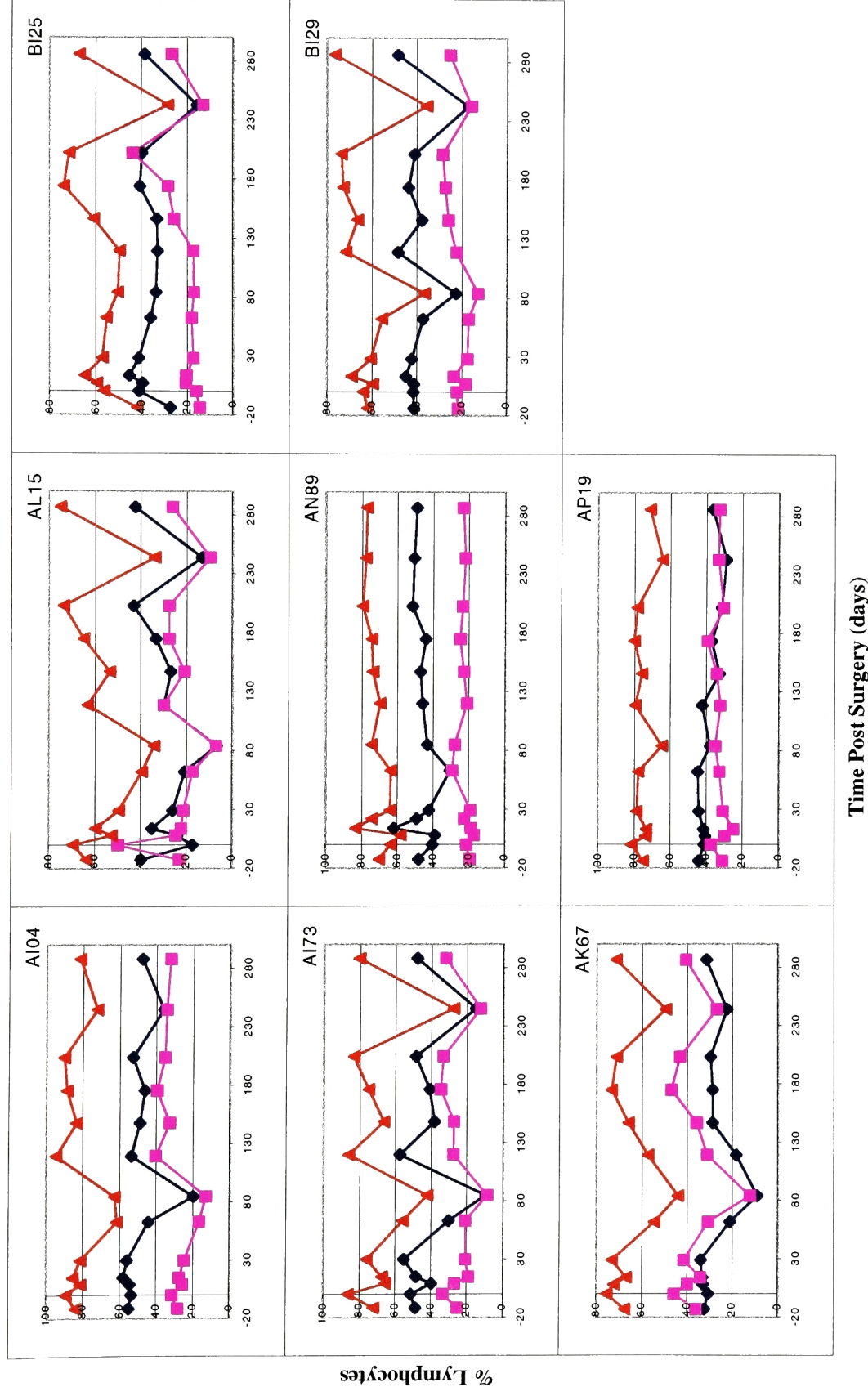


Figure 10b. % of CD3⁺, CD3⁺CD4⁺, and CD3⁺CD8⁺ T cells post thymectomy: sham macaques. Red triangles represent CD3⁺ cells, blue diamonds represent CD3⁺CD4⁺ cells, and purple squares represent CD3⁺CD8⁺ cells.

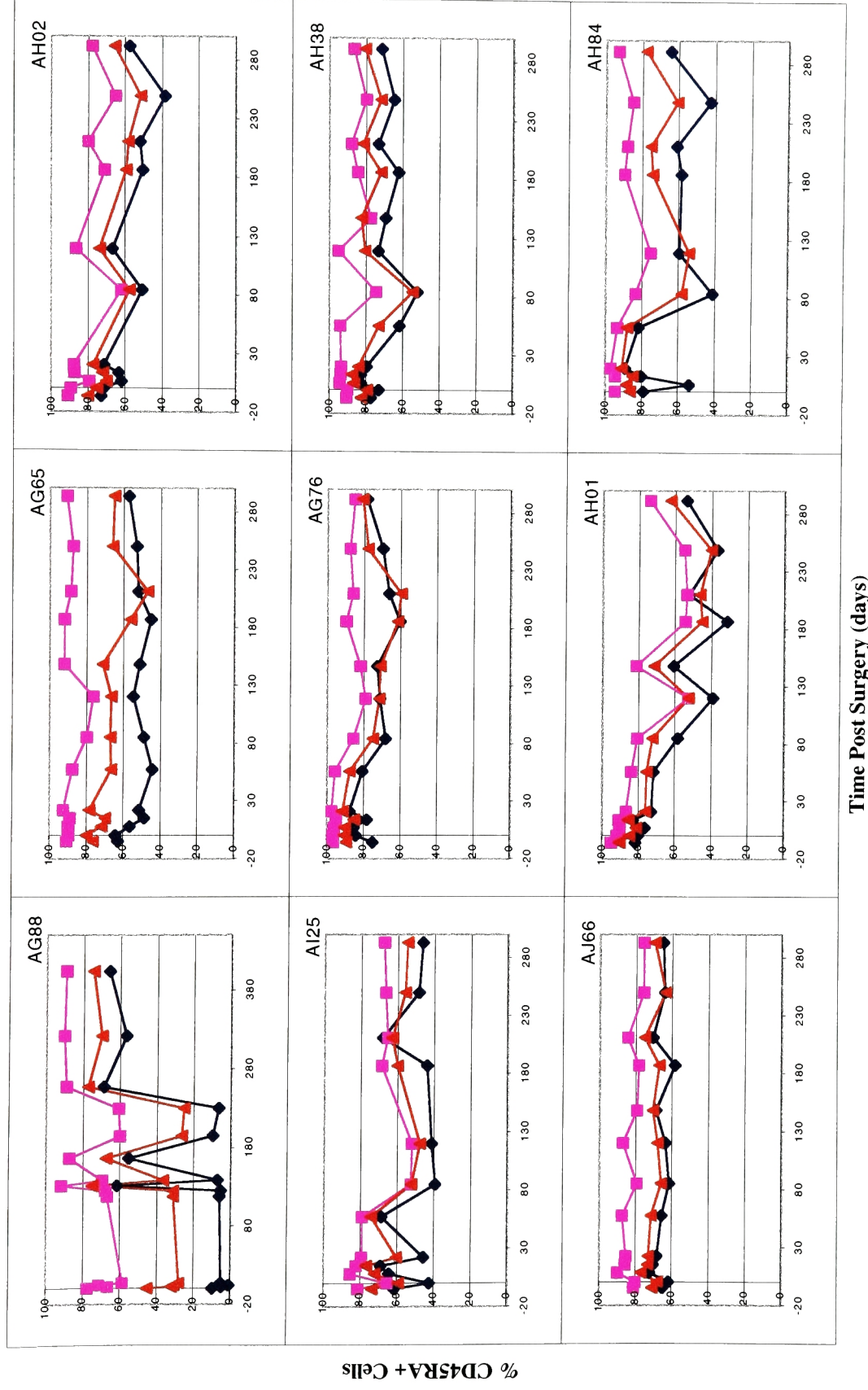
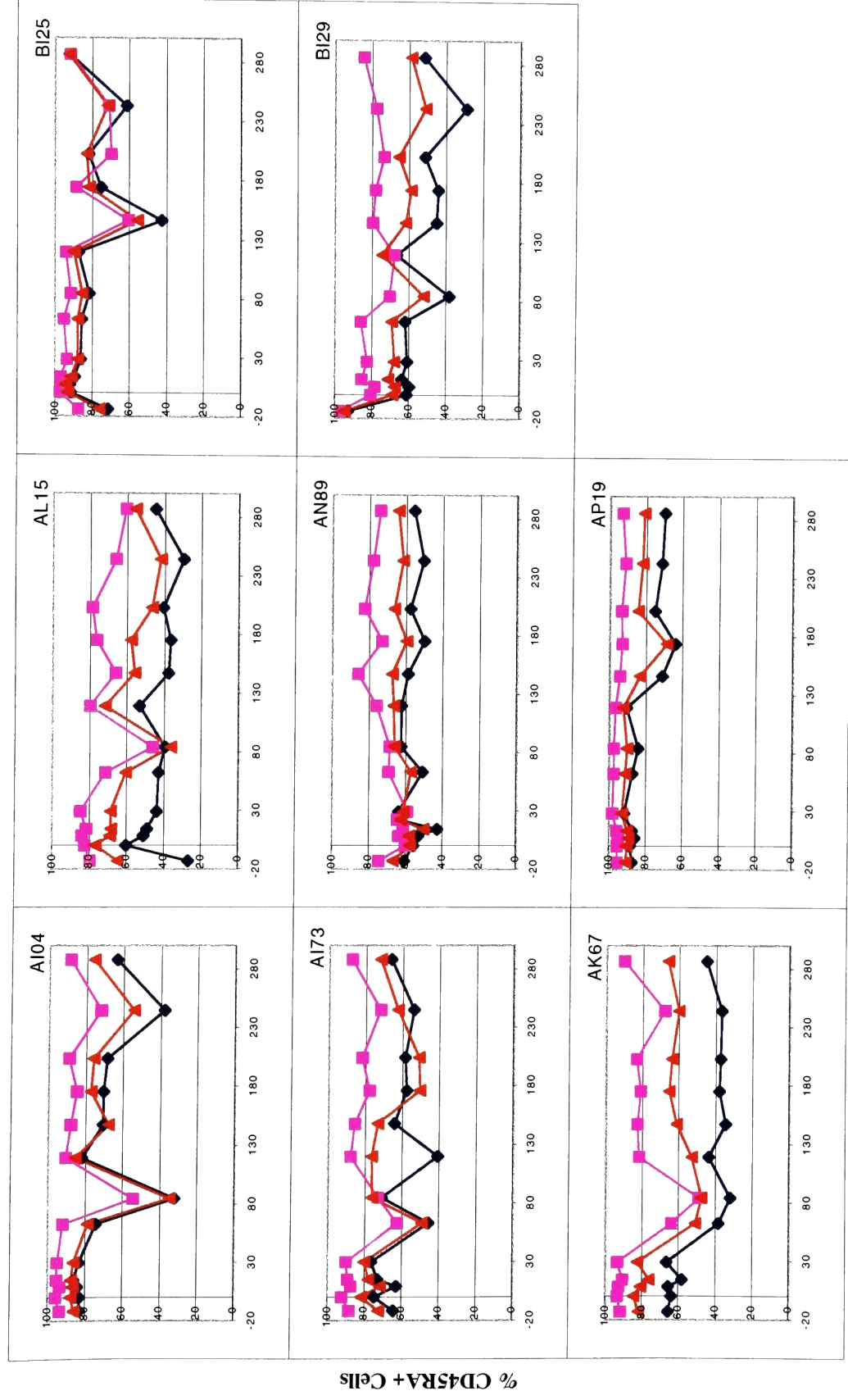


Figure 11a. % of CD45RA⁺ cells among CD3⁺, CD3⁺CD4⁺, and CD3⁺CD8⁺ T cells post thymectomy: thymectomized macaques. Red triangles represent CD3⁺ cells, blue diamonds represent CD3⁺CD4⁺ cells, and purple squares represent CD3⁺CD8⁺ cells.



Time Post Surgery (days)

Figure 11b. % of CD45RA⁺ cells among CD3⁺, CD3⁺CD4⁺, and CD3⁺CD8⁺ T cells post thymectomy: sham macaques. Red triangles represent CD3⁺ cells, blue diamonds represent CD3⁺CD4⁺ cells, and purple squares represent CD3⁺CD8⁺ cells.

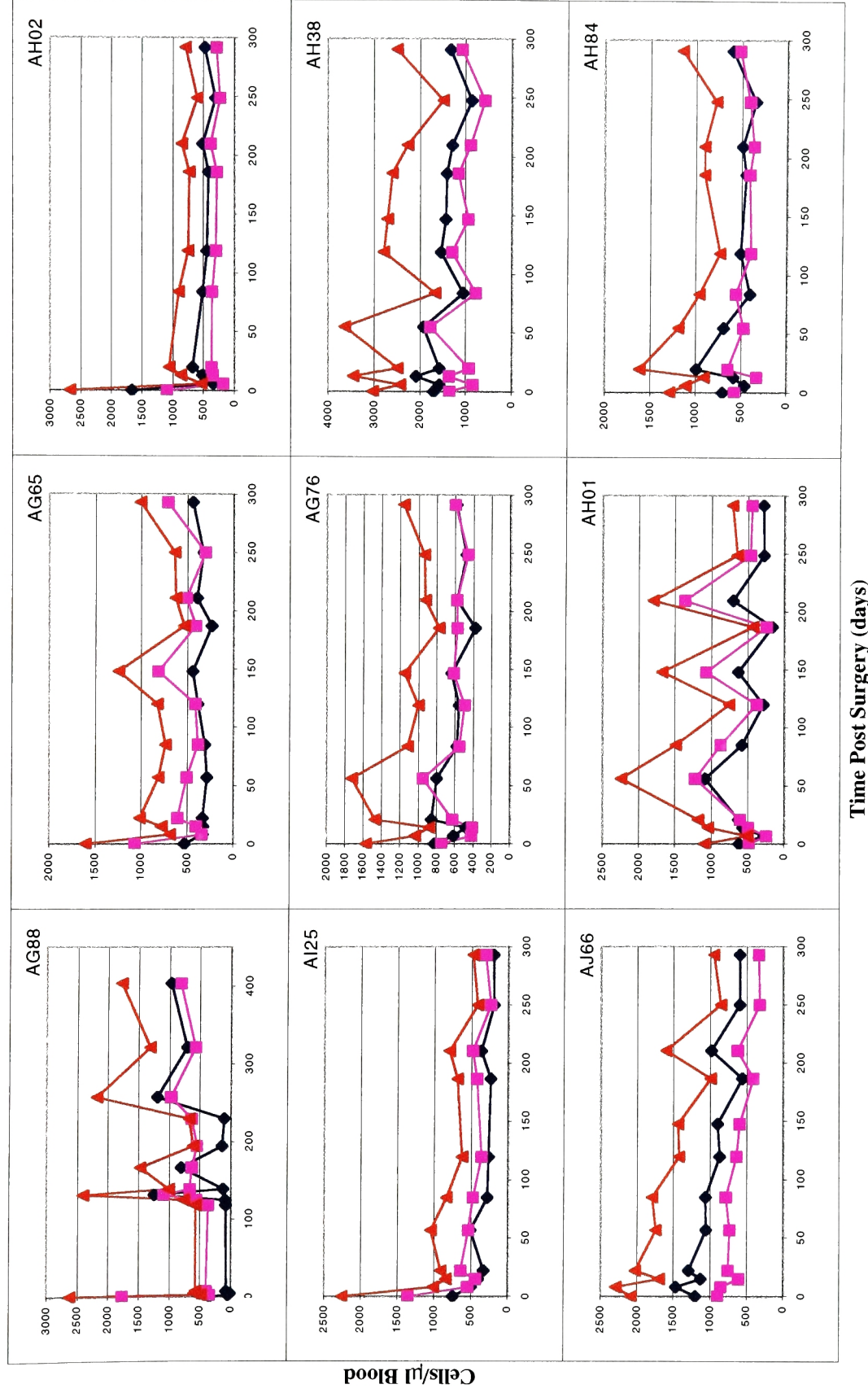


Figure 12a. Absolute naïve CD3, CD4, and CD8 counts post thymectomy: thymectomized macaques. Red triangles represent CD3⁺CD4⁺CD45RA⁺ cells, blue diamonds represent CD3⁺CD4⁺ cells, and purple squares represent CD8⁺ cells.

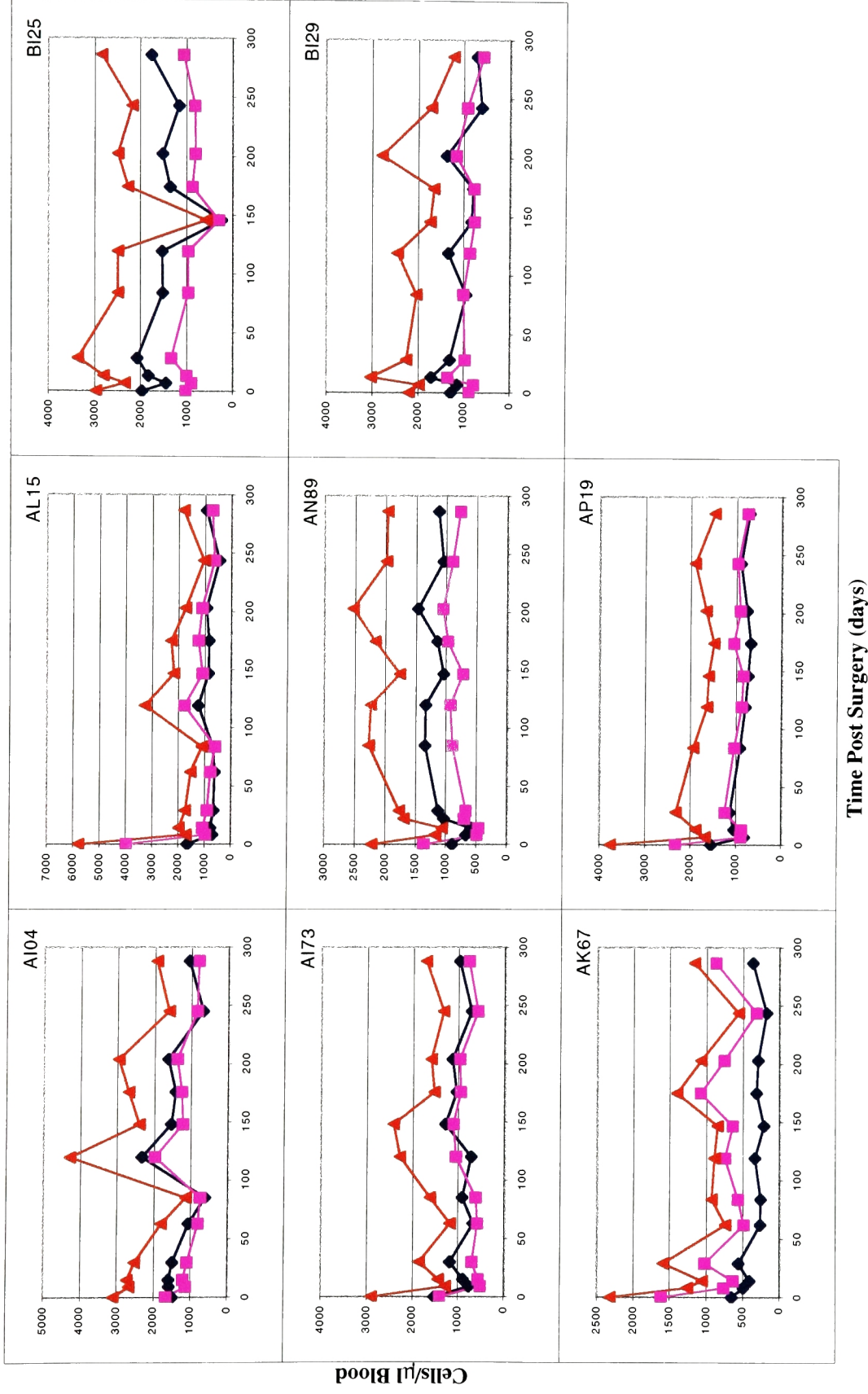


Figure 12b. Absolute naïve CD3, CD4, and CD8 counts post thymectomy: sham macaques.

Red triangles represent CD3⁺CD45RA⁺ cells, blue diamonds represent CD3⁺CD4⁺CD45RA⁺ cells, and purple squares represent CD3⁺CD8⁺CD45RA⁺ cells.

Table 3. Absolute naïve T cell decay slopes post thymectomy

		Slope (Day-1)		
		CD3 ⁺ CD45RA ⁺	CD4 ⁺ CD45RA ⁺	CD8 ⁺ CD45RA ⁺
Thymectomized	AG88	0.0018	0.0075	0.0007
	AI25	-0.0033	-0.0032	-0.0031
	AJ66	-0.0028	-0.0028	-0.0030
	AG76	-0.0011	-0.0012	-0.0002
	AH38	-0.0012	-0.0015	-0.0011
	AH84	-0.0010	-0.0013	-0.0006
	AG65	-0.0010	0.0001	-0.0003
	AH01	-0.0011	-0.0023	0.0003
	AH02	-0.0017	-0.0020	-0.0015
	Average	-0.0013	-0.0007	-0.0010
Sham	AI04	-0.0008	-0.0011	-0.0008
	AI73	-0.0003	-0.0002	0.0005
	AK67	-0.0017	-0.0025	-0.0013
	AL15	-0.0016	-0.0005	-0.0020
	AN89	0.0013	0.0015	0.0010
	AP19	-0.0016	-0.0016	-0.0016
	BI25	-0.0009	-0.0014	-0.0009
	BI29	-0.0015	-0.0023	-0.0010
	Average	-0.0009	-0.0010	-0.0008
p value		0.5006	0.5006	>.9999

5.2.4 T Cell Proliferation Post Surgery Based on the observation that thymectomy results in little quantitative change, if any, in the phenotypic makeup of the peripheral T cell pool, we wanted to address the question of whether peripheral proliferation of T cells was increased to fill the niche in the absence of the thymus. We used the nuclear antigen Ki67 as a marker for cell division(92). Figure 13 shows the percentages of Ki67⁺ CD3⁺CD4⁺ and CD3⁺CD8⁺ T cells measured post thymectomy. The percentages of proliferating T cells did not change significantly during the course of the study, and are overlapping at all time points between the thymectomized and sham group. Moreover, the range of proliferating cells (1-7% of CD3⁺CD4⁺ and 1-9% of CD3⁺CD8⁺) is within the normal range for rhesus macaques(191). We can conclude from this that peripheral proliferation is not significantly increased in response to the absence of a thymic source.

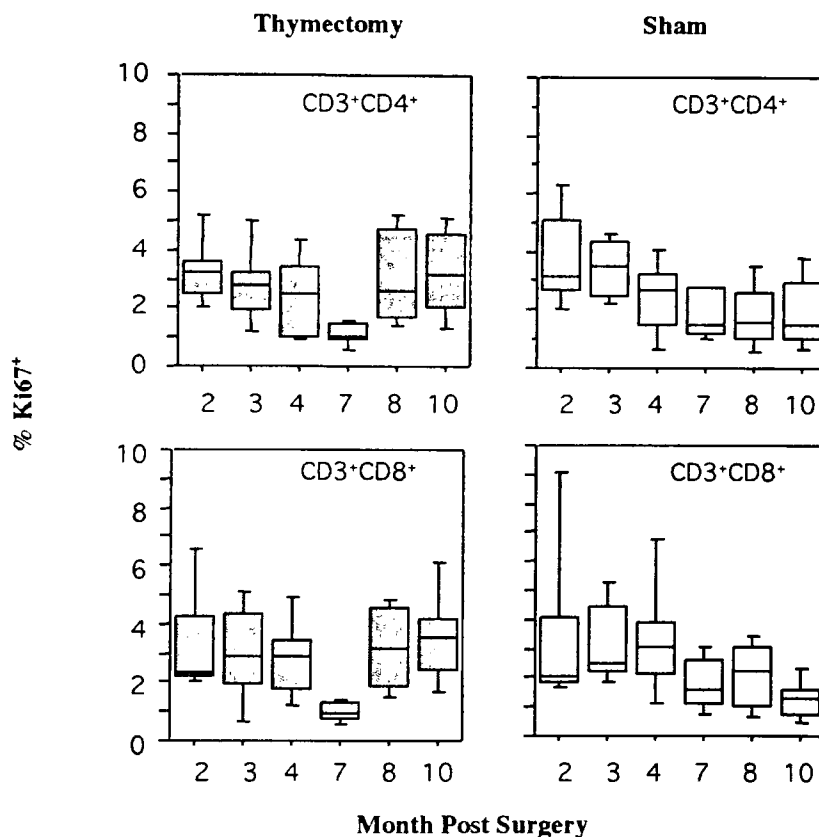


Figure 13. %Ki67⁺ CD3⁺CD4⁺ and CD3⁺CD8⁺ T cells post thymectomy. Shaded boxes indicate thymectomized animals, open boxes represent sham animals.

5.2.5 Thymectomy Results in a Decline in α 1 TRECBearing T cells At baseline, the PBMC α 1 TREC values of the nine animals assigned to the thymectomy

group and the eight animals assigned to the sham group were evenly matched (Fig. 14a). The median for the thymectomy group was $2.17 \times 10^4/10^6$ PBMC, whereas the median for the sham group was $1.99 \times 10^4/10^6$ PBMC (p value: 0.8474 by Mann-Whitney U test). Ten months post surgery, the two groups had significantly different $\alpha 1$ TREC values (Fig. 14b). The median for the thymectomy group had decreased nearly one log to $3.49 \times 10^3/10^6$ PBMC, while the median for the sham group was largely unchanged at $1.43 \times 10^4/10^6$ PBMC (p value: 0.0005 by Mann-Whitney U test), indicating a significant difference between the two groups.

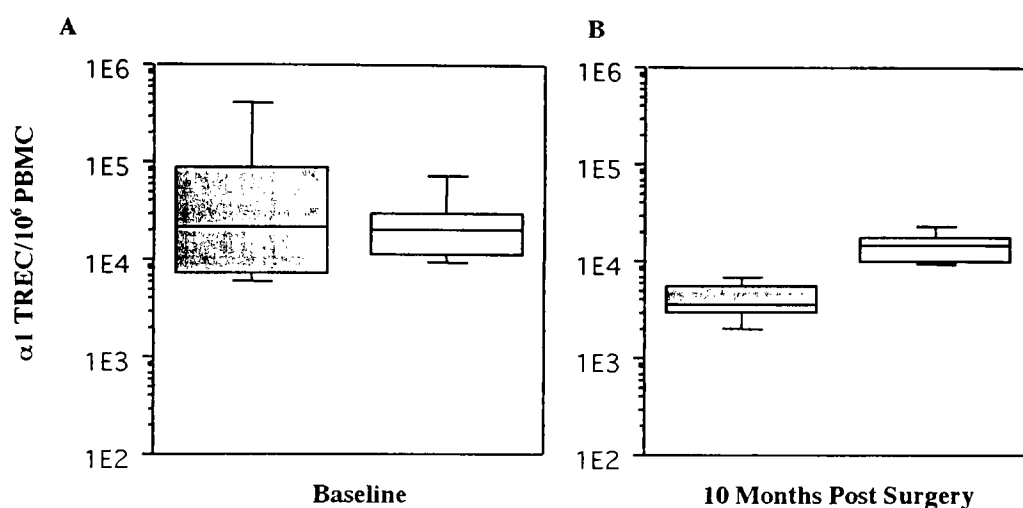


Figure 14. $\alpha 1$ TREC/ 10^6 PBMC at baseline and 10 months post surgery. Shaded boxes indicate thymectomized animals (n=9), open boxes represent sham animals (n=8). p value at baseline: 0.8474. p value at 10 months post surgery: 0.0005.

Figure 15 shows boxplots of $\alpha 1$ TREC decline in PBMC, CD4⁺, and CD8⁺ T cells after thymectomy. (For detailed plots of individual animals, see Appendix 1). While the concentration of $\alpha 1$ TREC positive cells in the PBMC of thymectomized animals declined after surgery, a comparison of the slopes between the two sets of animals was on the borderline of statistical significance (Table 4, p value= 0.0543 by Mann-Whitney U test). However, it was a concern that the effect of thymectomy on the $\alpha 1$ TREC positive concentrations in PBMC might be diluted by non-T cells in the population studied, so we

analyzed $\alpha 1$ TREC concentrations in sorted CD4⁺ and CD8⁺ T cells. As expected, $\alpha 1$ TREC decay in these T cell subsets was significantly increased by thymectomy (Table 4, p value for CD4⁺= 0.0015, CD8⁺= 0.0005). The average slopes correspond to a half-life of 129 days for $\alpha 1$ TREC in PBMC in the thymectomized macaques as compared to 561 days in the sham macaques (Table 5).

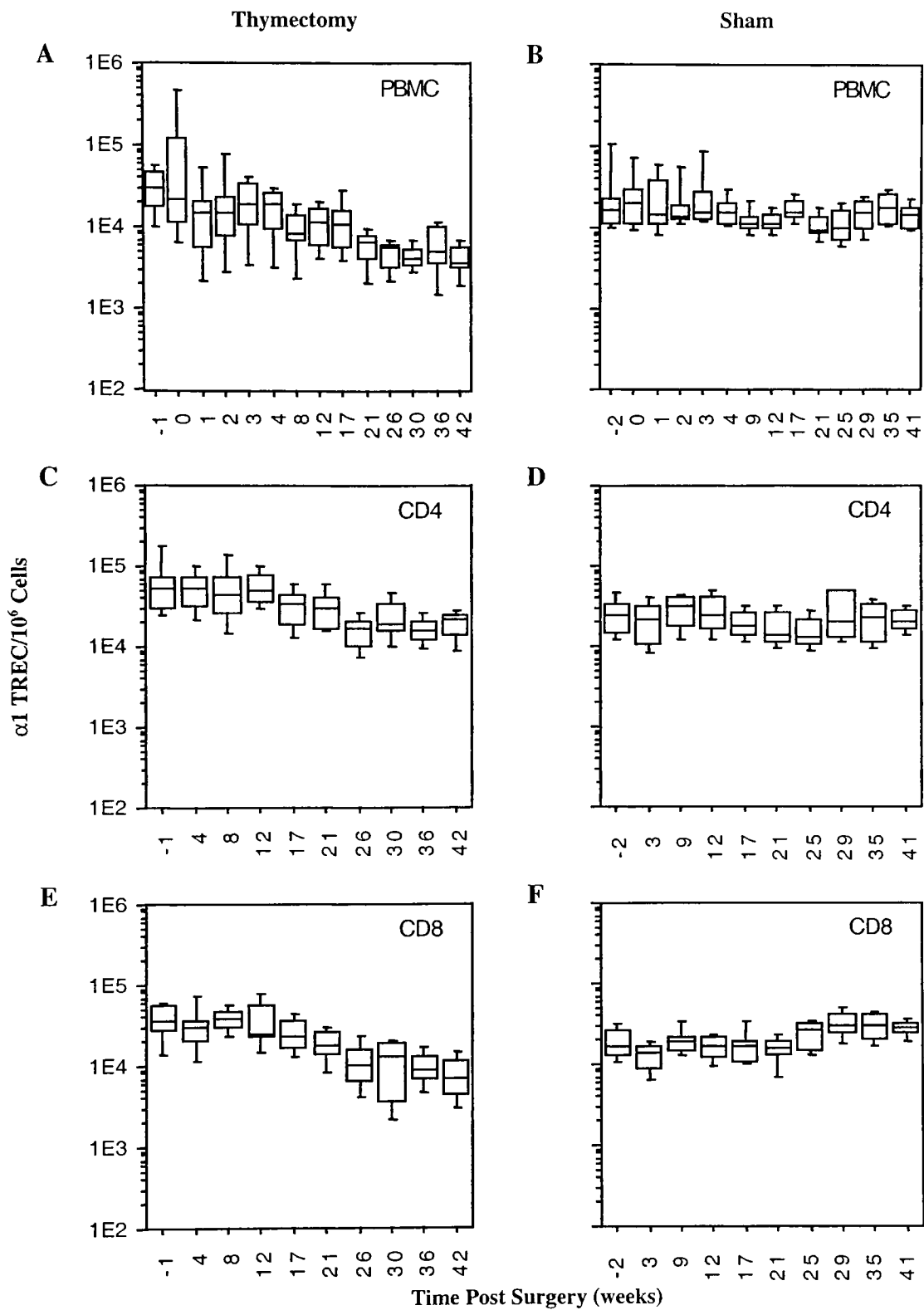


Figure 15. $\alpha 1$ TREC/10⁶ PBMC, CD4, and CD8 post surgery.
A, C, and E: Thymectomized macaques. B, D, and F: Sham controls.

Table 4. α 1 TREC decay slopes post thymectomy

		Slope (Day ⁻¹)		
		PBMC	CD4 ⁺	CD8 ⁺
Thymectomized	AG88	-0.0005	-0.0038	-0.0055
	AI25	-0.0006	-0.0063	-0.0097
	AJ66	-0.0042	-0.0030	-0.0082
	AG65	-0.0018	-0.0076	-0.0071
	AG76	-0.0122	-0.0078	-0.0075
	AH01	-0.0127	-0.0071	-0.0127
	AH02	-0.0063	-0.0021	-0.0052
	AH38	-0.0047	-0.0022	-0.0020
	AH84	-0.0055	-0.0018	-0.0003
	Average	-0.0054	-0.0046	-0.0065
Sham	AI04	-0.0050	-0.0010	0.0021
	AI73	-0.0019	0.0018	0.0044
	AK67	-0.0025	-0.0004	0.0021
	AL15	-0.0048	-0.0014	0.0016
	AN89	0.0020	-0.0007	0.0021
	AP19	0.0008	-0.0026	0.0010
	BI25	0.0002	0.0010	0.0030
	BI29	0.0015	-0.0010	0.0036
	Average	-0.0012	-0.0005	0.0025
p value		0.0543	0.0015	0.0005

Table 5. $\alpha 1$ TREC decay post thymectomy

	Average Slope (Day ⁻¹)		p value	T _{1/2} (d)	
	Thymectomy	Sham		Thymectomy	Sham
PBMC	-0.0054	-0.0012	0.0543	129	561
CD4	-0.0046	-0.0005	0.0015	150	1284
CD8	-0.0065	0.0025	0.0005	107	-277

5.2.6 Calculation of Thymic Export Rates in the Juvenile Rhesus Macaque

The decay slope of $\alpha 1$ TREC positive PBMC was calculated to be 0.0054 day⁻¹, or 0.5% of $\alpha 1$ TREC bearing cells per day. We can conclude that this decay rate is the output rate, or source, of 0.5% of $\alpha 1$ TREC bearing cells per day.

Given the median $\alpha 1$ TREC levels in both groups at baseline, and taking into account the fact that any one cell can contain either one or two $\alpha 1$ TREC depending on recombination on each chromosome, we can calculate a range of 1.1-2.2% of total T cells that are $\alpha 1$ TREC positive.

Based on the assumption that the average macaque has 10¹¹ total T cells and that $\alpha 1$ TREC are evenly distributed, we can calculate an absolute range of total T cells that are $\alpha 1$ TREC positive, 1.1-2.2x10⁹. 0.5% of this total yields an absolute thymic production rate of 5.5x10⁶ -1.1x10⁷ $\alpha 1$ TREC bearing cells per day (Fig. 16), a minor fraction of the total T cell pool.

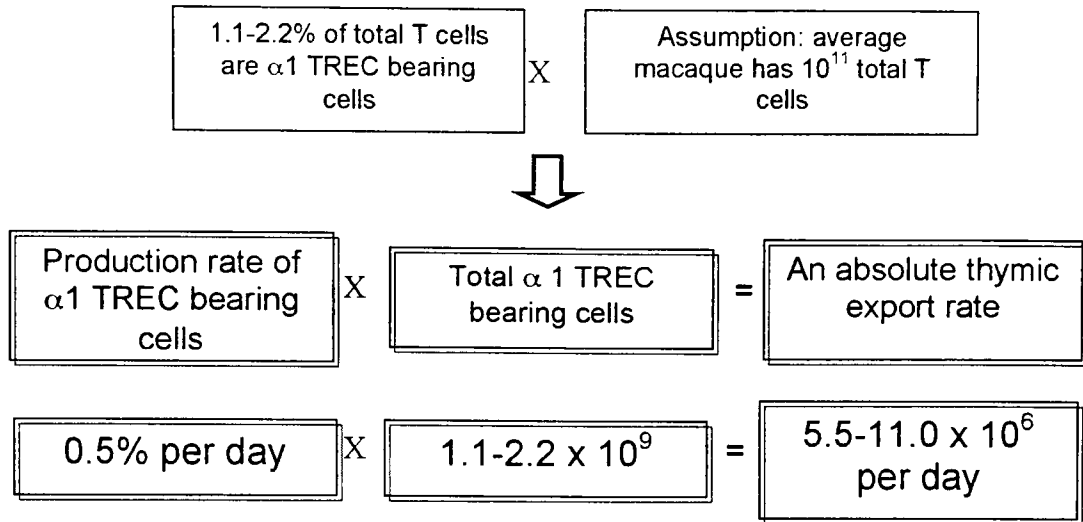


Figure 16. Calculation of an absolute thymic export rate.

The change in $\alpha 1$ TREC over time is equal to the input source minus proliferation and death, or

$$dTREC/dt = s_{TREC} - (p_{TREC} + d_{TREC}) \quad (1)$$

In our system, where s' is the source after thymectomy (assumed to be zero),

$$s'(\sim 0) - (p_{TREC} + d_{TREC}) = -0.0054/d \quad (2a)$$

$$s'(\sim 0) + 0.0054/d = p_{TREC} + d_{TREC} \quad (2b)$$

From this we see that $0.0054/d$ is a minimum estimate of source. Should s' be greater than 0, the actual source would be greater. Although residual thymic tissue was not detected on necropsy, even with a conservative assumption that the thymectomy was only 50% complete, the doubled thymic production rate, $1.1-2.2 \times 10^7$, is still a miniscule fraction of the total T cell pool.

There is a very low rate of $\alpha 1$ TREC decay in the PBMC of the sham animals as well, $-0.0012/d$. Adjusting the decay rate in the thymectomized animals for this

presumably age-related decline gives us a rate of -0.0042/d, or 0.4% of $\alpha 1$ TREC bearing cells per day, which translates to an even smaller output of $4.4\text{--}8.8 \times 10^6$ $\alpha 1$ TREC bearing cells per day.

Using our measured concentrations of $\alpha 1$ TREC bearing cells among single positive thymocytes, it is possible to estimate a total thymic export rate. As only 11% of single positive thymocytes are $\alpha 1$ TREC bearing cells, we must correct our measurements of $\alpha 1$ TREC bearing cell export by a factor of 11. This yields a total thymic export rate range of 6.1×10^7 – 1.2×10^8 .

5.3 Infection

5.3.1 Viral Loads and Disease Progression Approximately three hundred days after surgery, six thymectomized and six sham macaques were inoculated with 100AID₅₀ (animal infectious dose) of SIV_{MAC251}. Plasma viral loads are shown in Figure 17. Viral loads peaked at fourteen days post infection in both thymectomy and sham groups. The viral load plateau, or setpoint, was reached by day 89 in both groups. There was no statistically significant difference in peak viral load or average viral load at setpoint between the two groups (Fig. 18, $p = 0.0547$ for peak viral load, $p = 0.7488$ for setpoint by Mann-Whitney U test).

Within 200 days of infection, four thymectomized animals and two sham animals showed evidence of simian acquired immune deficiency syndrome (SAIDS) and opportunistic infections and were sacrificed. By 300 days post infection, a third sham animal had been sacrificed. Gross necropsy findings are reported in Table 6, and all findings were consistent with SAIDS. Viral load was a prognostic indicator in both thymectomy and sham groups. While some might argue that progression to disease appears to be faster among thymectomized animals, the small number of animals in each group makes it impossible to determine whether this is an effect of thymectomy or of individual response to pathogenesis. Death within six months to one year, one of the hallmarks of rapid progression in SIV, would be expected in this number of animals in either group, and would be predicted by high viral loads, as was observed. The absence of antibody response would confirm rapid progressor status in these animals. A study of

a larger cohort of animals would be necessary to determine whether thymectomy has an influence on rapid progression to disease and death.

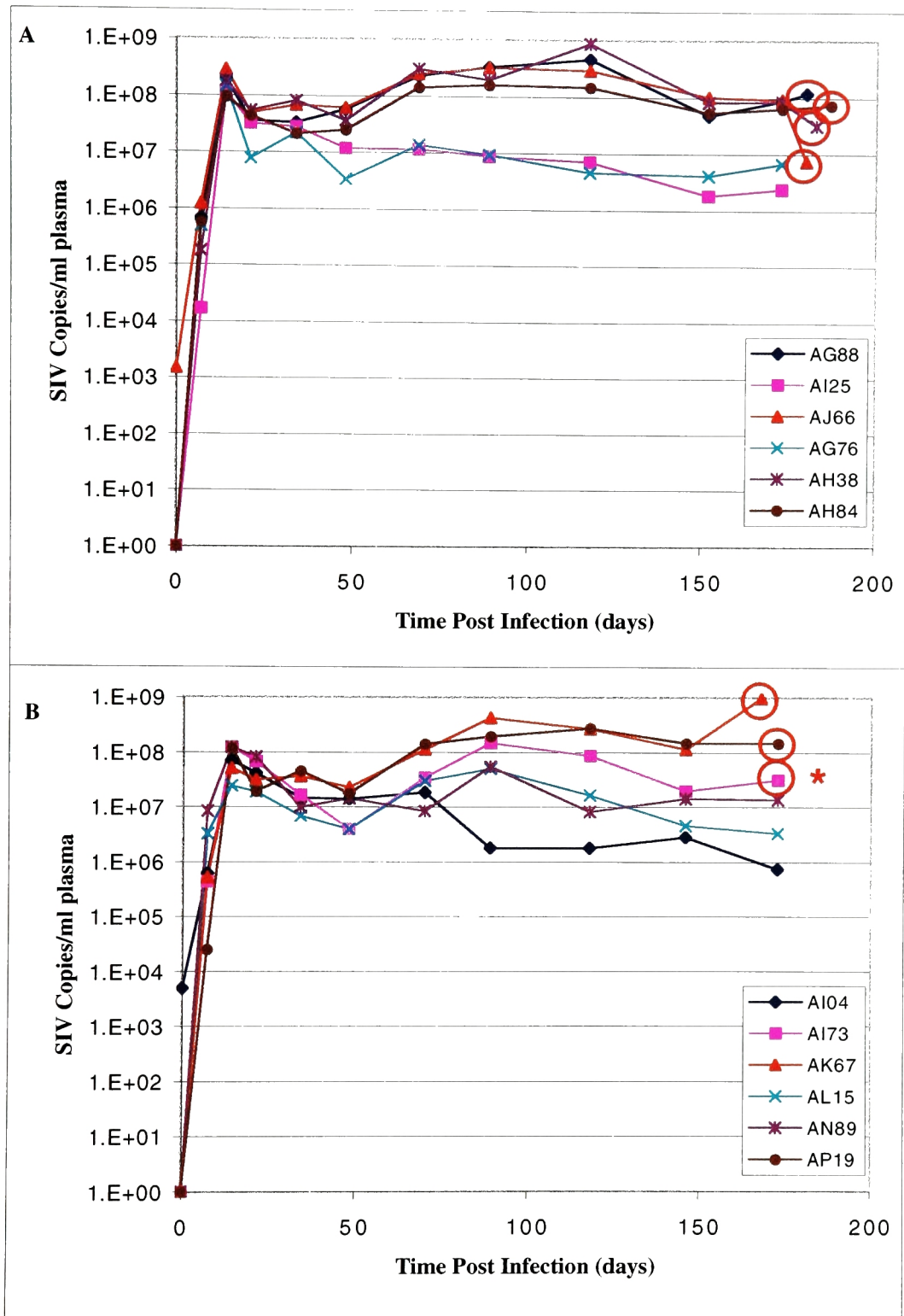


Figure 17. SIV viral loads A. Thymectomized macaques. B. Sham controls. Red circles indicate development of simian AIDS and sacrifice. Animal AI73, marked with an asterisk, died after the endpoint of this study (appx. day 300 post infection).

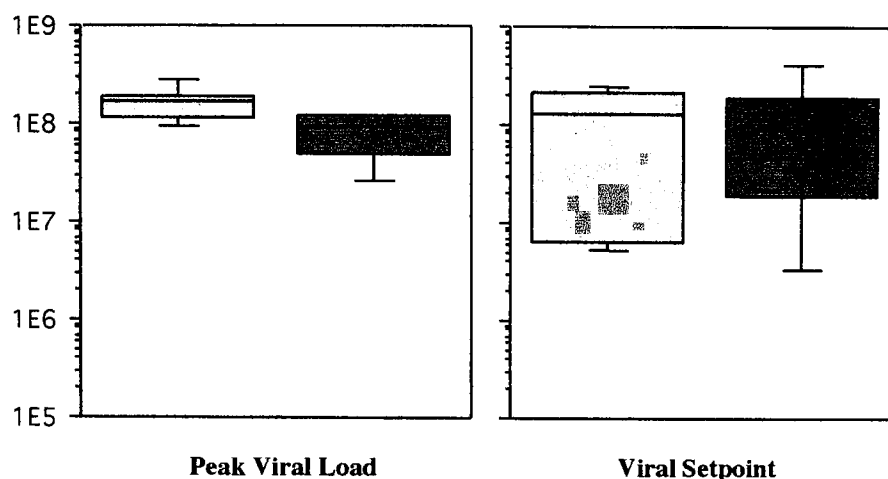


Figure 18. Boxplots of peak viral load and viral setpoint. Light shaded boxes represent thymectomized animals, dark shaded boxes represent sham animals. p value of peak viral load: 0.0547. p value of setpoint: 0.7488.

Table 6. Necropsy findings

Animal	Group	Necropsy Findings
AG88	Thymectomy	Chronic pneumonia. Severe diffuse SIV pneumonia. Severe disseminated M. avium infection. Pneumococcus cultured from the lung. Multifocal mild SIV encephalitis.
AJ66	Thymectomy	Chronic pneumonia. Lesions of severe diffuse interstitial pneumonia with multinucleated giant cells and severe pneumocystis carinii.
AH38	Thymectomy	Severe disseminated M. avium infection affecting the intestinal tract, bone marrow, and lymphoid tissues. SIV pneumonia and encephalitis also observed.
AH84	Thymectomy	Chronic pneumonia. Severe interstitial giant cell pneumonia. Disseminated M. avium infection. Pneumococcus cultured from the lung.
AK67	Sham	Cytomegaloviral pneumonia and intestinal cryptosporidiosis. SIV encephalitis and generalized giant cell disease. Acute myocarditis without inclusion bodies, possibly secondary to CMV.
AP19	Sham	Viral interstitial pneumonia. Chronic gastritis. Localized amyloidosis in the small intestine.
AI73	Sham	Pneumonia. Pathology report pending.

5.3.2 Effect of Infection on CD4⁺ T Cell Counts After infection, the absolute CD4⁺ T cell counts in the thymectomized animals began to decline (Fig. 19aA). Among the sham group, two of the infected animals, AI04 and AL15, had an observable drop in CD4/ μ l, but the others did not (Fig. 19bA). A comparison of the CD4 decline between preinfection and postinfection values indicated that the drop after infection was significant among the thymectomized animals ($p = 0.0104$, Table 7) but not among the sham controls ($p = 0.7488$). Uninfected macaques in both groups showed no overall CD4 decline (Figs. 19aB, 18bB, Table 7).

A comparison of the infected thymectomized and sham animals revealed that there was no statistical significance in the CD4 decay slopes between the two groups ($p = 0.2002$ (Table 8)). Although high viral load was associated with death within this study period, the animals with lower viral loads had lower CD4 counts.

The percentage of lymphocytes that were CD4⁺ also declined after infection in the thymectomized and some of the sham macaques, mirroring the decline in absolute CD4 counts (Fig. 20aA, 20bA). Again, uninfected controls had no change in the relative lymphocyte populations (Fig. 20aB, 20bB).

5.3.3 Effect of Infection on CD8⁺ T Cell Counts The impact of infection on the absolute CD8⁺ T cell counts in these animals varied. Among thymectomized animals, there was a decline in CD8/ μ l with transient increases that may reflect antigen-stimulated proliferation (Fig. 19aA). Among sham animals, two animals, AI04 and AL15, had a decline in CD8/ μ l that mirrored their decline in CD4/ μ l, while the others had sustained or slightly increased CD8 counts (Fig. 19bA). The overall CD8 trends were not significantly different from those preceding infection in either thymectomized or sham animals ($p = 0.6310$ for thymectomy, 0.7488 for sham (Table 7)). Uninfected macaques in both groups showed no overall CD8 decline (Figs. 19aB, 19bB, Table 7). There was no statistical significance in the CD8 slopes between the infected animals of the thymectomized and sham groups ($p > 0.9999$ (Table 8)).

The changes in the percentage of lymphocytes that were CD8⁺ also varied from animal to animal. In the thymectomy group, many of the animals had a steady increase in the percentage of CD8⁺ T cells, while others had very little change. One animal, AI25,

had a period of dramatic increase that was temporally correlated with the transient increase in absolute CD8 count (Fig. 20aA). In the sham group, only one animal, AK67, had a steady increase in the percentage of CD8⁺ T cells, while the others had relatively steady values (Fig. 20bA). Uninfected animals of both groups had no change in the relative lymphocyte populations (Fig. 20aB, 20bB).

5.3.4 CD4:CD8 Ratios After Infection After infection, the CD4:CD8 ratio in both thymectomized and sham animals dropped sharply, with all animals reversing the CD4:8 ratio (less than 1.0) by twenty-eight days post infection (Figs. 21aA, 21bA). One sham animal, AK67, seemed to have a rebound in CD4:8 ratio after 100 days post inoculation, but this was revealed to be secondary to a rapid drop in absolute CD8 count in the time points preceding death. In contrast, uninfected animals in both the thymectomized and sham groups had a stable CD4:8 ratio in this time period, at normal values of 1.5-2 (Figs. 21aB, 21bB).

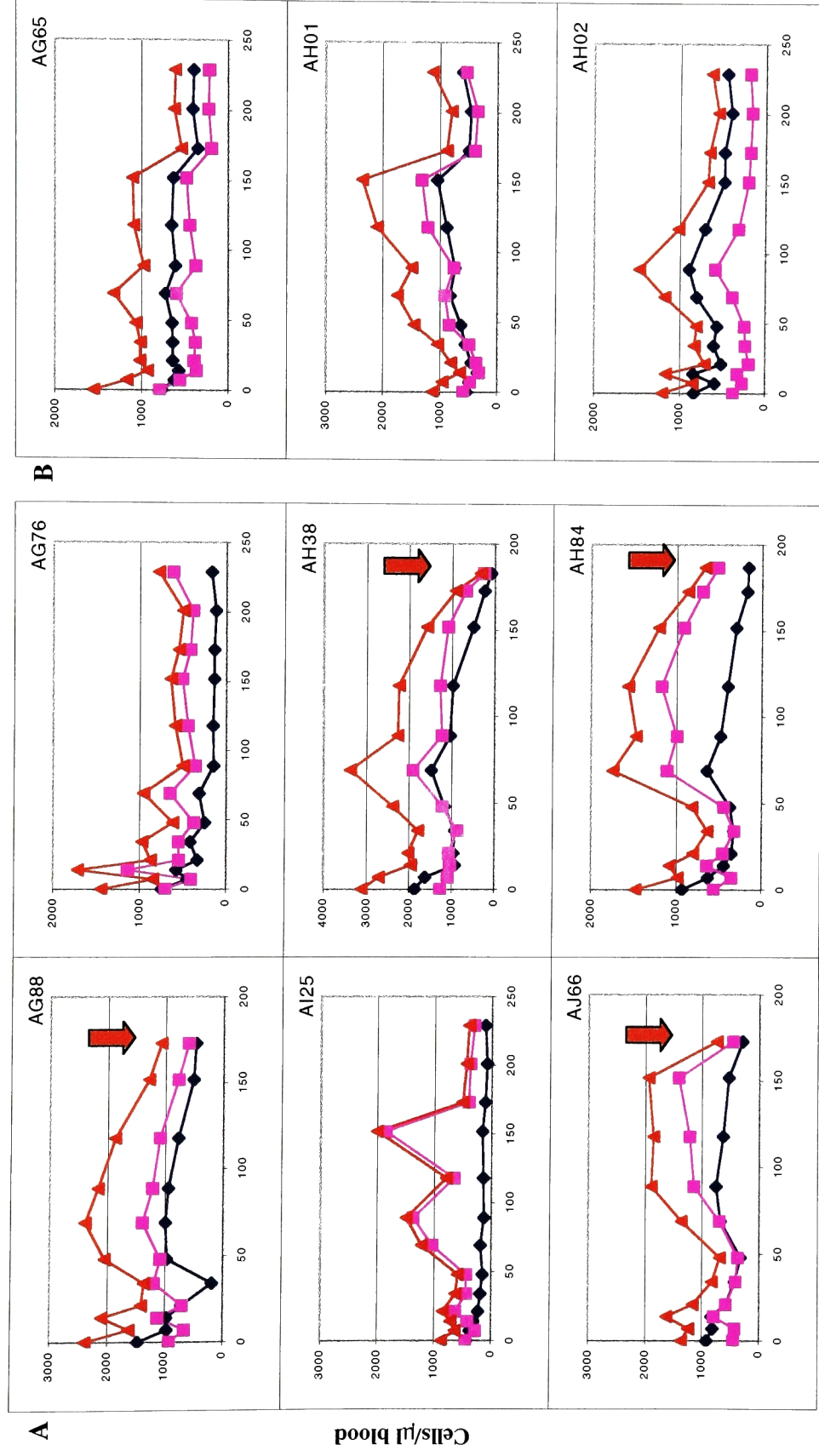


Figure 19a. Absolute CD3, CD4, and CD8 counts post infection: thymectomized macaques.

A. Infected macaques. B. Uninfected controls. Red triangles represent CD3⁺ cells, blue diamonds represent CD4⁺ cells, and purple squares represent CD8⁺ cells. Arrows indicate time of death.

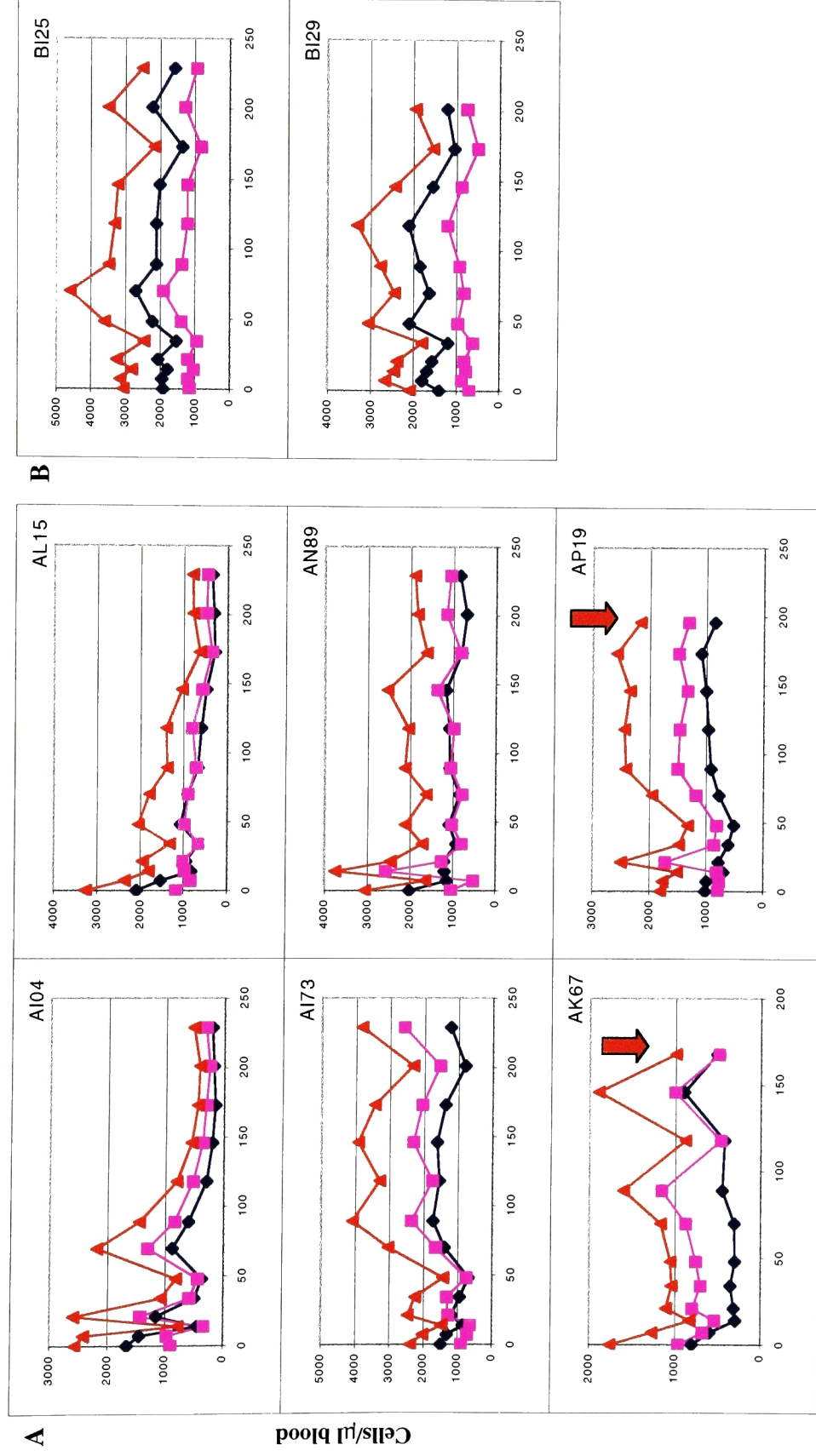


Figure 19b. Absolute CD3, CD4, and CD8 counts post infection: sham macaques.

A. Infected macaques. B. Uninfected controls. Red triangles represent CD3⁺ cells, blue diamonds represent CD4⁺ cells, and purple squares represent CD8⁺ cells. Arrows indicate time of death.

Table 7. Absolute T cell decay slopes, pre vs. post infection

CD3⁺		Average Slope (Day⁻¹)		
		preinfection	postinfection	p value
Infected	Thymectomized	-0.0011	-0.0021	0.7488
	Sham	0.0000	-0.0010	0.8728
Uninfected	Thymectomized	0.0000	-0.0013	0.5127
	Sham	-0.0006	-0.0008	0.4386
CD4⁺		Average Slope (Day⁻¹)		
		preinfection	postinfection	p value
Infected	Thymectomized	-0.0012	-0.0055	0.0104
	Sham	0.0004	-0.0017	0.7488
Uninfected	Thymectomized	-0.0002	-0.0011	0.5127
	Sham	-0.0002	-0.0011	>.9999
CD8⁺		Average Slope (Day⁻¹)		
		preinfection	postinfection	p value
Infected	Thymectomized	-0.0009	0.0001	0.6310
	Sham	-0.0004	-0.0003	0.7488
Uninfected	Thymectomized	0.0003	-0.0017	0.2752
	Sham	-0.0004	-0.0007	0.4386

Table 8. Absolute T cell decay slopes post infection, thymectomy vs. sham

		Slope (Day ⁻¹)		
		CD3 ⁺	CD4 ⁺	CD8 ⁺
Thymectomized	AG88	-0.0020	-0.0017	-0.0013
	AI25	-0.0016	-0.0051	0.0000
	AJ66	0.0010	-0.0027	0.0040
	AG76	-0.0027	-0.0062	-0.0010
	AH38	-0.0073	-0.0118	-0.0045
	AH84	0.0002	-0.0053	0.0033
	Average	-0.0021	-0.0055	0.0001
Sham	AI04	-0.0067	-0.0084	-0.0053
	AI73	0.0030	0.0008	0.0049
	AK67	0.0012	0.0037	-0.0005
	AL15	-0.0051	-0.0063	-0.0040
	AN89	-0.0009	-0.0016	0.0002
	AP19	0.0022	0.0019	0.0027
	Average	-0.0012	-0.0018	-0.0005
p value		0.3367	0.2002	>.9999

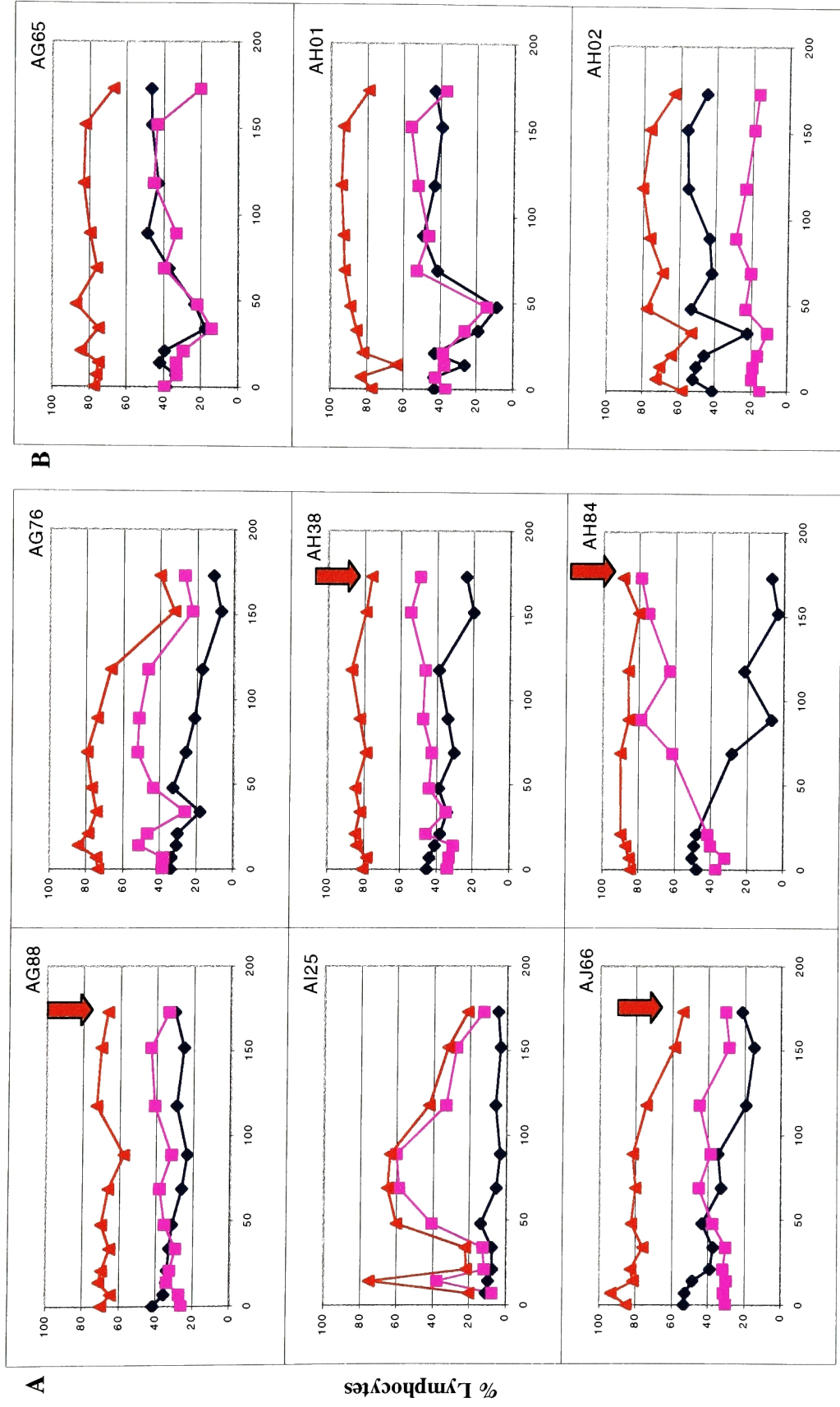
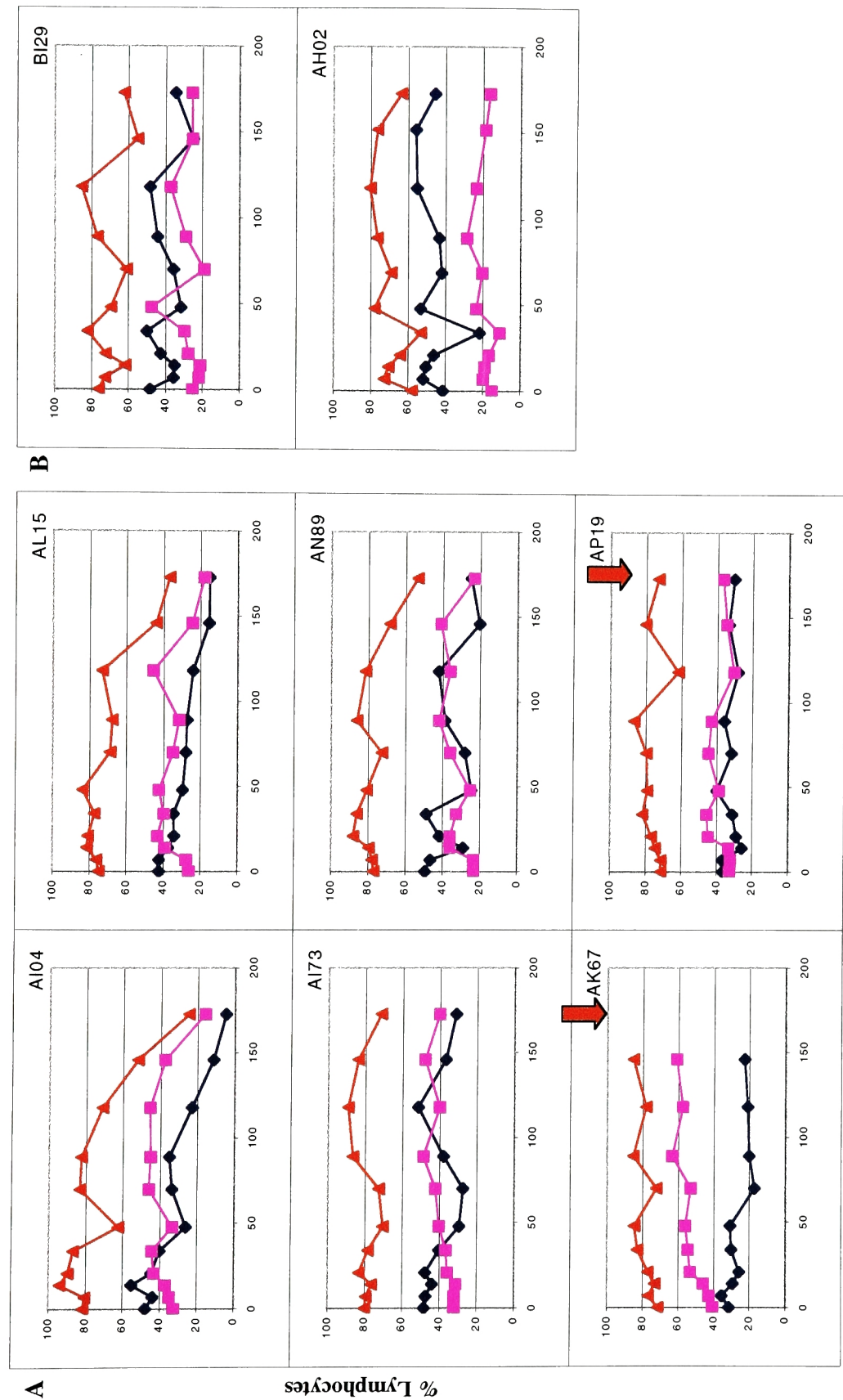


Figure 20a. % of CD3⁺, CD3⁺CD4⁺, and CD3⁺CD8⁺ cells post infection: thymectomized macaques. A. Infected macaques. B. Uninfected controls. Red triangles represent CD3⁺ cells, blue diamonds represent CD4⁺ cells, and purple squares represent CD8⁺ cells. Arrows indicate time of death.



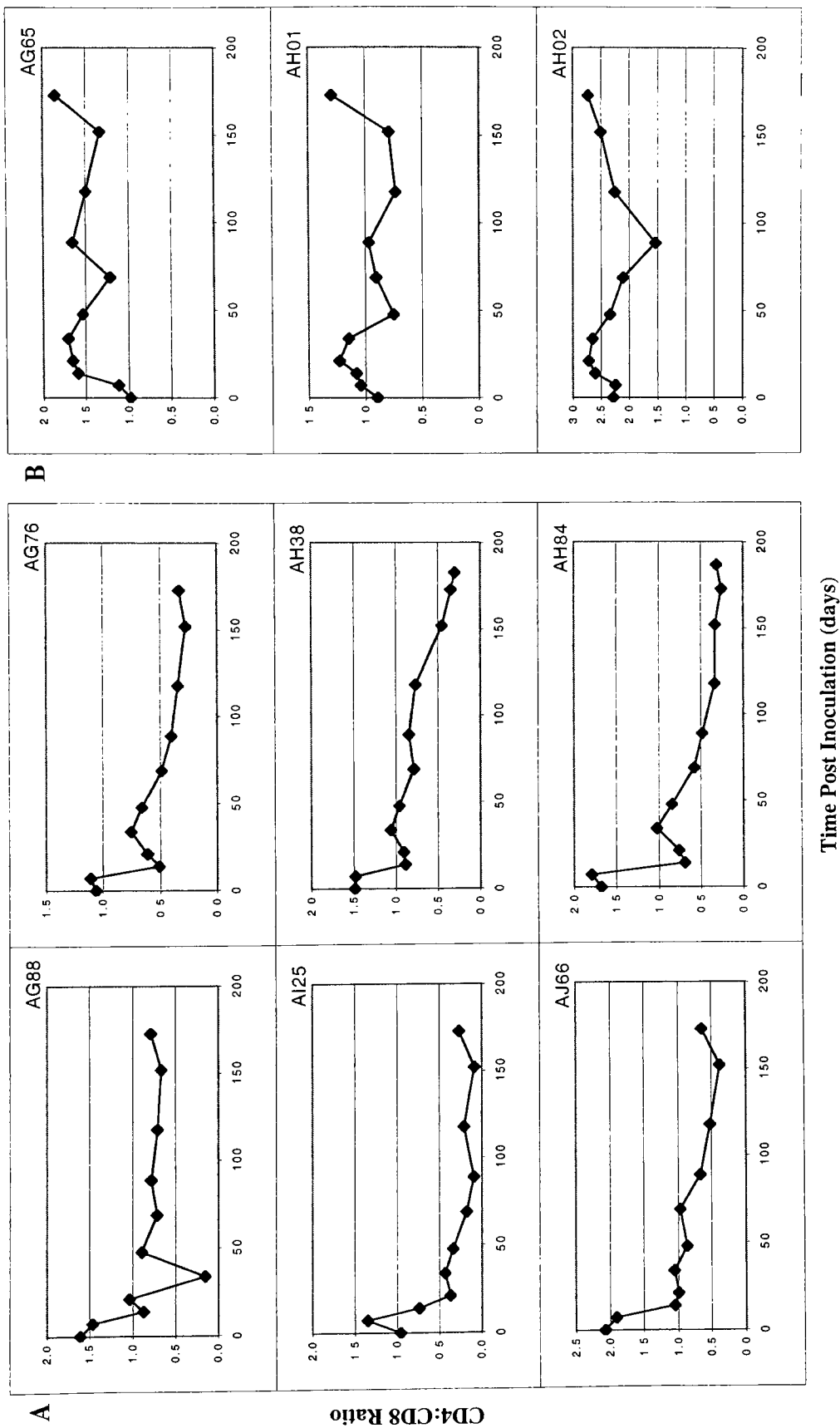


Figure 21a. CD4:CD8 ratio post infection: thymectomized macaques.

A. Infected macaques. B. Uninfected controls.

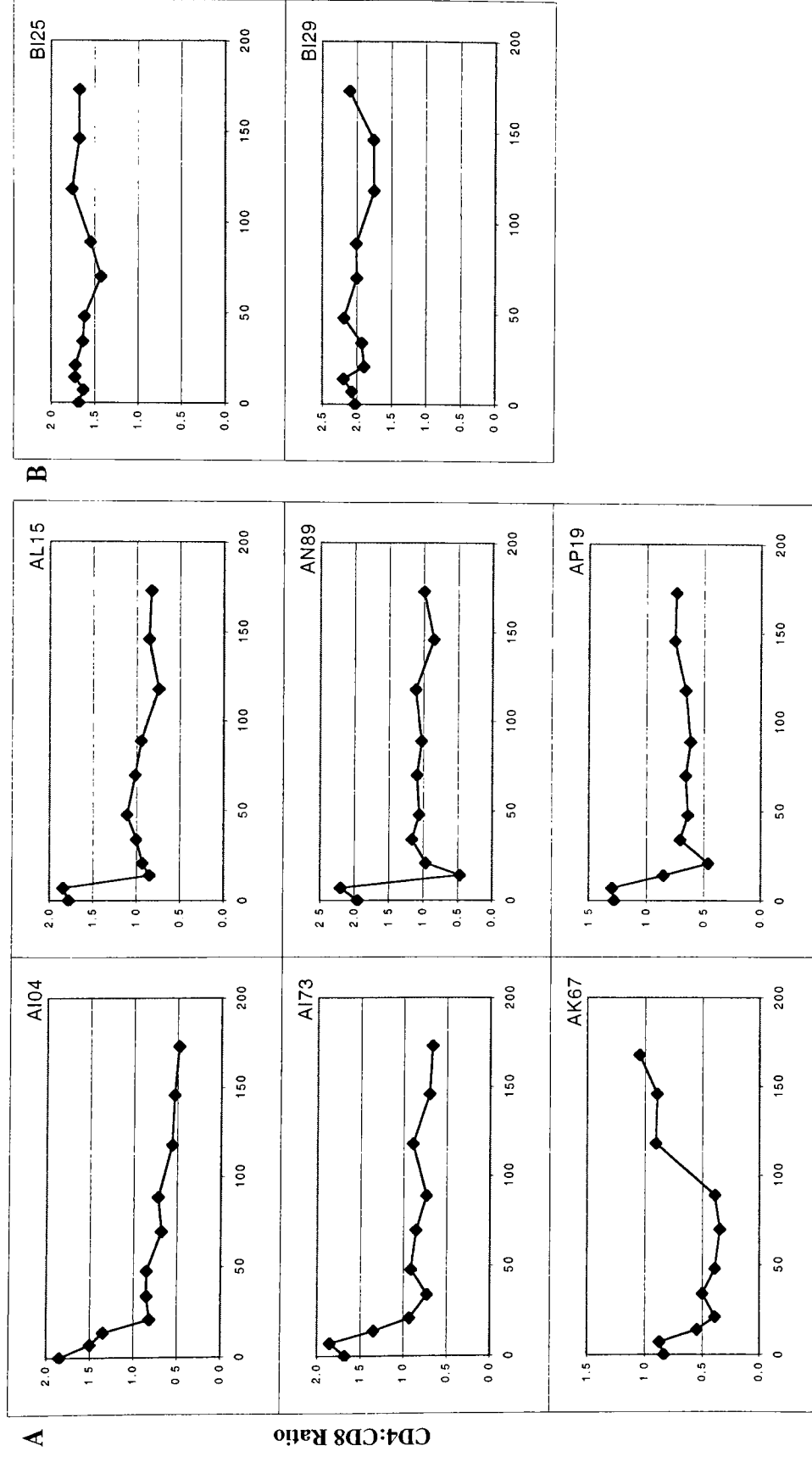


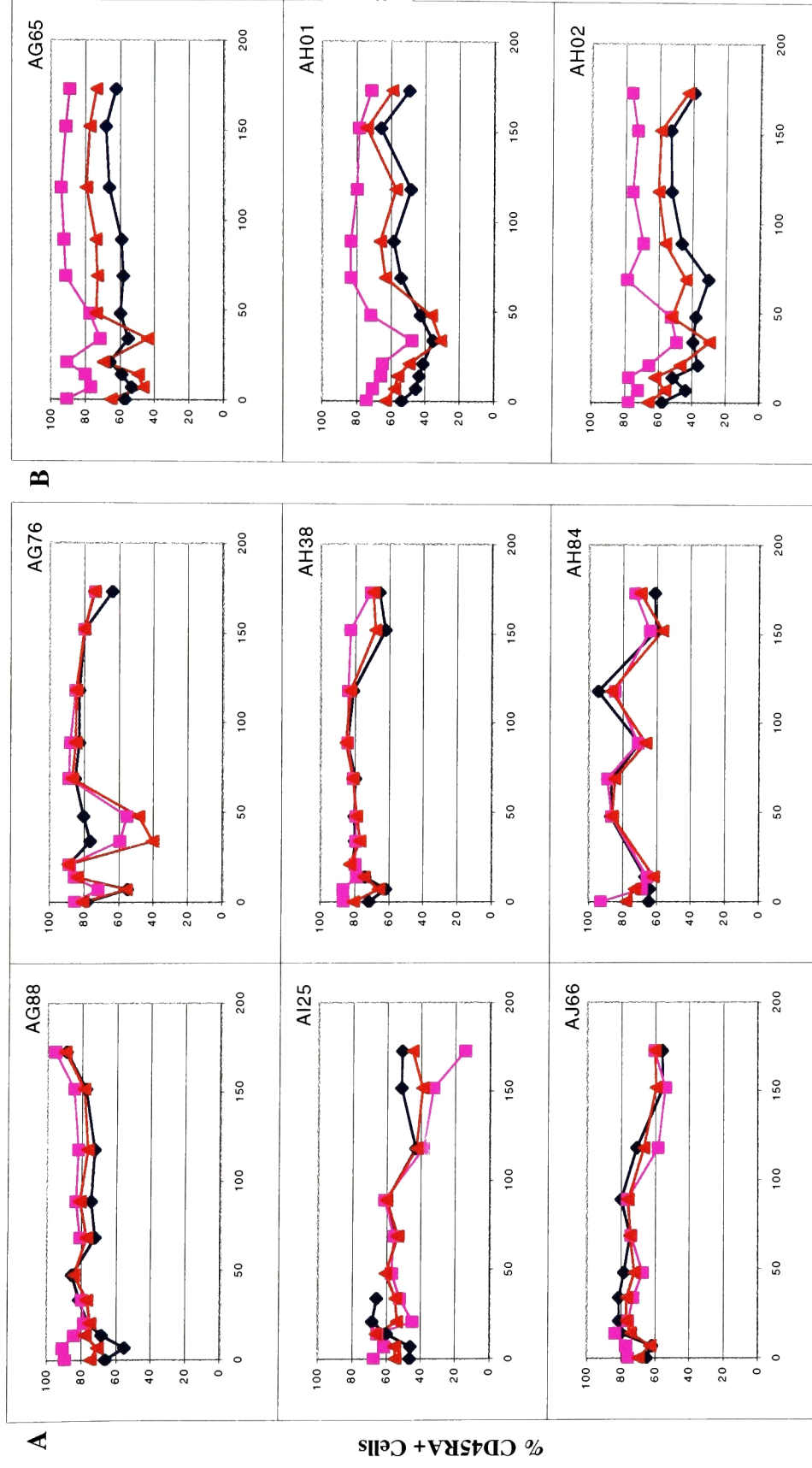
Figure 21b. CD4:CD8 ratio post infection: sham macaques.

A. Infected macaques. B. Uninfected controls.

5.3.5 Effect of Infection on Naïve T Cells Despite minor fluctuations in the percentages of CD45RA⁺ cells in the CD3⁺, CD4⁺, and CD8⁺ populations of the infected animals, the overall proportion of naïve cells remained unchanged, and fairly high (Figs. 22aA, 22bA). In uninfected macaques of both groups, the proportion of naïve cells was also stable (Figs. 22aB, 22bB).

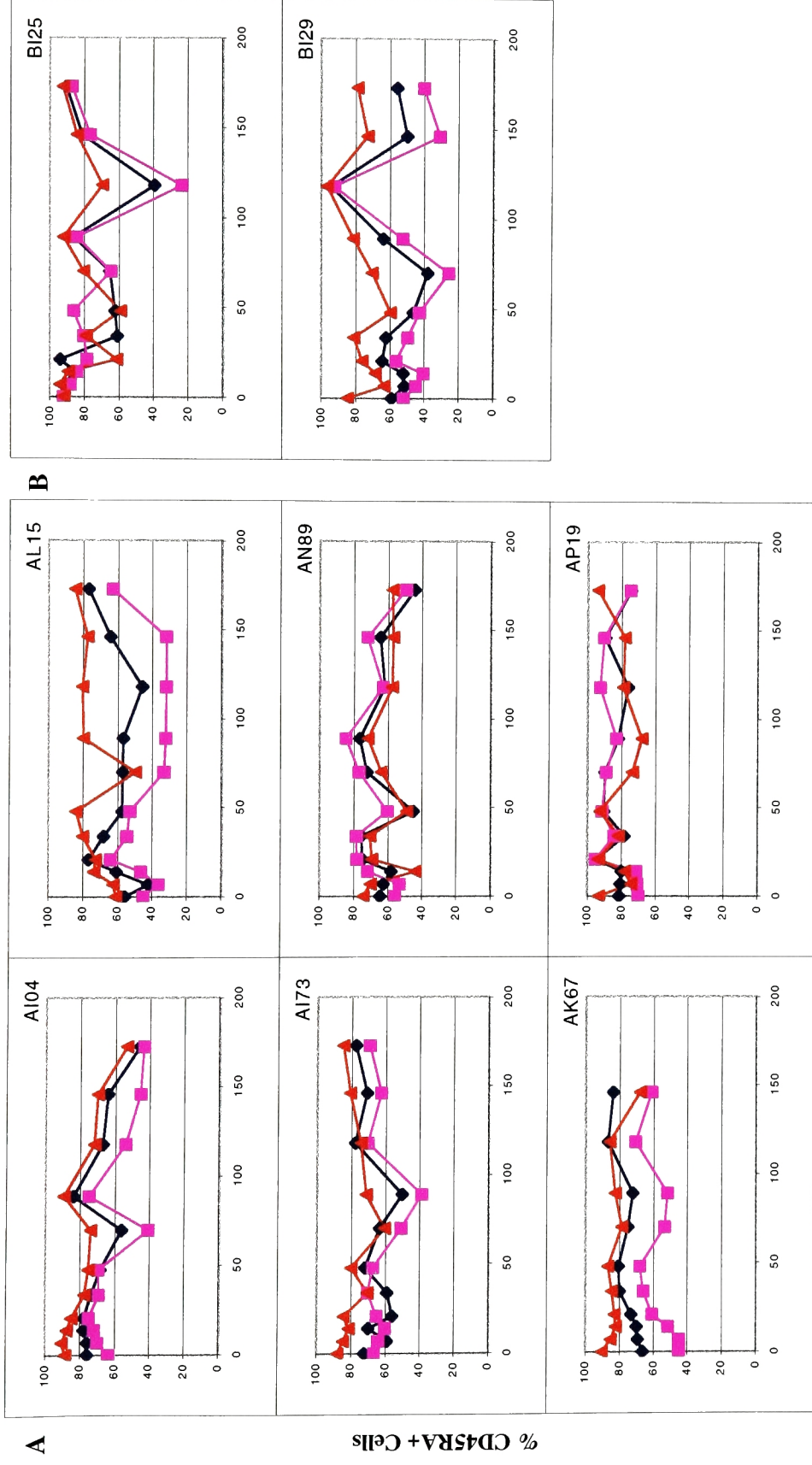
As the percentage of naïve cells was relatively stable throughout this period, the absolute CD45RA⁺ cell counts in each T cell subset was reflective of the changes in absolute CD3⁺, CD4⁺, and CD8⁺ populations (Figs. 23a, 23b). In all of the infected animals of the thymectomy group, there was a decline of naïve CD4⁺ T cells that was not significantly steeper than before infection ($p=0.0782$ (Table 9)). In the infected sham animals, there was no significant difference in the decay of naïve CD4⁺ T cells ($p= 0.5218$). There was no significant difference between the naïve CD4 decay between infected thymectomy and infected sham animals ($p= 0.3367$ (Table 10)). There was no change in the uninfected macaques during this period (Figs. 23aB, 23bB, Table 9).

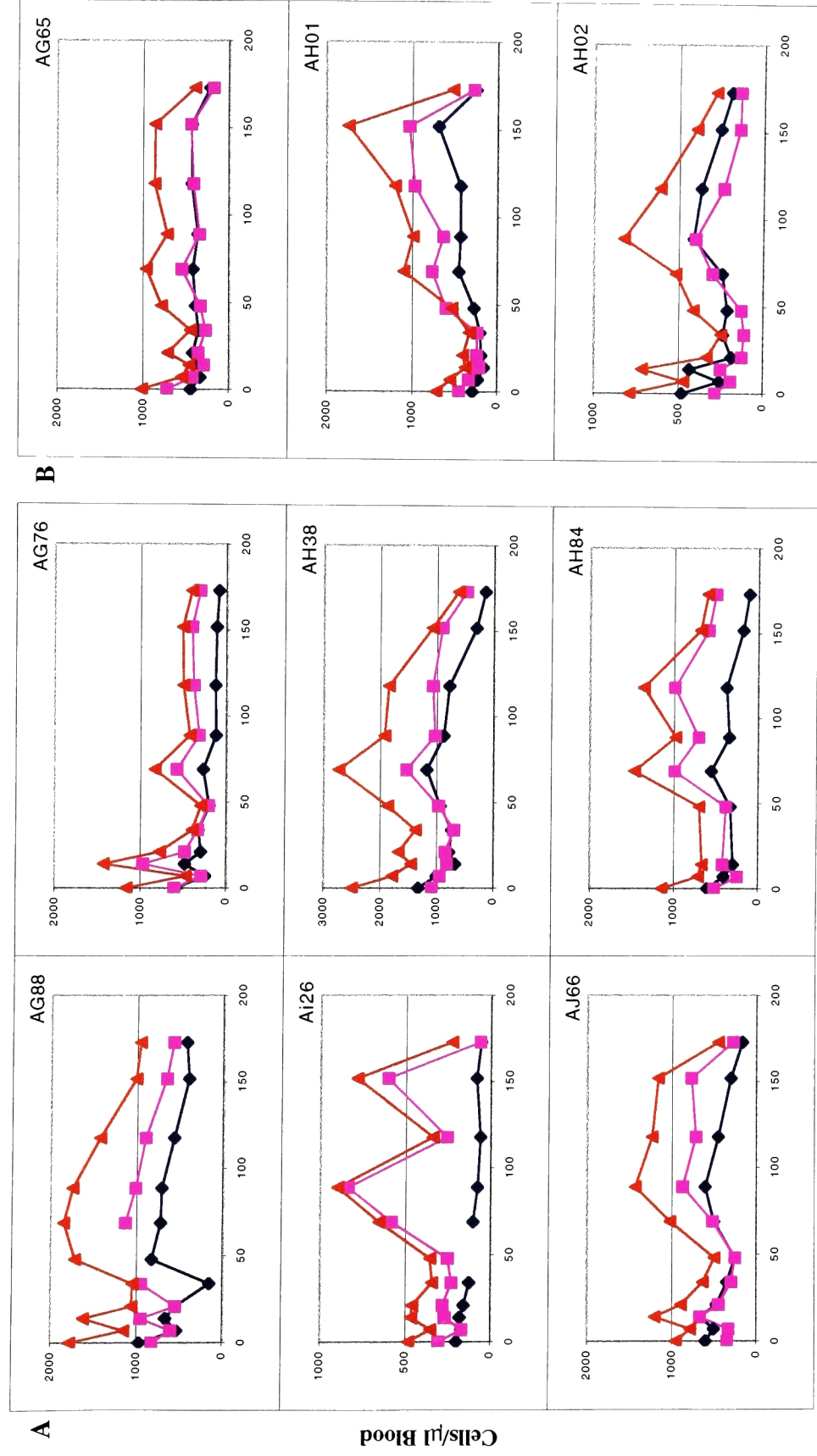
The overall absolute number of naïve CD8⁺ T cells was also stable during the period after infection. There was no significant decay as compared to the preinfection values in both the thymectomy and sham groups ($p= 0.1495$ for thymectomy, 0.2623 for sham (Table 9)). Neither was there any difference between the infected animals of the two groups ($p >0.9999$ (Table 10)). There was no change in the uninfected macaques during this period (Figs. 23aB, 23bB, Table 9).



Time Post Inoculation (days)

Figure 22a. % of CD45RA⁺ cells among CD3⁺, CD3⁺CD4⁺, and CD3⁺CD8⁺ T cells post infection: thymectomized macaques. A. Infected macaques. B. Uninfected controls. Red triangles represent CD3⁺ cells, blue diamonds represent CD3⁺CD4⁺ cells, and purple squares represent CD3⁺CD8⁺ cells.

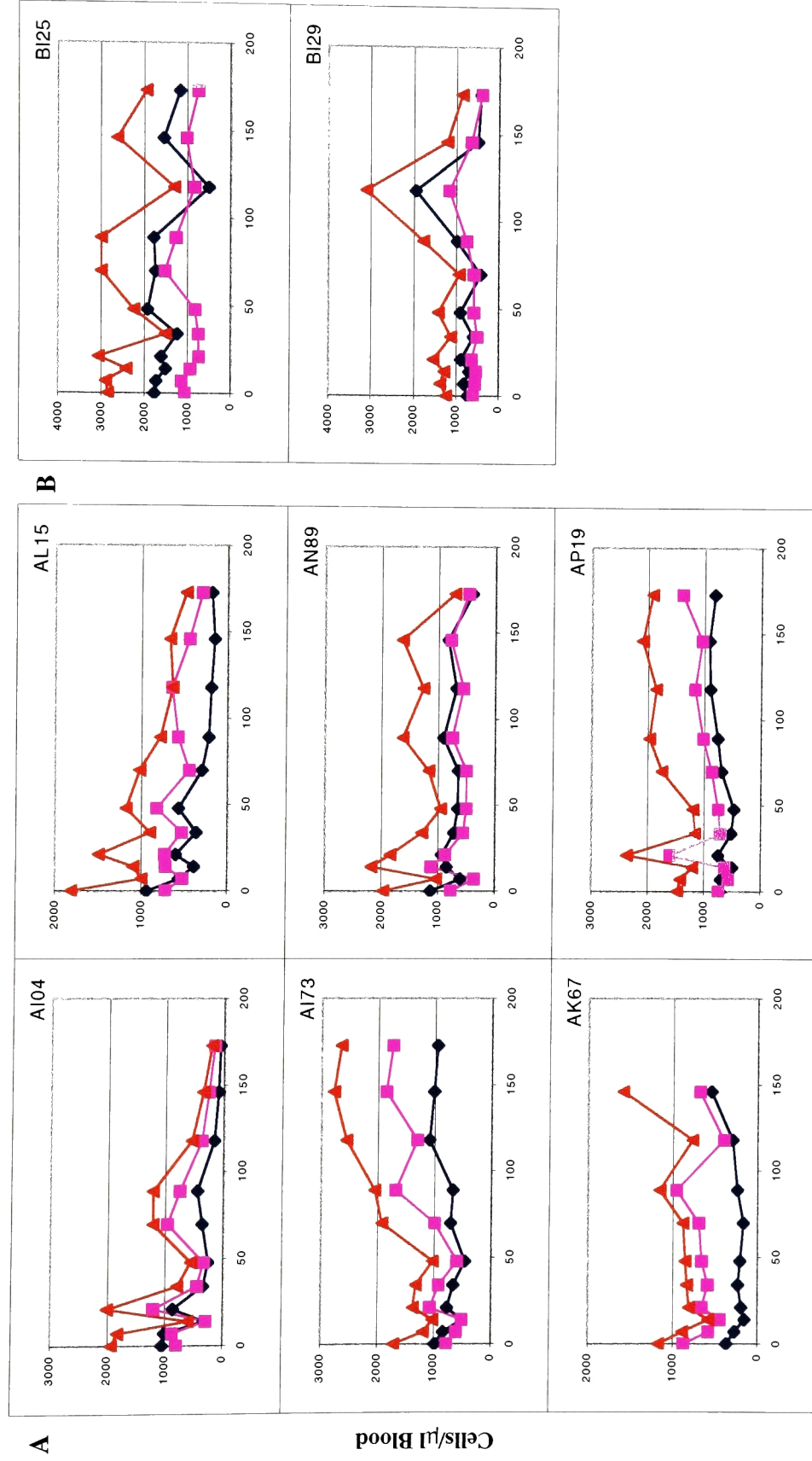




Time Post Inoculation (days)

Figure 23a. Absolute naïve CD3, CD4, and CD8 counts post thymectomy: thymectomized macaques.

A. Infected macaques. B. Uninfected controls. Red triangles represent CD3⁺CD45RA⁺ cells, blue diamonds represent CD3⁺CD4⁺CD45RA⁺ cells, and purple squares represent CD3⁺CD8⁺CD45RA⁺ cells.



Time Post Inoculation (days)

Figure 23b. Absolute naïve CD3, CD4, and CD8 counts post thymectomy: sham macaques.

A. Infected macaques. B. Uninfected controls. Red triangles represent CD3⁺CD45RA⁺ cells, blue diamonds represent CD3⁺CD4⁺CD45RA⁺ cells, and purple squares represent CD3⁺CD8⁺CD45RA⁺ cells.

Table 9. Absolute Naïve T cell decay slopes, pre vs. post infection

CD3⁺CD45RA⁺		Average Slope (Day⁻¹)		p value
		preinfection	postinfection	
Infected	Thymectomized	-0.0013	-0.0001	0.2623
	Sham	-0.0008	0.0000	0.5218
Uninfected	Thymectomized	-0.0013	0.0039	0.0495
	Sham	-0.0009	-0.0006	0.4386

CD4⁺CD45RA⁺		Average Slope (Day⁻¹)		p value
		preinfection	postinfection	
Infected	Thymectomized	-0.0004	-0.0043	0.0782
	Sham	-0.0008	-0.0021	0.5218
Uninfected	Thymectomized	-0.0007	0.0030	0.1266
	Sham	-0.0010	-0.0019	>.9999

CD8⁺CD45RA⁺		Average Slope (Day⁻¹)		p value
		preinfection	postinfection	
Infected	Thymectomized	-0.0012	0.0013	0.1495
	Sham	-0.0007	0.0011	0.2623
Uninfected	Thymectomized	-0.0010	0.0035	0.1266
	Sham	-0.0008	0.0004	0.1213

Table 10. Absolute Naïve T cell decay slopes post infection, thymectomy vs. sham

		Slope (Day ⁻¹)		
		CD3 ⁺ CD45RA ⁺	CD4 ⁺ CD45RA ⁺	CD8 ⁺ CD45RA ⁺
Thymectomized	AG88	-0.0012	-0.0005	-0.0007
	AI25	0.0001	-0.0069	-0.0016
	AJ66	0.0030	-0.0017	0.0052
	AG76	-0.0017	-0.0071	-0.0004
	AH38	-0.0006	-0.0035	0.0012
	AH84	-0.0001	-0.0062	0.0040
	Average	-0.0001	-0.0043	0.0013
Sham	AI04	-0.0071	-0.0120	-0.0046
	AI73	0.0060	0.0021	0.0069
	AK67	0.0012	0.0011	0.0004
	AL15	-0.0035	-0.0082	-0.0010
	AN89	0.0007	0.0007	0.0016
	AP19	0.0029	0.0038	0.0034
	Average	-0.0001	-0.0022	0.0010
p value		0.6310	0.3367	>.9999

5.3.6 Effect of Infection on T Cell Proliferation Figure 24 shows the effect of SIV infection on the percentages of Ki67⁺ cells in the CD3⁺CD4⁺ and CD3⁺CD8⁺ populations. In the infected macaques of the thymectomy group, the percentage of Ki67⁺ CD3⁺CD4⁺ T cells remained in the normal range, below 10%, until 16 weeks post infection, at which point the percentage of proliferating CD4⁺T cells began to increase, reaching a mean of 9.3% by week 24 post infection. Infected macaques of the sham group also showed a slight increase in the percentage of Ki67⁺ CD3⁺CD4⁺ T cells, but with few exceptions the values remained below 10%, reaching a mean of 3.9% at week 24 post infection. Uninfected macaques of both groups remained below 10% at all time points, with a few outlying points(192, 193).

In contrast, there was an immediate increase in the percentages of proliferating CD8⁺ T cells by week 2 post infection, reaching a mean of 24.9% in thymectomized animals and 20% in sham animals. This increase, no doubt due to antigen-stimulated proliferation of CD8⁺ T cells, was followed by a decline in the percentage of Ki67⁺ CD3⁺CD8⁺ T cells. Towards the later weeks of infection there was a second wave of increased Ki67⁺ CD3⁺CD8⁺ T cells, reaching a mean of 18.2% in the thymectomy group by week 24. The sham group did not have this second wave of increase, and the mean was 6.4% by week 24. Uninfected macaques of both groups remained in the normal range, below 10% at almost all time points.

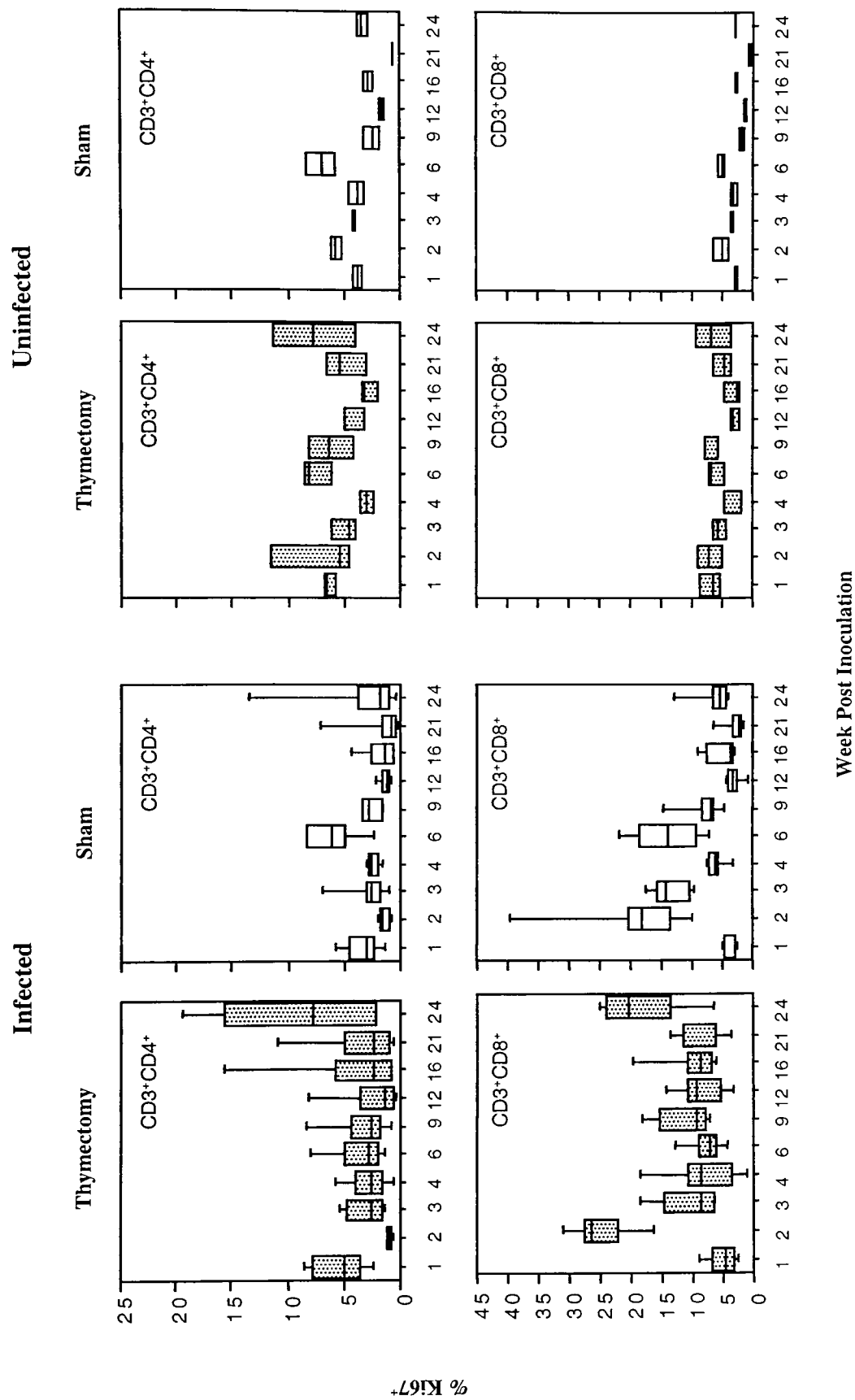


Figure 24. % Ki67⁺ CD3⁺CD4⁺ and CD3⁺CD8⁺ T cells post infection. Shaded boxes indicate thymectomized animals, open boxes represent sham animals.

5.3.7 α 1 TREC Decay Following Infection Figure 25, 26, and 27 show the changes in α 1 TREC in the PBMC, CD4, and CD8 T cells, respectively, during this study. (For detailed plots of individual animals, see Appendix 2). The α 1 TREC decay following thymectomy is shown in A and D, and the changes following infection are shown in B and E. Uninfected controls are represented in C and D.

Infection significantly increased the decay of α 1 TREC in PBMC in both the thymectomy and the sham groups ($p= 0.0250$ for both groups by Mann-Whitney U test) (Fig. 25B, 25E, Table 11). Uninfected control animals had α 1 TREC decay slopes comparable to those in the period before infection (Fig. 25C, 25F, Table 11).

In the sorted CD4 population, α 1 TREC decay increased after infection in both the thymectomy and sham groups ($p= .0062$ for thymectomy, 0.0374 for sham) (Fig. 26B, 26E, Table 11). In the sorted CD8 population, α 1 TREC decay increased after infection in both the thymectomy and sham groups, but surprisingly, only the sham group had a significant difference from the preinfection slope ($p= 0.2012$ for thymectomy, 0.0104 for sham) (Fig. 27B, 27E, Table 11).

The average slopes presented in Table 11 reveal that the thymectomized animals had a faster decline of α 1 TREC than sham animals after infection. However, to compare the α 1 TREC decay between the infected thymectomized and infected sham animals, it was necessary to adjust the slopes for the preexisting impairment resulting from thymectomy. This was done by subtracting the preinfection slope from the postinfection slope for each individual. Adjusted slopes, presented in Table 12, reveal no significant difference in the slope of α 1 TREC decay between thymectomized and sham animals ($p= 0.7488$ for CD3, 0.0679 for CD4, and 0.2733 for CD8). This indicates that infection had comparable impact on the α 1 TREC decay in thymectomized and euthymic animals, and that any difference observed was due to the preexisting impairment caused by thymectomy.

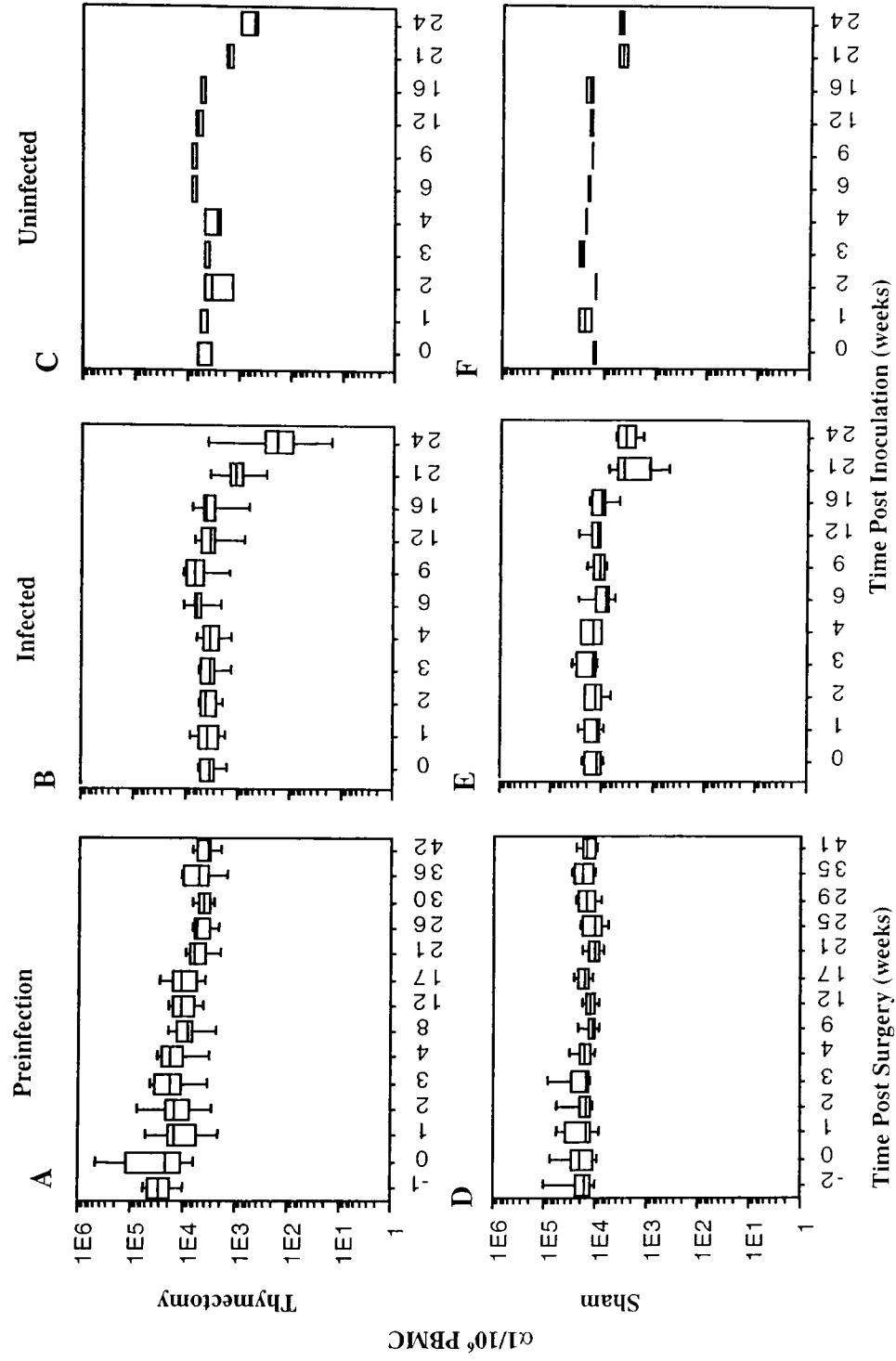


Figure 25. $\alpha 1$ TREC decay in PBMC following thymectomy and infection.
A, B, C: Thymectomized macaques. D, E, F: Sham controls. A and D represent changes following surgery, B and E represent changes following infection, C and F represent changes in uninfected macaques.

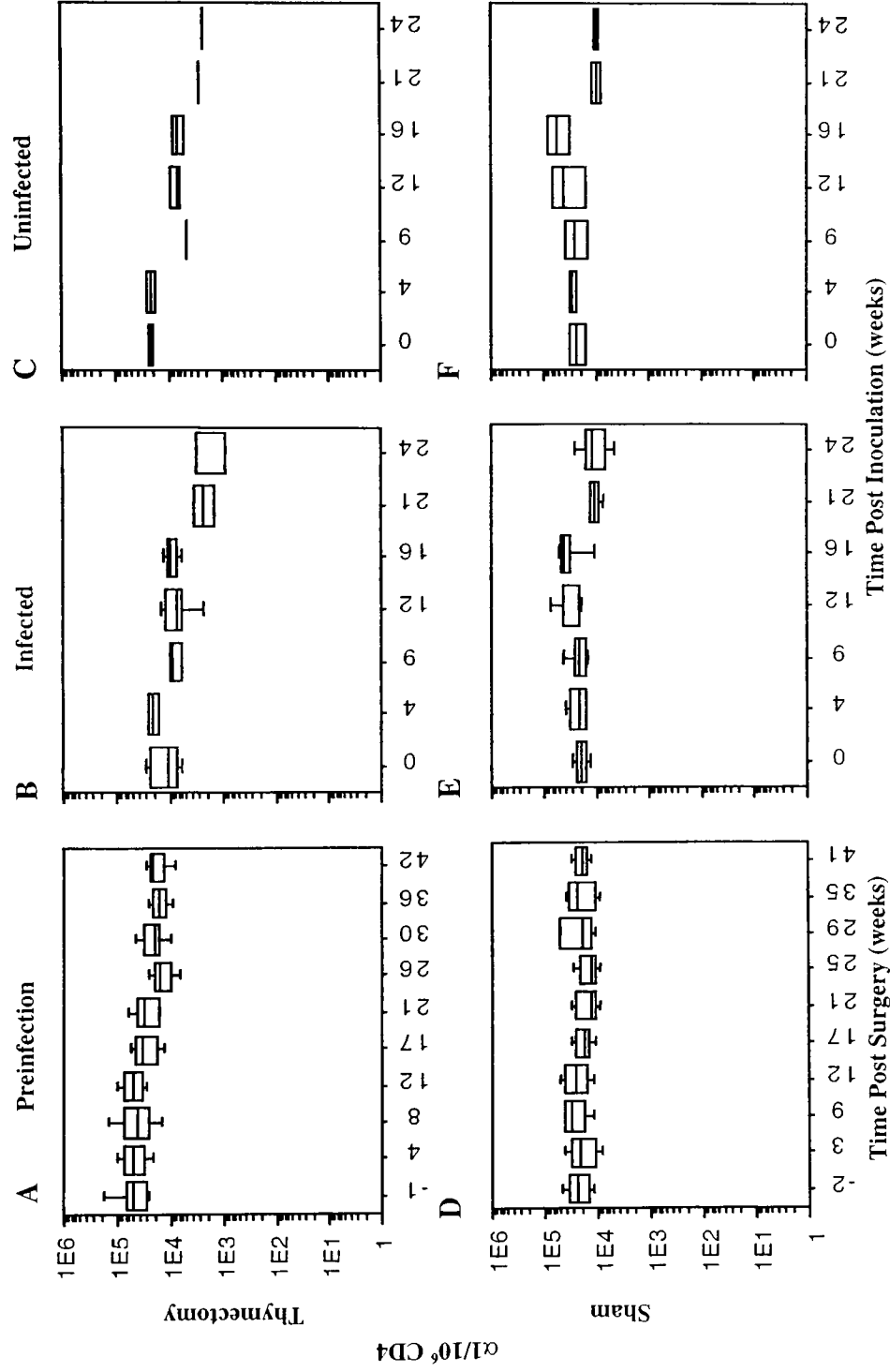


Figure 26. $\alpha 1$ TREC decay in CD4 following thymectomy and infection.
 A, B, C: Thymectomized macaques. D, E, F: Sham controls. A and D represent changes following surgery, B and E represent changes following infection, C and F represent changes in uninfected macaques.

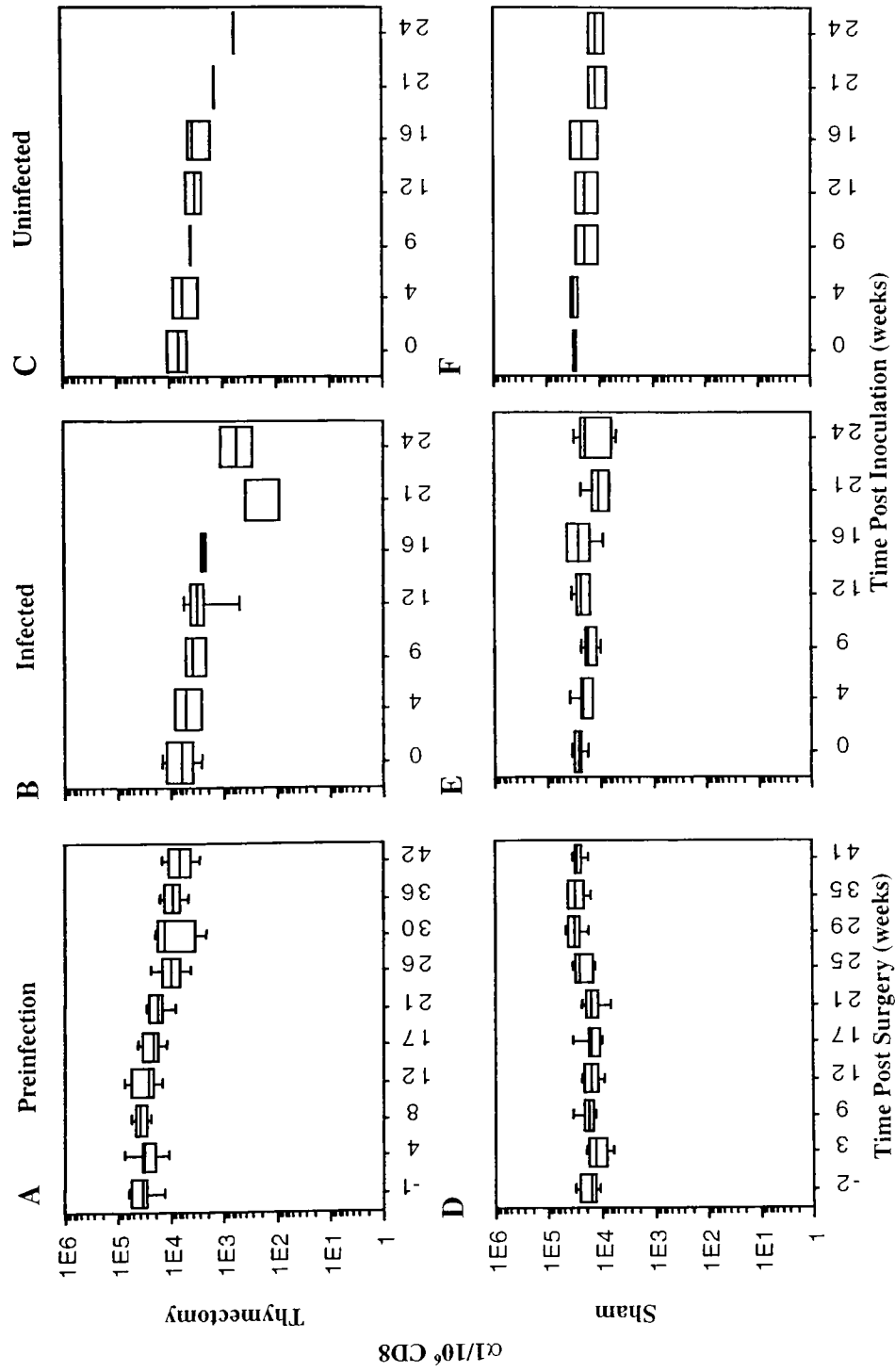


Figure 27. $\alpha 1$ TREC decay in CD8 following thymectomy and infection.
 A, B, C: Thymectomized macaques. D, E, F: Sham controls. A and D represent changes following surgery, B and E represent changes following infection, C and F represent changes in uninfected macaques.

Table 11. $\alpha 1$ TREC decay slopes, pre vs. post infection

PBMC		Average Slope (Day⁻¹)		p value
		preinfection	postinfection	
Infected	Thymectomized	-0.0046	-0.0142	0.0250
	Sham	-0.0019	-0.0096	0.0250
Uninfected	Thymectomized	-0.0069	-0.0077	0.0827
	Sham	0.0008	-0.0092	0.1213

CD4		Average Slope (Day⁻¹)		p value
		preinfection	postinfection	
Infected	Thymectomized	-0.0041	-0.0156	0.0062
	Sham	-0.0007	-0.0062	0.0374
Uninfected	Thymectomized	-0.0056	-0.0122	0.2752
	Sham	0.0000	-0.0078	0.1213

CD8		Average Slope (Day⁻¹)		p value
		preinfection	postinfection	
Infected	Thymectomized	-0.0055	-0.0179	0.2012
	Sham	0.0022	-0.0036	0.0104
Uninfected	Thymectomized	-0.0084	-0.0103	0.5127
	Sham	0.0033	-0.0065	0.1213

Table 12. Adjusted α 1 TREC decay slopes post infection

		Adjusted Slope (Day-1)		
		PBMC	CD4	CD8
Thymectomized	AG88	-0.0017	-0.0265	-0.0158
	AI25	-0.0178	-0.0041	0.0052
	AJ66	-0.0128	-0.0102	-0.0339
	AG76	-0.0056		
	AH38	-0.0081	-0.0081	-0.0155
	AH84	-0.0114	-0.0120	-0.0036
	Average	-0.0096	-0.0122	-0.0127
Sham	AI04	-0.0069	-0.0093	-0.0041
	AI73	-0.0064	-0.0012	-0.0026
	AK67	0.0022	-0.0031	-0.0023
	AL15	-0.0143	-0.0075	-0.0030
	AN89	-0.0147	-0.0073	-0.0126
	AP19	-0.0060	-0.0043	-0.0101
	Average	-0.0077	-0.0054	-0.0058
p value		0.7488	0.0679	0.2733

5.4 Tissues

5.4.1 Distribution of $\alpha 1$ TREC in Lymphoid Tissues Post Thymectomy, Before Infection Eight months after the surgery, four thymectomized and two sham macaques underwent tissue biopsy of multiple sites reported to be possible extrathymic sources of T cells (Fig. 28). The profile in the two control macaques was similar to that of the two normal juveniles presented in Figure 8, with an average $\alpha 1$ TREC concentration of 1.6% in PBMC, 2.2% of colonic lymph node, 0.8% of liver, and less than 0.6% of intestinal lymphocytes.

While overall $\alpha 1$ TREC concentrations were roughly twofold lower in the thymectomized macaques, the relative pattern was the same. The average $\alpha 1$ TREC concentration was 0.7% of PBMC, 1% of colonic lymph node, 0.3% of liver, and less than 0.15% of intestinal lymphocytes. This suggests that the decrease in $\alpha 1$ TREC in the peripheral blood of thymectomized macaques is reflected in an overall decrease in lymphoid tissues, and that none of the tissues surveyed displayed a compensatory increase in $\alpha 1$ TREC as would be expected in an alternate source.

5.4.2 Impact of SIV Infection on $\alpha 1$ TREC in the Lymph Nodes To assess the impact of SIV infection on the concentration of $\alpha 1$ TREC bearing cells in the lymph nodes, biopsies were taken two and nine weeks post inoculation. These data are presented in Figure 29, along with preinfection biopsy data and necropsy data from those animals that have expired.

At the time of inoculation, thymectomized animals had a lower concentration of $\alpha 1$ TREC bearing cells in the lymph nodes than sham controls. After infection, both thymectomized and sham macaques had a similar decrease in $\alpha 1$ TREC concentration in the lymph nodes. By nine weeks post inoculation, the average $\alpha 1$ TREC concentration in lymph nodes dropped almost one log, from $1.1 \times 10^4/10^6$ lymphocytes at the preinfection time point to $2.7 \times 10^3/10^6$ lymphocytes. The sham controls also dropped from $2.4 \times 10^4/10^6$ to $1.4 \times 10^4/10^6$ lymphocytes.

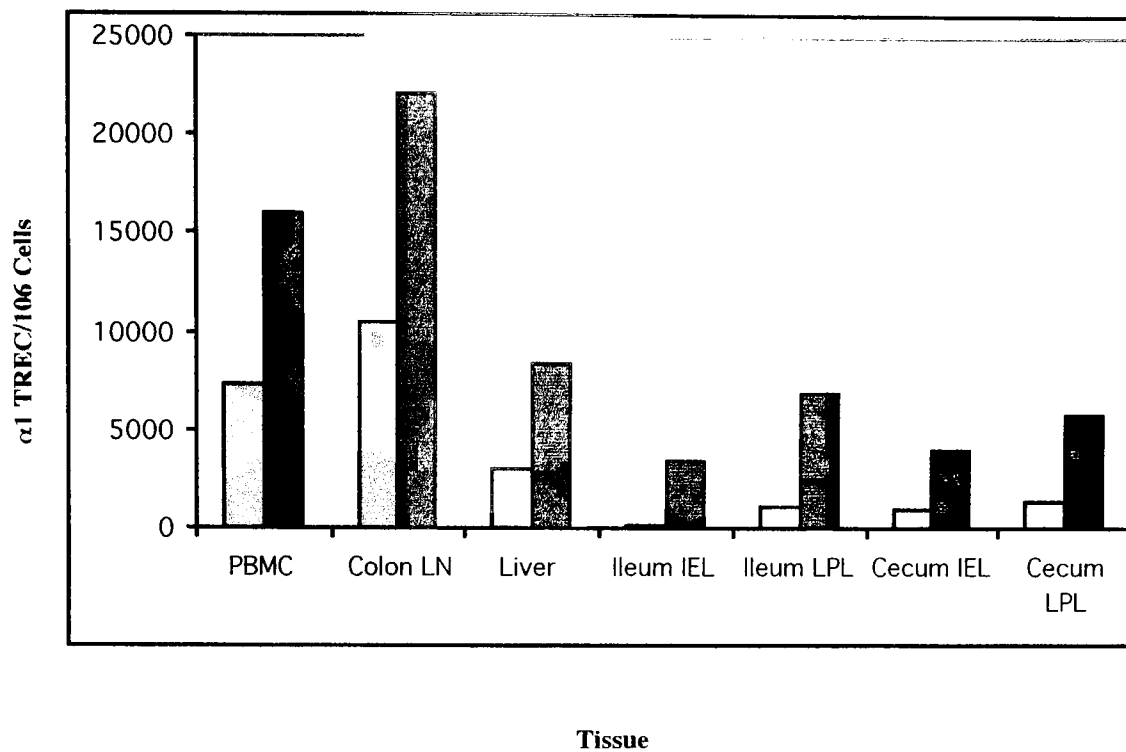


Figure 28. Tissue distribution of $\alpha 1$ TREC eight months post thymectomy. Light shaded columns indicate thymectomized macaques (n=4), dark columns indicate sham macaques (n=2).

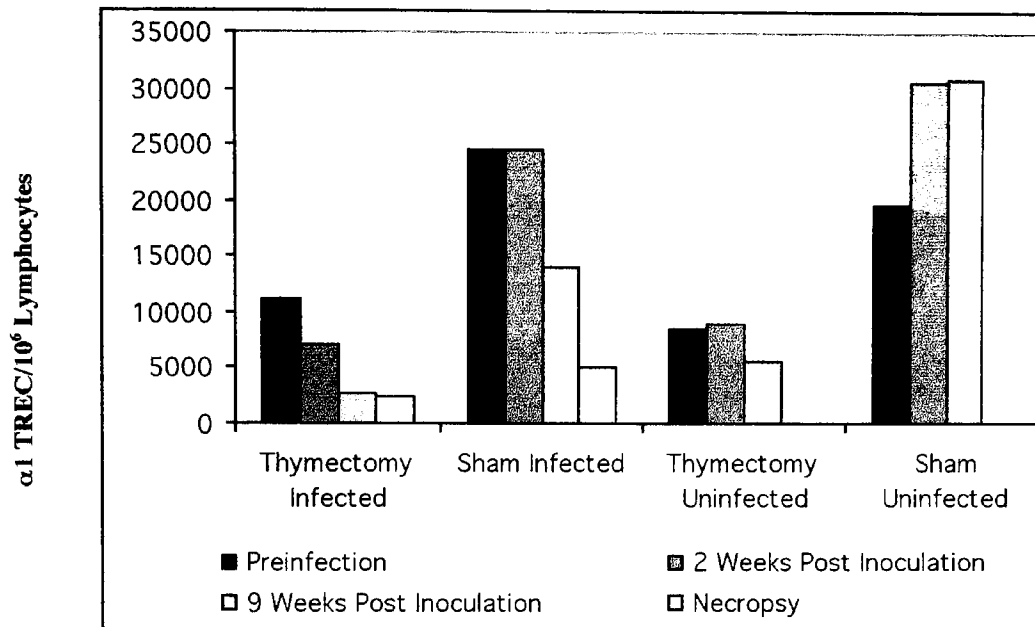


Figure 29. α1 TREC in Lymph Nodes Pre and Post Infection. Each bar represents the average of single biopsies from one or more animals. Necropsies include multiple lymph nodes from each animal. All animals involved in the study were biopsied at 2 and 9 weeks post inoculation (n=2-6 for various groups). Preinfection biopsies n=1-3, necropsy n=2-4.

The uninfected animals in both the thymectomy and sham group did not have the same dramatic decline in lymph node α1 TREC. The uninfected animals of the thymectomy group had a slight drop from $8.4 \times 10^3/10^6$ at the preinoculation time point to $5.5 \times 10^3/10^6$ at the nine-week point. In contrast, the uninfected animals of the sham group had an increase in lymph node α1 TREC from $1.9 \times 10^4/10^6$ to $3 \times 10^4/10^6$ during this time period.

5.4.3 Tissue Distribution of α1 TREC at Necropsy By six months post infection, four thymectomized and two sham macaques had expired from simian AIDS. α1 TREC concentrations in the tissues of these macaques are presented in Figure 30. Thymectomized macaques had lower concentrations of α1 TREC than sham controls in every tissue, but both groups had significantly lower concentrations than normal. The

average $\alpha 1$ TREC concentration in the lymph nodes was $2.5 \times 10^3/10^6$ in thymectomized animals, $5.7 \times 10^3/10^6$ in sham animals.

The most striking difference between the thymectomized and sham animals was in the spleen, where the $\alpha 1$ TREC concentration in sham animals was $1.8 \times 10^4/10^6$ cells, nearly two logs higher than the concentration in thymectomized animals, $6.2 \times 10^2/10^6$. Values obtained from the sham animals are very close to the value obtained from one uninfected macaque spleen, $1.28 \times 10^4/10^6$ cells (data not shown).

By the time of death, $\alpha 1$ TREC bearing intestinal lymphocytes were virtually undetectable in both groups, probably reflective of an overall loss of lymphocytes in the gut.

Thymic tissue was obtained from one sham macaque at necropsy. The concentration of $\alpha 1$ TREC in the thymus was $3.33 \times 10^4/10^6$ thymocytes, threefold lower than the average normal concentration of $9.1 \times 10^4/10^6$. This was reflected in the disruption of the architecture of the thymus of the same macaque (Fig. 31). Thymic tissue displayed severe atrophy, infiltration of fat, and cortical thinning with small islands of thymocytes.

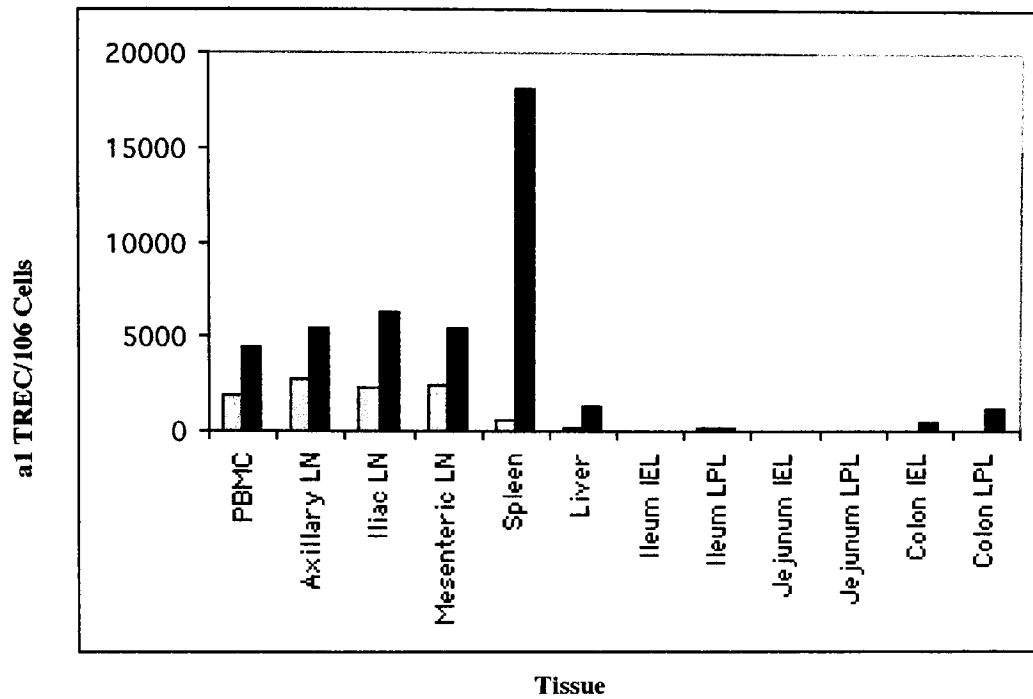


Figure 30. Tissue distribution of $\alpha 1$ TREC at necropsy. Light shaded columns indicate thymectomized macaques (n=4, n=2 for intestinal lymphocytes), dark columns indicate sham macaques (n=2)

5.4.4 $\alpha 1$ TREC in the Tissues: Summary Table 13 shows a summary of $\alpha 1$ TREC concentrations in the tissues expressed as the percentage of $\alpha 1$ TREC bearing cells. Overall, these studies indicate that thymectomy results in a decrease of $\alpha 1$ TREC in the lymphoid tissues. This decrease reflects that seen in the peripheral blood of thymectomized macaques, indicating that there may be circulation of $\alpha 1$ TREC bearing cells, rather than compartmentalization in sites protected from the effects of thymectomy. SIV infection also causes a decrease in the $\alpha 1$ TREC bearing cells in the lymphoid tissues of both thymectomized and sham macaques.

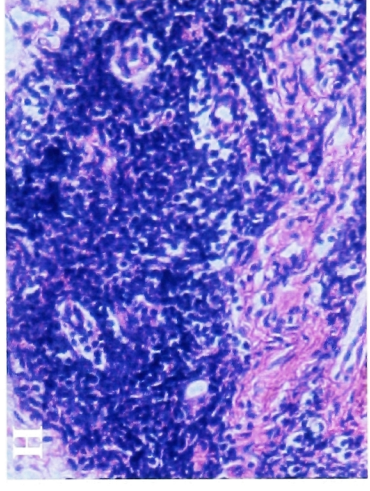
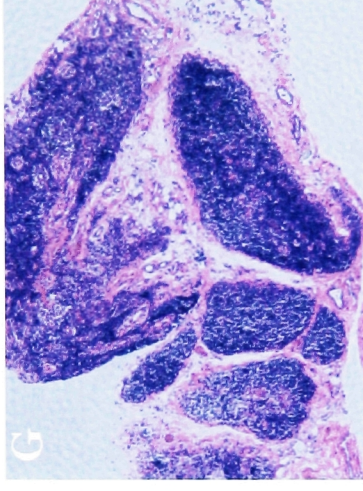
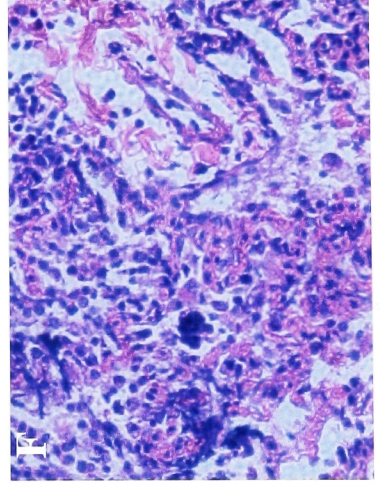
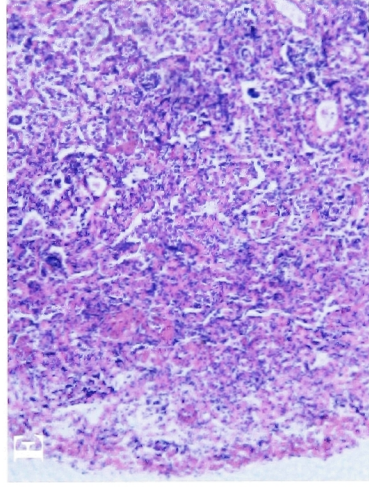
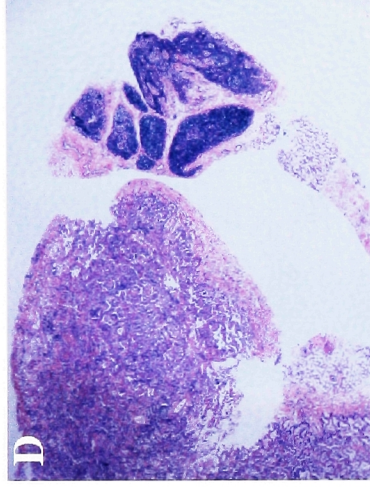
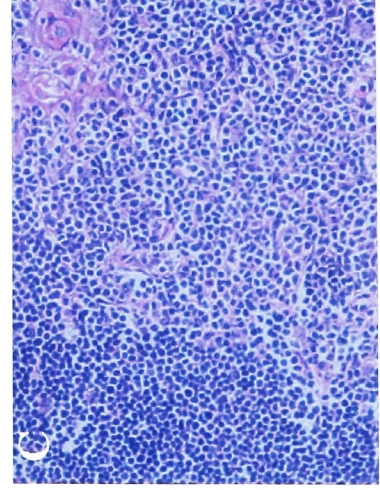
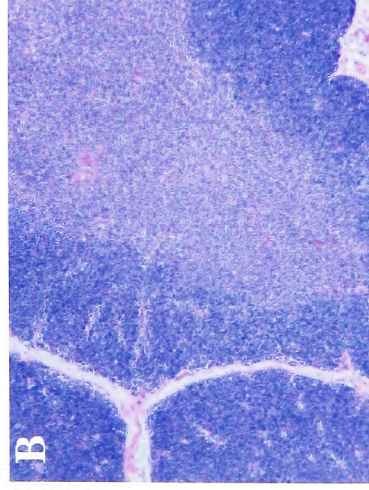
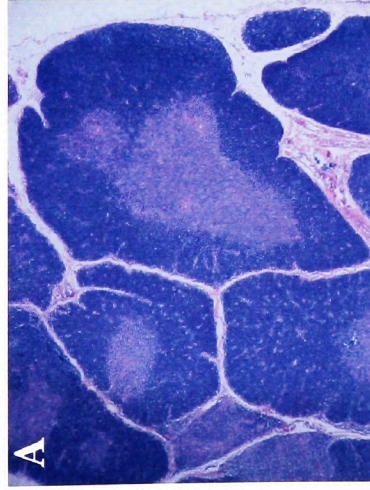


Figure 31. Thymic Histopathology of SIV, hematoxylin and eosin stain.

A-C. Normal thymus, with dense cortex and lighter medulla. C shows corticomedullary junction with Hassall's corpuscle. D-H. SIV-infected thymus with disrupted architecture and thinning of the cortex. F shows loss of cellularity and infiltration of fat. A and D, 40x. B, E, and G, 100x. C, F, and H, 400x.

Table 13. Percentage of $\alpha 1$ TREC-bearing cells in lymphoid tissues

Normal Macaques							
Tissue		Average	Range				
PBMC	n=85	1.98	0.02	to 28.00			
Thymus	n=10	9.10	5.50	to 20.14			
Lymph Node	n=2	2.85	1.20	to 4.54			
Ileum IEL		0.28	0.22	to 0.35			
Ileum LPL		0.51	0.44	to 0.59			
Jejeunum IEL		0.12	0.09	to 0.14			
Jejeunum LPL		0.28	0.12	to 0.44			
Colon IEL		0.30	0.25	to 0.35			
Colon LPL		0.29	0.18	to 0.40			
Post Surgery							
Thymectomy				Sham			
Tissue		Average	Range			Average	Range
PBMC	n=4	0.73	0.33	to 1.05	n=2	1.61	1.41 to 1.81
Lymph Node		1.05	0.84	to 1.36		2.21	1.96 to 2.45
Liver		0.30	0.00	to 0.63		0.84	0.27 to 1.41
Ileum IEL		0.02	0.00	to 0.08		0.35	0.20 to 0.49
Ileum LPL		0.11	0.05	to 0.17		0.69	0.30 to 1.07
Cecum IEL		0.10	0.00	to 0.40		0.40	0.38 to 0.41
Cecum LPL		0.14	0.00	to 0.29		0.58	0.29 to 0.87
Necropsy							
Thymectomy				Sham			
Tissue		Average	Range			Average	Range
PBMC	n=4	0.19	0.01	to 0.41	n=2	0.45	0.38 to 0.52
Lymph Node		0.25	0.10	to 0.42		0.57	0.17 to 0.92
Spleen		0.06	0.00	to 0.13		1.81	0.50 to 3.13
Liver		0.01	0.00	to 0.04		0.12	0.02 to 0.23
Ileum IEL	n=2	0.00				0.00	
Ileum LPL		0.01	0.00	to 0.01		0.02	0.00 to 0.03
Jejunum IEL		0.00				0.00	
Jejunum LPL		0.00				0.00	
Colon IEL		0.00				0.05	0.00 to 0.09
Colon LPL		0.00				0.12	0.01 to 0.22
Thymus					n=1	3.33	

5.5 TCR β CDR3 Profile The quantity of peripheral T cells did not decrease appreciably following thymectomy. However, these data do not yield any information about the quality of the immune panel after surgery. Therefore, we used TCR β CDR3 length polymorphism as an indicator of the diversity of the TCR repertoire among the PBMC of representative thymectomized and sham animals.

Twenty-five V β families were studied, and Fig. 32 shows the qualitative changes in one representative V β family from each of four macaques over the course of this study. The four animals chosen were AI25, thymectomized and infected, AH02, thymectomized and uninfected, AP19, sham and infected, and BI25, sham and uninfected.

The top panels indicate the profile at baseline, the middle panels indicate the profiles eight months post surgery, and the bottom panels indicate the profiles three months post infection. For the two animals that were not infected, AH02 and BI25, the three month post inoculation time point represents thirteen months post surgery.

Genescan software was used to define the number of species in each V β family at each time point, and these data are summarized in Table 14.

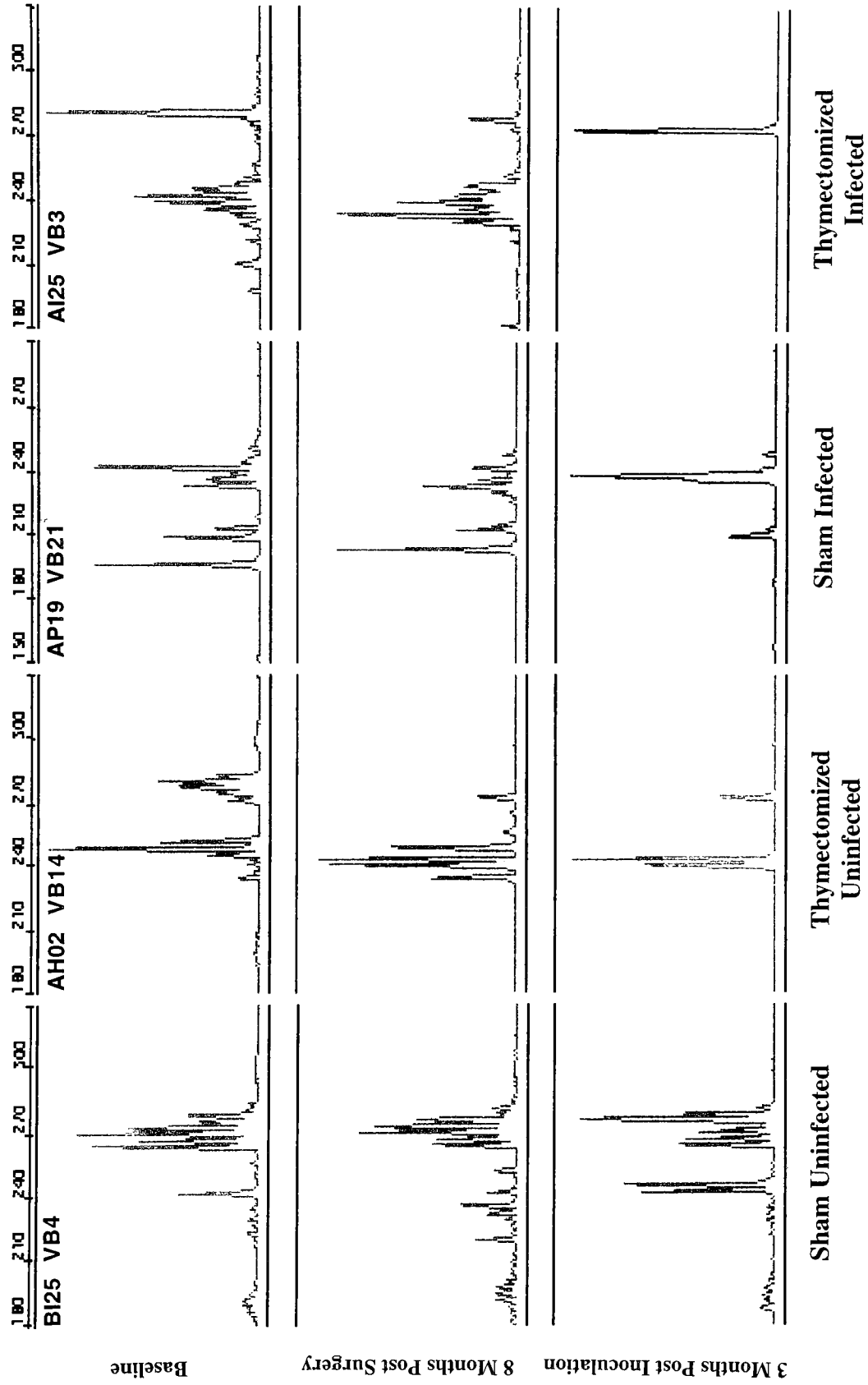


Figure 32. TCR Vβ length polymorphism profiles

Table 14. Number of species in each V β family

**Thymectomized Infected
AI25**

1	2	3	4	5	6	7	8	9	10	11	12	13.1	13.2	14	15	16	17	18	19	20	21	22	23	24	SUM
14	17	19	29	23	20	11	17	10	12	10	11	11	9	13	16	20	11	14	30	21	10	11	16	27	402
21	18	19	28	30	22	10	10	18	12	13	20	9	20	12	24	24	25	15	32	19	17	16	27	42	503
4	4	4	9	10	7	5	2	1	4	3	1	2	1	1	1	5	4	10	8	8	3	13	0	1	111

**Baseline
8 Months Post Thymectomy
3 Months Post Infection**

**Thymectomized Uninfected
AH02**

1	2	3	4	5	6	7	8	9	10	11	12	13.1	13.2	14	15	16	17	18	19	20	21	22	23	24	SUM
13	6	16	13	23	4	15	12	12	7	11	8	11	10	14	10	22	7	28	23	12	8	24	7	6	322
23	17	3	12	20	12	9	8	22	11	2	8	6	7	7	10	17	6	7	11	21	10	8	13	5	275
0	10	3	5	10	3	2	3	4	0	2	4	4	2	6	1	6	10	2	6	16	5	9	9	7	129

**Baseline
8 Months Post Thymectomy
13 Months Post Thymectomy**

**Sham Infected
AP19**

1	2	3	4	5	6	7	8	9	10	11	12	13.1	13.2	14	15	16	17	18	19	20	21	22	23	24	SUM
10	17	12	11	20	16	9	14	11	16	0	8	3	4	12	9	15	13	12	10	26	18	13	13	6	298
13	11	6	8	17	18	9	7	14	8	2	1	8	2	6	7	12	7	3	6	20	13	6	10	10	224
14	8	8	7	11	13	19	6	6	0	0	3	6	8	7	5	8	5	4	1	10	7	5	3	7	171

**Baseline
8 Months Post Thymectomy
3 Months Post Infection**

**Sham Uninfected
BI25**

1	2	3	4	5	6	7	8	9	10	11	12	13.1	13.2	14	15	16	17	18	19	20	21	22	23	24	SUM
12	19	13	14	26	13	14	18	24	24	9	13	12	13	16	16	17	20	11	22	18	17	8	21	15	405
13	18	19	15	20	18	25	18	26	15	18	20	16	10	13	19	20	20	16	19	31	23	33	26	11	482
18	22	9	13	13	16	16	12	18	10	9	18	20	12	16	13	12	9	36	17	21	13	16	15	14	388

**Baseline
8 Months Post Thymectomy
13 Months Post Thymectomy**

5.5.1 Thymectomy Results in Restriction of the TCR Repertoire Eight months post thymectomy, the V β profiles in both thymectomized and sham animals were virtually unchanged. Minor shifts in the relative frequencies of species within each family were observed in all animals, but the overall profile was of a broad, sustained polyclonal population with myriad species in all of the 25 V β families assayed (Fig. 32).

However, by thirteen months post thymectomy, there was evidence of restriction in the immune panel in the uninfected thymectomized macaque AH02. While the sham control BI25 remained stable throughout this time period, AH02 showed evidence of oligoclonality within many, though not all, of the V β families.

This observation is confirmed by comparing the number of species within each V β family (Table 14). Eight months post surgery, neither the number of species within each family nor the sum of species changed appreciably in the thymectomized animals AI25 and AH02. However, thirteen months post thymectomy, the number of species within many families of animal AH02 have decreased, and the sum of species is 40% of the sum at baseline. The sham control BI25 showed no evidence of restriction during the thirteen month time period, ruling out age-related restriction as an explanation for this phenomenon.

5.5.2 Infection Results in Dramatic Restriction of the TCR Repertoire Three months post infection, both thymectomized animal AI25 and sham animal AP19 showed evidence of dramatic restriction of the TCR repertoire. Visually this is evidenced by a dramatic shift from multiple peaks, or species, within each V β family, to a single dominant species or a small number of species (Fig. 32). This is confirmed by the decrease in the number of species in each V β family, both in the thymectomized and the sham infected macaque (Table 14).

In the sham infected macaque, AP19, the sum of species after infection was less than 60% of that at baseline. This decrease, though remarkable, was nowhere near that observed in the thymectomized macaque AI25. After infection the sum of species in AI25 was 27% of that at baseline. This suggests that there is a combined effect of thymectomy over the long term and the deleterious effect of SIV infection on the TCR repertoire in this animal.

6. Discussion

6.1 Development of an Assay to Detect $\alpha 1$ T Cell Receptor Excisional Circles in the Rhesus Macaque The development of a PCR-based assay for the $\alpha 1$ TREC enables the examination of a population of cells that can be defined as recent thymic emigrants, where ‘recent’ refers to the number of cell divisions since leaving the site of recombination, rather than the time elapsed. This assay, used in conjunction with other methods of defining phenotypically naïve cells, allows a more refined examination of the effects of thymectomy than has previously been possible.

It has been reported that adult thymectomy is not associated with immunological deficit(30-32, 53). This is consistent with multiple lines of evidence that both thymic mass and thymic output decline with age. However, initial studies using $\alpha 1$ TREC as a marker for thymic output in humans revealed that the thymus functions well into old age(16, 17). This raised the question of the significance of postnatal thymic output and its role in T cell homeostasis.

While many studies on the role of the thymus in peripheral T cell homeostasis have been done on mice and sheep, the rhesus macaque model affords this study two benefits. The first is the evolutionary proximity of macaques to humans, and the second is the large body of work on infection of the rhesus macaque with SIV as a model for HIV-1 infection. We thus sought to confirm observations made in the clinical setting using $\alpha 1$ TREC as a marker for thymic output with a controlled animal study.

The rhesus macaque model has some limitations compared to the mouse model. Large numbers of animals cannot be enrolled in a rhesus study, which limits the n values and thus the power of comparisons between experimental groups. The absence of congenic strains of rhesus results in a high level of inter-animal variation in many parameters, including normal values of T cells and $\alpha 1$ TREC bearing cells as well as response to viral infection. Finally, there are restrictions on the amount of blood and tissue that can be obtained from rhesus macaques, limiting the scope of experiments that can be performed on the cohort.

The study of $\alpha 1$ TREC has many benefits over previous methods for the study of thymic output. It is the first direct measure of recent thymic emigrants in mammalian species, fulfilling an experimental need in the absence of a cell-surface phenotypic marker. The PCR-based assay can be performed on up to eighty-four samples in under six hours, making it an efficient means of assessing thymic output in a large-scale study such as this one. The assay is sensitive down to 10 copies, dynamic within a 6-log range, and accurate (10% coefficient of variance)(17). The episome is stable in the cell(194) and thus lends itself to long-term studies of recent thymic emigrants, in contrast to fluorescent dye studies which are limited by the half-life of the dye within the cell. Finally, the assay can be used on stored samples, allowing retrospective studies of thymic output in various disease states.

With these benefits also come drawbacks. The $\alpha 1$ TREC is known to occur in ~70% of the δ locus deletion recombination events in humans(169). While this means that the $\alpha 1$ TREC is a dominant species and readily measurable, an estimate of thymic output based on the $\alpha 1$ TREC is based on a fraction of the total recombination events and is thus an underestimate of the total T cell production. Next, a study of cells bearing the $\alpha 1$ TREC is limited to $\alpha\beta$ T cells. While these cells comprise the majority of cells released from the thymus, a study based on $\alpha 1$ TREC does not take into account processes involving $\gamma\delta$ T cells. Finally, real-time PCR with molecular beacon assays require access to expensive reagents and equipment that is not yet common to all research facilities.

An important consideration in the study of $\alpha 1$ TREC is the cell population examined. While initial studies in the field focused on PBMC as the denominator for fraction of $\alpha 1$ TREC bearing cells, it is more precise to examine $\alpha 1$ TREC bearing cells as a fraction of total T cells or CD4 and CD8 subsets. This would control for variations in the T cell to non-T cell ratio among PBMC, which may skew concentrations of $\alpha 1$ TREC bearing cells.

The need for an assay to detect recent thymic emigrants in the peripheral blood and tissues far outweighs the limitations of the $\alpha 1$ TREC as a marker for RTE. However, we must be cautioned against regarding $\alpha 1$ TREC as a broad marker for thymic function, and focus instead on the specific population of $\alpha\beta$ T cells being studied. Like other assay

systems, this assay carries more weight in conjunction with other studies of peripheral T cell processes such as flow cytometry and TCR V β CDR3 length polymorphism analysis.

6.2 α 1 TREC in the Normal Macaque Before beginning a study of the impact of thymectomy on the α 1 TREC population, it was necessary to understand the frequency and distribution of α 1 TREC in the normal macaque. We began by measuring α 1 TREC in the PBMC of 96 normal rhesus macaques, ranging in age from 1.4 to 5.6 years (Fig. 6). Mean and median α 1 TREC value were calculated for animals between 1 and 4 years of age, as this was the age range of the macaques involved in the thymectomy study. The mean α 1 TREC concentration in macaques aged 1-4 years was $1.98 \times 10^4 / 10^6$ PBMC, and the median was $6.18 \times 10^3 / 10^6$ PBMC.

There was an individual variation of up to two logs between animals within any age category. A similar degree of individual variation has been described in normal humans(17). As discussed above, this variation may be the result of skewing due to the use of PBMC rather than T cells as the denominator of the α 1 TREC calculation. An age-related curve could not be determined from this cohort as the number of animals above age four was small ($n=11$), and samples from older macaques could not be obtained. A steep drop in α 1 TREC concentrations has been described in humans between the ages of 15 and 20(17). A corresponding drop in macaques would be expected to occur after six years of age. A future study of age-related decline in normal rhesus would benefit from evaluating α 1 TREC in sorted CD3 T cells, and from access to a larger cohort of animals, particularly over the age of 6.

It was expected that the concentrations of α 1 TREC would be significantly higher in the thymus, where α locus recombination is taking place. Thymic tissue was obtained from ten juvenile and three neonatal macaques. The mean concentration of α 1 TREC in the thymus of juvenile macaques was about 1 TREC in 10 cells, $9.1 \times 10^4 / 10^6$ thymocytes (Fig. 7). This value is nearly one log higher than the mean in the PBMC of macaques in the same age range. The mean concentration of α 1 TREC in the thymus of neonatal macaques was $6.28 \times 10^4 / 10^6$ thymocytes, within the same range. This indicates that thymic recombination activity does not significantly decrease in the first years of life.

These values were obtained from total thymocytes, a population that includes immature thymocytes (not yet recombined at the α locus) as well as mature thymocytes (which may have divided multiple times since recombination and generation of an $\alpha 1$ TREC). It can therefore be assumed that the actual frequency of cells that recombine to generate an $\alpha 1$ TREC is higher than the concentration measured from these samples.

To assess the normal distribution of $\alpha 1$ TREC in the lymphoid tissues, two normal juvenile macaques were sacrificed (Fig.8). As expected, the $\alpha 1$ TREC concentration in the thymus of these animals was higher than that in the PBMC, a tenfold increase in one animal and a twentyfold increase in the other.

$\alpha 1$ TREC concentrations in the lymph nodes of each animal varied from values similar to those obtained in the PBMC to values fourfold higher. This may reflect ongoing local processes of stimulation and proliferation of $\alpha 1$ TREC bearing cells. Alternately, as DNA is extracted from the total cells residing in the lymph node, variation in $\alpha 1$ TREC concentrations may be due to local differences in the T cell to non-T cell ratio in various lymph nodes.

Intestinal intraepithelial and lamina propria lymphocytes were isolated from the ileum, jejunum, and colon of these two animals to determine whether there was a significant population of $\alpha 1$ TREC bearing cells in these sites. As the gut has been implicated as an extrathymic source of T cells, we wanted to be able to compare the intestinal lymphocytes of thymectomized macaques to normal values. In the normal macaques, the IEL and LPL in the gut contained fewer than 0.5% $\alpha 1$ TREC bearing cells. These low levels indicate both the absence of significant $\alpha\beta$ TCR rearrangement in the gut and the absence of large-scale trafficking of $\alpha 1$ TREC bearing cells from the thymus to the gut. It must be remembered that no conclusion can be made about $\gamma\delta$ TCR rearrangement using this assay.

6.3 Impact of Thymectomy on the Peripheral T Cell Pool The functional significance of the postnatal thymus has long been the subject of debate. Here we present evidence that despite persistent and measurable thymic output, the thymic contribution to the peripheral T cell pool is quantitatively insignificant.

Figure 33A presents a model of the steady-state peripheral T cell pool, in which the thymic source (s) and proliferation (p) contribute to the pool, while death (d) depletes the pool. In the steady-state, $s+p = d$. Figure 33B shows the same model with the source cut off by complete surgical thymectomy. In this situation, there must either be a decline in the total T cell pool or a new steady-state reached with p balancing d.

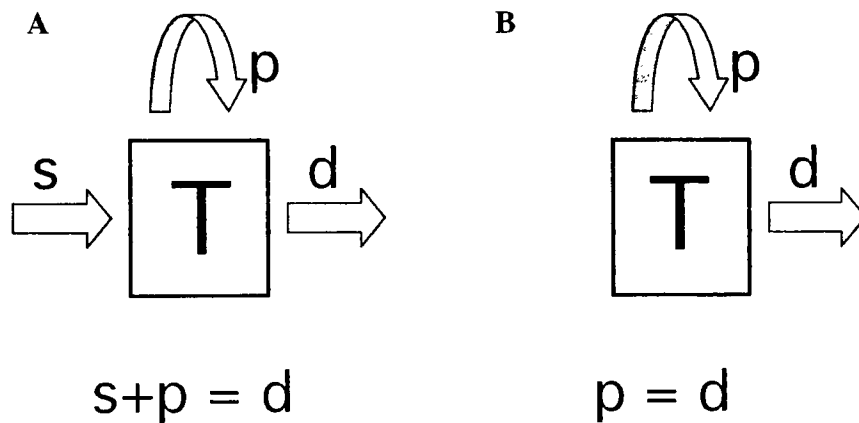


Figure 33. Model of peripheral T cell homeostasis. A. Normal macaque. B. Thymectomized macaque.

From our analysis, we observed that surgical thymectomy did not significantly decrease peripheral $CD3^+$, $CD4^+$, or $CD8^+$ T cells (Fig. 9, 10, Table 2). Thymectomy also had no effect on the naïve populations as measured by the CD45RA isoform (Fig. 11, 12, Table 3). The persistence of a steady-state T cell pool could be explained by 1) an increase in proliferation, 2) a decrease in death, or 3) no change in proliferation and death required because the source before thymectomy was not significantly contributing to the pool. We can rule out explanation 1 immediately because flow cytometry analysis of the T cell pool using Ki67 as a marker for cell proliferation revealed no increase in proliferation in response to thymectomy (Fig. 13). Although we were not able to measure the death rate in this study to directly rule out explanation 2, we will see from the $\alpha 1$

TREC analysis that indeed the source before thymectomy is so small as to be insignificant, therefore not requiring peripheral compensation to maintain the steady-state.

While we observed no change in these parameters during the ten months post surgery, it might be expected that a longer period of time would reveal a slow but measurable decline of T cells, particularly naïve T cells. While the number of cells produced by the thymus each day is quite small, the cumulative effects of thymectomy over the lifespan of the rhesus might become more apparent. In this study, the phase of thymectomy alone was meant to set the stage for a comparison of athymic and euthymic animals in infection, and after the ten months studied the majority of animals were infected with SIV. The number of uninfected animals remaining is too small to draw any conclusions as to long-term effects of thymectomy, but may in the coming years provide an indication of what is to be expected from a larger study of thymectomy without infection.

This phase of the study was also limited by technical aspects of the flow cytometry. Flow cytometry provides a fairly accurate profile of the cells studied, but may lack the quantitative ability to distinguish small changes in the subsets studied. It is possible that processes occurring post thymectomy result in small changes in the peripheral T cell pool, too small to be detected using flow cytometry.

Moreover, the use of additional markers for naïve cells and for T cell proliferation might reveal changes in the peripheral pool not detected by this study. Future studies might include double staining with CD45RA and CD62L (not used in this study due to limitations created by freezing cells) for a more specific assessment of naïve cells. While antibodies to the CD45RO isoform that cross react with rhesus cells are not currently available, the creation of these antibodies will allow a direct study of memory cells. In addition to the use of Ki67 as a marker for cell proliferation, the early activation marker CD69 would also provide evidence of peripheral processes that would affect TREC concentrations. Finally, the use of TUNEL or annexin V staining would yield information on cell death in this cohort.

6.4 Impact of Thymectomy on $\alpha 1$ TREC Bearing Cells A model of the impact of thymectomy on peripheral $\alpha 1$ TREC bearing cells is diagrammed in Figure 34, A and B. In the normal state (Fig. 34A), the source of TREC (s_{TREC}) increases the pool of TREC bearing cells, while proliferation (p_{TREC}) and death (d_{TREC}) of those cells decrease the TREC concentration. Cell division decreases the concentration of TREC in the T cell pool, while the death of a TREC-bearing cell results in the loss of the episome itself, either one or two copies. Note that s_{TREC} , p_{TREC} , and d_{TREC} are not the same as s , p , and d for the total T cell pool, unless one makes the assumption that TREC bearing cells are evenly distributed among processes involving the total T cell pool.

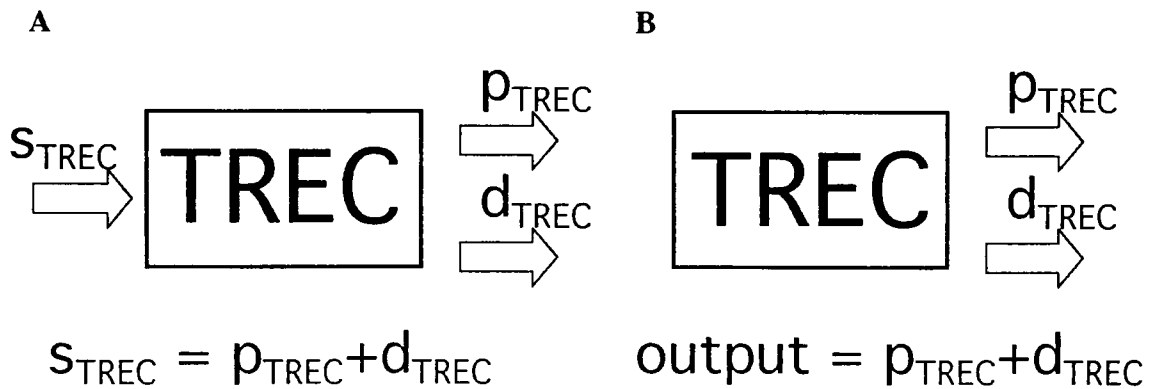


Figure 34. Model of $\alpha 1$ TREC homeostasis. A. Normal macaque.
B. Thymectomized macaque.

After thymectomy (Fig. 34B), there can be no maintenance of the presurgical state, as the thymus is the only source for $\alpha 1$ TREC bearing cells. While it is possible that the proliferation or death rate of that population could decrease to maintain the population of recent thymic emigrants, various lines of evidence indicate that this is unlikely. First, naïve cells are long-lived and divide slowly(195). Second, many studies argue against feedback or cross-talk between the thymus and the periphery(24-26). Most importantly, data presented here on the increased decay of $\alpha 1$ TREC in the thymectomized macaques provides evidence that interruption of the source is not compensated by peripheral processes.

The decay of $\alpha 1$ TREC bearing cells after thymectomy is reflective of the input rate from the source (Fig. 14, 15, Table 4). Our calculation, based on the slope of $\alpha 1$

TREC decay in the PBMC of the thymectomized macaque (Fig. 16), is based on some numerical assumptions. The first is that the average juvenile macaque has 10^{11} total T cells. This is tenfold less than humans, based on size. The second is the percentage of total T cells in the juvenile macaque that are $\alpha 1$ TREC positive. Our data shows that the baseline median TREC levels in the seventeen animals enrolled at the study was 2.2% of PBMC. As any cell can contain one or two $\alpha 1$ TREC, depending on recombination at each chromosome, this translates to a total of $1.1\text{--}2.2 \times 10^9$ total $\alpha 1$ TREC bearing cells. We make the assumption that $\alpha 1$ TREC bearing cells are evenly distributed among the T cell compartments; although some lymphoid tissues have higher concentrations than others, our tissue $\alpha 1$ TREC data supports the assumption that $\alpha 1$ TREC bearing cells circulate between the blood and tissues, rather than being sequestered (discussed below).

With these assumptions, we can multiply the decay rate of $\alpha 1$ TREC bearing cells in the PBMC (0.5% of their number per day) by the total $\alpha 1$ TREC bearing cells ($1.1\text{--}2.2 \times 10^9$) to obtain an absolute thymic production rate, $5.5\text{--}1.1 \times 10^6$ cells per day. As only 11% of single positive thymocytes are $\alpha 1$ TREC positive, we expect the total thymic export rate to be 11-fold higher, 6.1×10^7 to 1.2×10^8 cells per day. This value is within the range obtained for mice ($1\text{--}2 \times 10^6$ cells/day)(1, 3) and sheep ($8.5 \times 10^7\text{--}4 \times 10^8$ cells/day)(6). As a juvenile macaque is intermediate in size between these two species, it makes sense that the thymic output, which is believed to be based on thymic mass, is intermediate as well(1, 2, 4-6). One might expect that a 7kg monkey, approximately 250 times larger than a mouse, would have a 250 fold greater thymic output, of 2.5×10^8 cells per day. Our calculated export rate of 1.2×10^8 cells per day approaches that value.

While our calculation gives us an estimate of thymic output, it does not take into account the age-related decline in $\alpha 1$ TREC concentrations seen in euthymic controls. While thymectomized animals have a decay rate of 0.5% of $\alpha 1$ TREC per day, sham controls had a decay rate of 0.1% per day. Adjusting for the age-related decline yields a thymic output of $4.4\text{--}8.8 \times 10^6$ $\alpha 1$ TREC bearing cells per day, or $4.8\text{--}9.7 \times 10^7$ total cells per day.

Our calculations of thymic output provide a minimum estimate. Residual thymic tissue, while not detected on necropsy, would slow the decay of $\alpha 1$ TREC bearing cells after surgery and decrease our measurement of the actual production rate.

We have thus demonstrated a persistent and measurable thymic output in the juvenile macaque, approximately 6.1×10^7 to 1.2×10^8 cells per day. This number represents 0.1 % of the rhesus T cell pool of 10^{11} cells, a small fraction of the total. As the loss of this input was not measurable by flow cytometry within the 300 days studied, we believe that this output is so small as to require no compensation. While normal levels of peripheral proliferation may have been able to maintain the pool over the course of this study, it is unknown whether these levels can maintain the pool quantitatively in the long run. Over a longer period of time, maintenance of the T cell pool by proliferation alone would be expected to result in a qualitative restriction of the TCR repertoire. This is consistent with the TCR V β restriction observed in the single animal studied 13 months post thymectomy.

6.5 $\alpha 1$ TREC in the Lymphoid Tissues After Thymectomy Having ascertained that the thymus is the sole source of $\alpha 1$ TREC bearing cells in the normal juvenile macaque, we addressed the issue of whether an extrathymic source might develop in response to thymectomy. Eight months post surgery, four thymectomized and two sham macaques underwent tissue biopsy of lymph node, liver, and intestine, the latter sites chosen as they have been reported to be extrathymic sources of T cells (64, 65, 74). The appendix has been implicated as a significant site of interest in the intestine. As rhesus macaques do not have an appendix, the terminal ileum and cecum were biopsied instead.

While the two sham controls had a similar profile to the normal juvenile macaques, the $\alpha 1$ TREC concentrations in the tissues of the thymectomized macaques were roughly twofold lower in all tissues studied (Fig. 28, Table 13). This is consistent with the decline in $\alpha 1$ TREC in the PBMC during this period. That removal of the source impacts upon the lymphoid tissues as well as the peripheral blood lends support to the assumption that there is circulation of $\alpha 1$ TREC bearing cells between the blood and lymphoid tissues.

Extrathymic recombination to produce $\alpha \beta$ T cells would result in a localized increase in $\alpha 1$ TREC concentration at the site of recombination. No such increase was seen in the tissues of the thymectomized macaques, evidence that none of the tissues

studied were behaving as an alternate site of compensatory $\alpha\beta$ T cell production. Again, $\gamma\delta$ T cell recombination events are outside of the scope of this study.

Moreover, the absence of overall changes in the peripheral T cell pool provide no homeostatic pressure for the development of an extrathymic source. Indeed, as thymic output is calculated to be so small as to be insignificant, its absence would not be expected to be a driving force for compensatory changes in potential extrathymic sites for T cell production.

6.6 TCR Repertoire Restriction After Thymectomy While the quantitative changes following thymectomy provide information about thymic output and peripheral T cell processes, they do not address the quality of the immune panel following surgery. Previous reports that adult thymectomy is not associated with immunological deficit (30-32, 53) suggest that the qualitative aspects of the T cell pool are unchanged by thymectomy. To address this issue in our study, we used TCR V β CDR3 length polymorphism as an indicator of the diversity of the TCR repertoire.

One representative animal was chosen from each group of the study; thymectomized infected, thymectomized uninfected, sham infected, and sham uninfected. The twenty-four V β families were studied at baseline, eight months after surgery, and three months after infection (thirteen months post surgery).

Eight months after surgery, the V β profiles in the two thymectomized and two sham animals were virtually unchanged (Fig. 32). There were minor shifts in the relative frequencies of species within each family in all animals, most likely reflective of normal ongoing antigen-recognition processes. However, in all four animals the V β profiles were diverse, reflecting a broad immune panel. This is consistent with our observation that there was no significant loss of T cells after surgery, and no increase in peripheral proliferation that might lead to clonal expansion of individual V β species.

While two of these four animals were assigned to the infection group, the remaining uninfected controls allowed the study of the impact of thymectomy over a longer period of time. Thirteen months post thymectomy, uninfected animal AH02 showed evidence of restriction in the immune panel, while the euthymic control BI25 continued to have a broad polyclonal TCR panel. This may reflect a slow loss of T cells

without thymic replacement, too small to be detected by flow cytometry but evidenced by TCR repertoire restriction. Alternately, the number of T cells may be maintained by a level of peripheral proliferation that is not marked as elevated by FACS but that results in an oligo- or monoclonal expansion of peripheral T cells.

In an effort to substantiate the observation that thymectomy resulted in restriction of the TCR panel beyond the pictorial changes displayed in Figure 32, we used Genescan software to define the number of species in each V β family at each time point (Table 14). At baseline, the four animals had varying numbers of species within each family, but a similar total number of species, ranging from 298 to 405. Eight months post thymectomy, there were no consistent changes in number in thymectomized or sham animals. However, by thirteen months post thymectomy, the uninfected animal AH02 had a clear decrease in the sum of species to 40% of the sum at baseline. In the same time period, the uninfected sham control BI25 had a slight decrease to 96% of baseline, ruling out age-related restriction as an explanation for this phenomenon. It must be stressed that this is only one animal, and further studies must be done before a generalized conclusion is made.

It is believed that a diverse TCR repertoire relies on thymopoiesis, while expansion of peripheral T cells is limited to the existing population and results in a suboptimal immune panel (reviewed in(196)). Thus it is not surprising that there is evidence of restriction in the immune panel following thymectomy. The extent of this restriction in a larger population and the impact on antigen recognition and immune response will require further study on a larger cohort. As there is clinical evidence that adult thymectomy does not result in immune deficit, it might be hypothesized that restriction of the immune panel after thymectomy is a slow process, and that observable deficits might not develop for many years.

6.7 Thymectomy in the Context of SIV Infection While the hallmark of HIV-1 and SIV infection is the progressive loss of T cells, it is not clear whether this loss is due to pathogenic effects of the virus on the thymus, direct and indirect cell killing in the periphery, or, most likely, some combination of the two. Infection is known to increase proliferation by immune activation(96, 197) and to increase cell death(96). It is also

believed that there may be an increase in thymic activity after infection(96, 129). A ‘tap and drain’ model has been proposed for HIV-1 infection in which thymic output and peripheral proliferation are increasingly outpaced by T cell death. Eventually, the balance of input and loss is tipped towards the progressive loss of T cells, resulting in immunodeficiency and death.

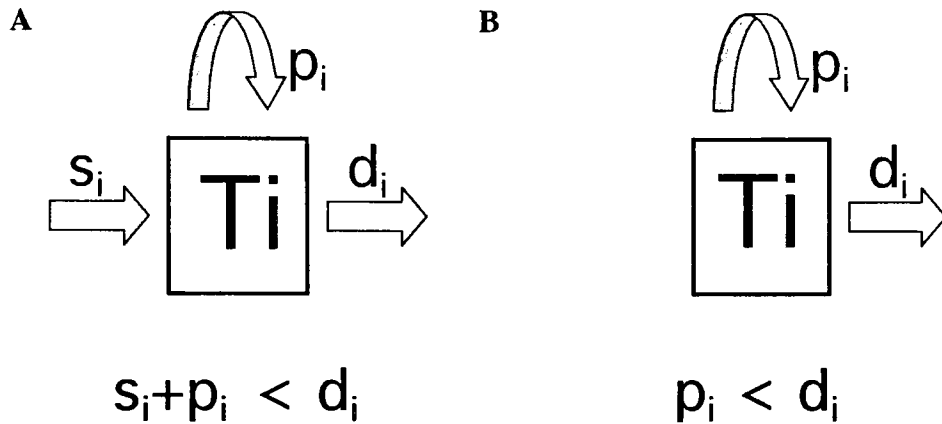


Figure 35. Model of peripheral T cell decay in SIV infection. A. Normal macaque. B. Thymectomized macaque.

We have demonstrated that thymectomy has a limited quantitative impact on the steady-state peripheral T cell pool in the juvenile rhesus macaque. We next wanted to perturb that steady-state to assess the role of the thymus in a situation of T cell decay. We inoculated six thymectomized and six sham macaques with SIV_{MAC251}. In our model of peripheral T cell homeostasis (Fig. 35), the ‘tap’ in the euthymic macaques would include both thymic output and peripheral proliferation, and proliferation alone in the thymectomized animals (Fig. 35A, 35B).

It was hypothesized that the absence of thymic output, however minimal, would take on greater significance in the context of lymphopenia, and that thymectomy would result in a faster rate of CD4 decline. However, this was not observed (Fig. 19, Table 8). The slope of CD4 decay in the thymectomized animals was not significantly steeper than that of the sham animals. Paradoxically, only the animals in the thymectomy group had a significantly steeper decline of CD4 cells compared to their own preinfection values. This may suggest a more rapid onset of CD4 decline in the thymectomized animals,

possibly due to the lack of thymic rebound in early infection, but does not ultimately translate to lower CD4 counts or faster progression to death.

There was also no discernible difference in naïve T cell decay between the thymectomized and sham animals (Fig. 23, Table 10). While it is believed that HIV-1 and SIV preferentially infect activated T cells, leading to a decline in the memory population, this is a long-term effect of chronic infection that would not be expected in the time period under examination(192, 193).

These observations are consistent with anecdotal evidence that thymectomy before HIV-1 infection did not preclude peripheral CD4⁺ T cell reconstitution or clinical response to HAART(53), and suggest that the absence of the thymus does not increase the quantitative effects of viral infection on the peripheral T cell pool.

An increase in T cell proliferation, beyond that observed in infection of a euthymic host, might compensate somewhat for the absence of the thymus. We observed that thymectomized animals had an increase in Ki67⁺ CD4 T cells as early as 16 weeks post infection (Fig. 24). In contrast, sham animals showed a slight increase in Ki67⁺ CD4 T cells, with only a few animals exceeding normal values in the 24 weeks studied.

Antigen stimulation provides a driving force for CD8 proliferation, and in both thymectomized and sham animals, there were two phases of increased Ki67⁺ CD8 T cells. There was an initial burst of CD8 proliferation at 2 weeks post infection, temporally correlated with the peak viral load. The percentage of proliferating CD8⁺ T cells declined slightly but remained above normal in the thymectomy group, with a second phase of increase at week 24. In the sham group, the percentage of proliferating CD8⁺ T cells declined to the normal range between weeks 9 and 24, and began to increase slightly again at week 24.

The higher percentage of Ki67⁺ CD8 T cells in the thymectomized macaques may reflect compensation for the absence of source. Alternately, it may reflect a higher level of antigen stimulation. There was no clear-cut correlation between viral load and percentage of Ki67⁺ T cells in individual animals of either group. If Ki67 levels indeed reflect compensation for the absence of thymic output, it would suggest that in the context of SIV infection, thymic output plays a role in the effort to keep a steady-state T cell pool. However, a comparison between thymectomy and sham animals indicates that

there is adequate compensation for the loss of the thymus. Future studies using more markers for T cell activation and proliferation may clarify these issues.

Finally, thymectomy did not increase progression to death in this cohort. In the first six months following infection, four thymectomized and two sham animals progressed to simian AIDS and had to be euthanized. This timing is consistent with rapid progression, a phenomenon that occurs in SIV-infected macaques. For these animals, both thymectomized and sham, viral load was the strongest predictor of death. A third sham animal, AI73, had to be euthanized nine months post infection. Although this was after the endpoint of this study, it should be noted that this animal had the highest viral load among surviving animals at the last time point of the study. This observation is consistent with reports that thymectomy in patients with myasthenia gravis does not result in general immune deficit(30-32), or greater pathogenesis of HIV-1 infection(11, 53). The caveat to this observation is the small number of animals in each cohort. It is impossible with this number of animals to determine whether the progression to death seen in our study was a factor of thymectomy or inter-animal variation in immune response to viral pathogenesis. However, the overall similarities between the thymectomized and sham animals in other parameters support our conclusion that progression to death was not related to thymectomy in these animals.

6.8 α 1 TREC in the Context of SIV Infection Pathogenic effects of the virus on the thymus and in the periphery are reflected in the decay of α 1 TREC in the infected host, and the study of α 1 TREC as a marker for recent thymic emigrants affords the opportunity to examine the relative contribution of these two arms of attack on the T cell pool.

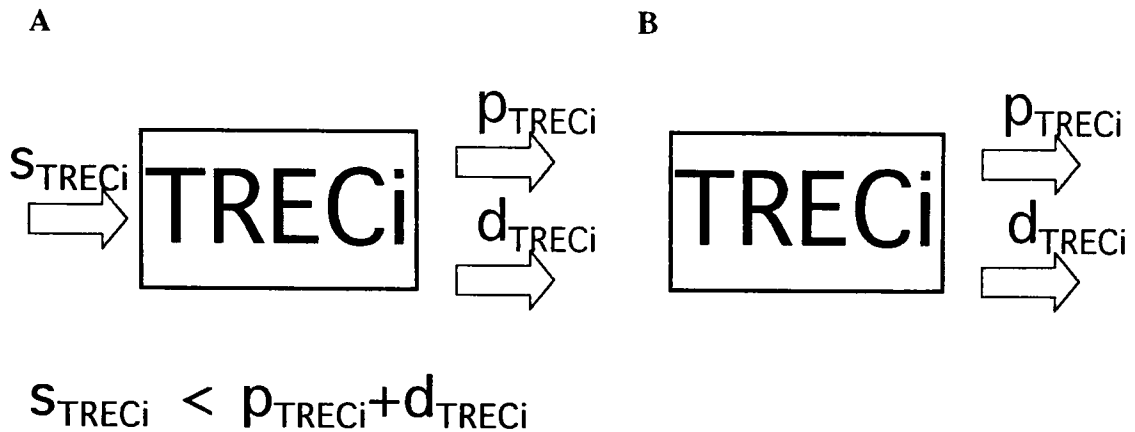


Figure 36. Model of $\alpha 1$ TREC decay in SIV infection. A. Normal macaque.
B. Thymectomized macaque.

HIV-1 and SIV infection could decrease the concentration of $\alpha 1$ TREC bearing cells in the periphery by blocking thymic production of new $\alpha 1$ TREC bearing cells (s_{TREC}), by killing $\alpha 1$ TREC bearing cells in the periphery (d_{TREC}), or by stimulating the division rate of $\alpha 1$ TREC bearing cells (p_{TREC}) (Fig 36, A and B). It has been suggested that the decrease in $\alpha 1$ TREC is entirely based on pathogenic effects on the thymus(16). As support for this theory, Douek *et al.* assert that peripheral proliferation of naïve cells occurs slowly, if at all(195), and that it is unlikely that recent thymic emigrants are susceptible to HIV infection(192, 193). The same group suggests that HAART increases $\alpha 1$ TREC by increasing thymic output. However, it is equally plausible that HAART decreases proliferation and death rates, alternate explanations for the increase in $\alpha 1$ TREC following treatment(17).

A more sophisticated study of the impact of viral pathogenesis on $\alpha 1$ TREC demonstrate that peripheral processes, rather than thymic impairment, account for the decline in $\alpha 1$ TREC after infection. By combining $\alpha 1$ TREC measurements in naïve T cells with mathematical modeling, Hazenberg *et al.* were able to predict the effect of changing individual parameters on $\alpha 1$ TREC. Blocking thymic production barely influenced the average TREC content or naïve cell numbers. Increasing death led to a decrease in the number of naïve T cells along with an increase in the TREC concentration of those cells. Finally, increasing proliferation increased naïve cells and decreased

TREC. A model of HIV-1 infection involving increased proliferation and death predicted a loss in $\alpha 1$ TREC and a slow decrease in naïve T cell numbers(198).

Although we assayed $\alpha 1$ TREC in CD4 and CD8 cells, rather than in naïve populations, our data support Hazenberg's predictions. In CD4 cells, infection significantly increased the decline of $\alpha 1$ TREC in both the thymectomized and sham macaques (Fig. 26). Infection also increased the decay rate of $\alpha 1$ TREC in the CD8 cells, although the decline after infection in the thymectomized animals was not significantly faster than that before infection (Fig. 27).

A comparison of the postinfection $\alpha 1$ TREC decay between thymectomy and sham indicated that the thymectomized animals had a faster decay rate (Table 12). This difference is an immediate indication that the absence of the thymus results in a greater loss of recent thymic emigrants in SIV infection. However, we hypothesized that this was not due to greater viral pathogenesis in the thymectomized macaques, but rather to the preinfection disparity in $\alpha 1$ TREC decay caused by thymectomy. To clarify this issue, we adjusted the postinfection $\alpha 1$ TREC decay slopes for the preinfection values. The adjusted decay rates revealed no significant difference between the two groups, confirming our suspicion that the impact of infection on $\alpha 1$ TREC decay is unrelated to the thymus. This indicates that it is peripheral processes disturbed by viral pathogenesis, and not blockage of the source, that forms the greater factor $\alpha 1$ TREC decay in SIV infection. This supports Hazenberg *et al.*'s modeling of various parameters on $\alpha 1$ TREC decay in infection.

These data contradict previous assertions that impaired production forms the basis for CD4⁺ T cell decline in HIV-1 infection(16). This hypothesis is based on observations of $\alpha 1$ TREC decay in infected individuals as well as reports that HIV-1 infects thymocytes and disrupts thymic architecture(98, 115, 129, 199). We agree that the thymus is affected by SIV and present evidence that its architecture and function is indeed damaged by infection (Fig. 31, Table 13). However, the comparison of euthymic and thymectomized animals presented here indicates that disruption of thymic function is not as great a factor in predicting $\alpha 1$ TREC decay and overall CD4⁺ T cell decline as are peripheral processes.

Our data support multiple reports that peripheral processes are the predictor of CD4⁺ T cell decline in HIV-1 infection(84-88, 92-97). These studies argue that increased proliferation and accelerated destruction result in eventual immune collapse. That our thymectomized animals have comparable peripheral T cell dynamics and disease progression to euthymic animals indicates that peripheral processes play a major role in viral pathogenesis. While it would be impossible to draw a firm conclusion as to the relative contributions of impaired production and accelerated destruction in T cell decline, it is most likely a balance of the two that eventually leads to opportunistic infection and death.

Due to the rapid loss of most of our infected animals, this study was not able to address T cell reconstitution following antiretroviral therapy. We expect thymic output to be crucial in T cell regeneration following therapy. Our hypothesis is that thymectomized animals would not be able to fully correct the loss of CD4 T cells, and that T cells regenerated by peripheral expansion would be memory cells. We also suspect that thymectomized animals would not be able to regain a diverse TCR panel. Future studies will be able to focus on treatment and the role of the thymus in reconstitution in the rhesus macaque. A study of $\alpha 1$ TREC increases following treatment in euthymic animals may yield quantitative information on the ability of the thymus to reconstitute the peripheral T cell pool.

6.9 $\alpha 1$ TREC in the Lymphoid Tissues After Infection To examine the impact of SIV infection on the concentration of $\alpha 1$ TREC bearing cells in the lymph nodes, biopsies were taken from all animals at two and nine weeks post inoculation. To strengthen the observations made in these samples, we added the lymph node data from those animals that had tissue biopsies eight months post thymectomy, before infection, as well as data from tissue collected from infected animals at necropsy (Fig. 29).

As thymectomy resulted in a decreased concentration of $\alpha 1$ TREC in the lymphoid tissues, the thymectomized animals had lower concentrations than the sham animals at the start of infection. By nine weeks post infection, both thymectomized and sham animals had a drop of approximately one log, from $1.1 \times 10^4/10^6$ lymphocytes to $2.7 \times 10^3/10^6$ lymphocytes in the thymectomized animals and $2.4 \times 10^4/10^6$ to $1.4 \times 10^4/10^6$

lymphocytes in the sham animals. That both groups had a similar drop due to infection indicates that the lower $\alpha 1$ TREC concentrations in the thymectomized animals is due to the preexisting deficit in $\alpha 1$ TREC bearing cells. However, a one log drop in the thymectomized group represents a greater relative decline than that in the sham group, suggesting a greater pathogenic effect on the thymectomized animals.

At necropsy, thymectomized animals had lower concentrations than sham controls in every lymphoid tissue studied (Fig. 30, Table 13). However, both groups had significantly lower concentrations than normal. This suggests that SIV infection has a pathogenic effect on $\alpha 1$ TREC bearing lymphocytes in the tissues as well as the blood, and that $\alpha 1$ TREC bearing cells may circulate freely between the blood and tissues such that the effects of viral pathogenesis are evenly distributed.

The only tissue that had a normal $\alpha 1$ TREC in the infected sham macaques was the spleen. In the thymectomized animal the $\alpha 1$ TREC concentration in the spleen was nearly two logs lower. It is possible that an increased $\alpha 1$ TREC concentration is associated with inflammatory processes in this tissue. Two thymectomized animals with granulomatous inflammation of the spleen secondary to *Mycobacterium avium* had higher $\alpha 1$ TREC concentrations in the spleen. Although one sham animal did not show histologic evidence of inflammation of the spleen, the pathology report on the other has not yet been obtained. A final caveat is that $\alpha 1$ TREC were measured as a fraction of total splenocytes rather than T cells in the spleen, and thus may reflect disparate overall T cell counts in that organ between the two groups.

$\alpha 1$ TREC bearing intestinal lymphocytes were virtually undetectable in both thymectomized and sham groups. This is most likely reflective of the overall loss of lymphocytes in the gut, and the possibility that those remaining are not canonical $\alpha \beta$ T cells.

Finally, seven animals were examined for the presence of residual thymic tissue at necropsy. No thymic remnants were found in the four thymectomized macaques, assurance that surgical thymectomy was complete. Involuting thymic tissue was present in the three sham animals. The concentration of $\alpha 1$ TREC in one thymus sample was $3.33 \times 10^4/10^6$ thymocytes, threefold lower than the average normal concentration of $9.1 \times 10^4/10^6$. Histological examination of the same thymic tissue on necropsy revealed

further evidence of pathogenic effects on the thymus, including atrophy, loss of cellularity, and infiltration of fat (Fig. 31). This is consistent with multiple lines of evidence that HIV-1 and SIV infect the thymus (reviewed in(50)).

6.10 TCR Repertoire Restriction After Infection Three months after infection, the one thymectomized and one sham animal studied both showed evidence of dramatic restriction of the TCR repertoire by CDR3 length polymorphism analysis (Fig. 32). Visual inspection reveals a marked decrease in the species within each family, from multiple peaks of varying frequency to a single dominant peak or a small number of peaks. This shift from polyclonal to mono- or oligoclonal response is reflective of the antigenic simulation and clonal expansion processes taking place in infection.

Analysis of the sum of species in these two macaques indicates that the restriction was more profound in the thymectomized animal than in the sham control (Table 14). Three months post infection, the sum of species in the sham animal AP19 was 60% of that at baseline for the study, while the sum of species in thymectomized animal AI25 was 27% of that at baseline. This difference is not surprising, as thymectomy alone over this period resulted in a 40% decrease in the sum of species.

It was initially reported that SIV_{MAC} infection does not result in restriction of the TCR V β repertoire(179). However, that study was based on estimates obtained from autoradiograms of PCR product, and focused in the relative frequency of each V β family. This technique cannot be used to examine the changes in species within each family. In fact, a shift from multiple species of similar length to a single species might not affect the cpm detected from a band on a gel. Using PCR based spectratyping, differences in length as small as a single base pair can be detected within each family. Our results are consistent with Chen *et al.*'s initial study in that the overall contribution of each V β family to the total is not dramatically changed, however we had the opportunity to monitor minute changes within each family. It must be noted that neither technique has the ability to detect base pair substitutions in a species of a given length.

More recent studies by Chen *et al.* using the Genescan based length polymorphism assay revealed that there was indeed clonal dominance among CD4⁺ T cells in macaques infected with SIV(200). These findings are consistent with our own,

although we studied total PBMC rather than sorted CD4 cells. This study suggests that the dominant clones are SIV-specific cells. Other studies, using this method of spectratyping as well as V β -chain specific monoclonal antibodies, have also demonstrated skewing in the CD8⁺ T cell population(152, 201) and sorted CD45RA⁺ and CD45RO⁺ populations(202) in HIV-1 and SIV infected hosts.

A future study of particular interest in this area will involve the treatment of thymectomized, infected animals with HAART, to ascertain whether any restoration of the TCR repertoire is possible. There is evidence for a polyclonal background underlying dominant CDR3 populations in SIV infected macaques(200) as well as HIV-1 infected humans (L. Zhang, personal communication). The extent of this background in the thymectomized host has yet to be determined.

7. Conclusion

Here we present evidence that the quantitative contribution of the thymus to the peripheral T cell pool is minimal. Surgical thymectomy in the juvenile macaque did not cause a detectable loss of peripheral T cells or a shift in naïve and memory populations. No compensatory extrathymic source was detected, nor was proliferation induced as a compensatory mechanism. This is consistent with previous studies that described minimal immunological deficits following thymectomy in the clinical setting.

It has long been believed that after the initial seeding of the T cell pool, the thymus ceases to play a role in T cell homeostasis. Initial studies on the $\alpha 1$ TREC as a marker for recent thymic emigrants in humans proposed the novel conclusion that thymic function is present well into old age. This study of $\alpha 1$ TREC decay in the thymectomized macaque provides evidence that thymic output, while measurable, is numerically minimal in the context of the total T cell pool.

SIV infection has a profound impact on T cell homeostasis. SIV has destructive effects on T cells in the thymus and the periphery, and results in high levels of antigen-stimulated proliferation. Our results demonstrate that the absence of the thymus does not create a situation of higher viral load, greater T cell decay or progression to death. The increased proliferation in the thymectomized animals may be due to antigen stimulation or to compensate for the absence of thymic output. In either case, it is sufficient to maintain the declining T cell pool at the same levels seen in the euthymic controls.

Infection can decrease the concentration of $\alpha 1$ TREC bearing cells in the periphery by a combination of blocking the source, increasing proliferation, and increasing death. Our data demonstrates that the $\alpha 1$ TREC decay after infection is mainly predicted by proliferative dilution.

Taken together, these data show that peripheral processes, rather than thymic output, form the basis for peripheral T cell dynamics, both in the normal macaque and in the context of SIV infection.

8. Bibliography

1. Scollay, R.G., E.C. Butcher, and I.L. Weissman. 1980. Thymus cell migration. Quantitative aspects of cellular traffic from the thymus to the periphery in mice. *European Journal of Immunology* 10, no. 3:210.
2. Binns, R.M., R. Pabst, and S.T. Licence. 1988. Subpopulations of T lymphocytes emigrating in venous blood draining pig thymus labelled in vivo with fluorochrome. *Immunology* 63, no. 2:261.
3. Tough, D.F., and J. Sprent. 1994. Turnover of naive- and memory-phenotype T cells. *Journal of Experimental Medicine* 179, no. 4:1127.
4. Cahill, R.N., W.G. Kimpton, C.P. Cunningham, and E.A. Washington. 1997. An immune system switch at birth triggers a change in the lifespan of peripheral T cells. *Seminars in Immunology* 9, no. 6:355.
5. Cahill, R.N., W.G. Kimpton, E.A. Washington, J.E. Holder, and C.P. Cunningham. 1999. The ontogeny of T cell recirculation during foetal life. *Seminars in Immunology* 11, no. 2:105.
6. Witherden, D.A., W.G. Kimpton, N.J. Abernethy, and R.N. Cahill. 1994. Changes in thymic export of gamma delta and alpha beta T cells during fetal and postnatal development. *European Journal of Immunology* 24, no. 10:2329.
7. Steinmann, G.G. 1986. Changes in the human thymus during aging. *Current Topics in Pathology* 75:43.
8. Haagensen, C.D., N. Lane, and R. Lattes. 1972. Neoplastic proliferation of the epithelium of the mammary lobules: adenosis, lobular neoplasia, and small cell carcinoma. *Surgical Clinics of North America* 52, no. 2:497.
9. Kendall, M.D., H.R. Johnson, and J. Singh. 1980. The weight of the human thymus gland at necropsy. *Journal of Anatomy* 131, no. 3:483.
10. Moore, A.V., M. Korobkin, W. Olanow, D.K. Heaston, P.C. Ram, N.R. Dunnick, and P.M. Silverman. 1983. Age-related changes in the thymus gland: CT-pathologic correlation. *AJR. American Journal of Roentgenology* 141, no. 2:241.
11. Haynes, B.F., and L.P. Hale. 1998. The human thymus. A chimeric organ comprised of central and peripheral lymphoid components. [republished in *Immunol Res* 1998;18(3):175-92]. *Immunologic Research* 18, no. 2:61.
12. Mackall, C.L., and R.E. Gress. 1997. Pathways of T-cell regeneration in mice and humans: implications for bone marrow transplantation and immunotherapy. *Immunological Reviews* 157:61.
13. McCune, J.M., R. Loftus, D.K. Schmidt, P. Carroll, D. Webster, L.B. Swor-Yim, I.R. Francis, B.H. Gross, and R.M. Grant. 1998. High prevalence of thymic tissue in adults with human immunodeficiency virus-1 infection. [see comments]. *Journal of Clinical Investigation* 101, no. 11:2301.
14. Cunningham, C.P., W.G. Kimpton, J.E. Holder, and R.N. Cahill. 2001. Thymic export in aged sheep: a continuous role for the thymus throughout pre- and postnatal life. *European Journal of Immunology* 31, no. 3:802.
15. Jamieson, B.D., D.C. Douek, S. Killian, L.E. Hultin, D.D. Scripture-Adams, J.V. Giorgi, D. Marelli, R.A. Koup, and J.A. Zack. 1999. Generation of functional thymocytes in the human adult. *Immunity* 10, no. 5:569.

16. Douek, D.C., R.D. McFarland, P.H. Keiser, E.A. Gage, J.M. Massey, B.F. Haynes, M.A. Polis, A.T. Haase, M.B. Feinberg, J.L. Sullivan, B.D. Jamieson, J.A. Zack, L.J. Picker, and R.A. Koup. 1998. Changes in thymic function with age and during the treatment of HIV infection. [see comments]. *Nature* 396, no. 6712:690.
17. Zhang, L., S.R. Lewin, M. Markowitz, H.H. Lin, E. Skulsky, R. Karanickolas, Y. He, X. Jin, S. Tuttleton, M. Vesanen, H. Spiegel, R. Kost, J. van Lunzen, H.J. Stellbrink, S. Wolinsky, W. Borkowsky, P. Palumbo, L.G. Kostrikis, and D.D. Ho. 1999. Measuring recent thymic emigrants in blood of normal and HIV-1-infected individuals before and after effective therapy. *Journal of Experimental Medicine* 190, no. 5:725.
18. Poulin, J.F., M.N. Viswanathan, J.M. Harris, K.V. Komanduri, E. Wieder, N. Ringuette, M. Jenkins, J.M. McCune, and R.P. Sekaly. 1999. Direct evidence for thymic function in adult humans. *Journal of Experimental Medicine* 190, no. 4:479.
19. Ginaldi, L., M. De Martinis, A. D'Ostilio, L. Marini, F. Loreto, M. Modesti, and D. Quaglino. 2001. Changes in the expression of surface receptors on lymphocyte subsets in the elderly: quantitative flow cytometric analysis. *American Journal of Hematology* 67, no. 2:63.
20. Ginaldi, L., M. De Martinis, M. Modesti, F. Loreto, M.P. Corsi, and D. Quaglino. 2000. Immunophenotypical changes of T lymphocytes in the elderly. *Gerontology* 46, no. 5:242.
21. Xu, X., I. Beckman, M. Ahern, and J. Bradley. 1993. A comprehensive analysis of peripheral blood lymphocytes in healthy aged humans by flow cytometry. *Immunology & Cell Biology* 71, no. Pt 6:549.
22. Tanchot, C., and B. Rocha. 1995. The peripheral T cell repertoire: independent homeostatic regulation of virgin and activated CD8+ T cell pools. *European Journal of Immunology* 25, no. 8:2127.
23. Mackall, C.L., F.T. Hakim, and R.E. Gress. 1997. T-cell regeneration: all repertoires are not created equal. *Immunology Today* 18, no. 5:245.
24. Berzins, S.P., R.L. Boyd, and J.F. Miller. 1998. The role of the thymus and recent thymic migrants in the maintenance of the adult peripheral lymphocyte pool. *Journal of Experimental Medicine* 187, no. 11:1839.
25. Berzins, S.P., D.I. Godfrey, J.F. Miller, and R.L. Boyd. 1999. A central role for thymic emigrants in peripheral T cell homeostasis. *Proceedings of the National Academy of Sciences of the United States of America* 96, no. 17:9787.
26. Gabor, M.J., R. Scollay, and D.I. Godfrey. 1997. Thymic T cell export is not influenced by the peripheral T cell pool. *European Journal of Immunology* 27, no. 11:2986.
27. Tanchot, C., and B. Rocha. 1997. Peripheral selection of T cell repertoires: the role of continuous thymus output. *Journal of Experimental Medicine* 186, no. 7:1099.
28. Mackall, C.L., C.V. Bare, L.A. Granger, S.O. Sharrow, J.A. Titus, and R.E. Gress. 1996. Thymic-independent T cell regeneration occurs via antigen-driven expansion of peripheral T cells resulting in a repertoire that is limited in diversity and prone to skewing. *Journal of Immunology* 156, no. 12:4609.

29. Mackall, C.L., T.A. Fleisher, M.R. Brown, M.P. Andrich, C.C. Chen, I.M. Feuerstein, I.T. Magrath, L.H. Wexler, D.S. Dimitrov, and R.E. Gress. 1997. Distinctions between CD8+ and CD4+ T-cell regenerative pathways result in prolonged T-cell subset imbalance after intensive chemotherapy. *Blood* 89, no. 10:3700.
30. Melms, A., G. Malcherek, U. Gern, N. Sommer, R. Weissert, H. Wietholter, and H.J. Buhning. 1993. Thymectomy and azathioprine have no effect on the phenotype of CD4 T lymphocyte subsets in myasthenia gravis. *Journal of Neurology, Neurosurgery & Psychiatry* 56, no. 1:46.
31. Scadding, G.K., A.D. Webster, M. Ross, H.C. Thomas, and C.W. Havard. 1979. Humoral immunity before and after thymectomy in myasthenia gravis. *Neurology* 29, no. 4:502.
32. Sempowski, G., J. Thomasch, M. Gooding, L. Hale, L. Edwards, E. Cialfaloni, D. Sanders, J. Massey, D. Douek, R. Koup, and B. Haynes. 2001. Effect of thymectomy on human peripheral blood T cell pools in myasthenia gravis. *Journal of Immunology* 166, no. 4:2808.
33. Miller, J.F.A.P. 1961. Immunological Function of the Thymus. *The Lancet*:748.
34. Miller, J.F., S. Doak, and A.M. Cross. 1963. Role of the thymus in recovery of the immune mechanism in the irradiated adult mouse. *Proceedings of the Society of Experimental Biological Medicine* 112:785.
35. Cole, G.J., and B. Morris. 1971. The cellular and humoral response to antigens in lambs thymectomized in utero. *Australian Journal of Experimental Biology & Medical Science* 49, no. 1:55.
36. Fahey, K.J., P.M. Outteridge, and C. Burrells. 1980. The effect of pre-natal thymectomy on lymphocyte sub-populations in the sheep. *Australian Journal of Experimental Biology & Medical Science* 58, no. 6:571.
37. Wells, W.J., R. Parkman, E. Smogorzewska, and M. Barr. 1998. Neonatal thymectomy: does it affect immune function? *Journal of Thoracic & Cardiovascular Surgery* 115, no. 5:1041.
38. Brearley, S., T.A. Gentle, M.I. Baynham, K.D. Roberts, L.D. Abrams, and R.A. Thompson. 1987. Immunodeficiency following neonatal thymectomy in man. *Clinical & Experimental Immunology* 70, no. 2:322.
39. Bosma, G.C., R.P. Custer, and M.J. Bosma. 1983. A severe combined immunodeficiency mutation in the mouse. *Nature* 301, no. 5900:527.
40. Fischer, A. 1992. Severe combined immunodeficiencies. *Immunodeficiency Reviews* 3, no. 2:83.
41. Hong, R. 1991. The DiGeorge anomaly. *Immunodeficiency Reviews* 3, no. 1:1.
42. Hong, R. 1998. The DiGeorge anomaly (CATCH 22, DiGeorge/velocardiofacial syndrome). *Seminars in Hematology* 35, no. 4:282.
43. Parkman, R., and K. Weinberg. 1998. DiGeorge syndrome: still an enigma. [letter; comment]. *Journal of Pediatrics* 132, no. 1:3.
44. Stephan, J.L., V. Vlekova, F. Le Deist, S. Blanche, J. Donadieu, G. De Saint-Basile, A. Durandy, C. Griscelli, and A. Fischer. 1993. Severe combined immunodeficiency: a retrospective single-center study of clinical presentation and outcome in 117 patients. *Journal of Pediatrics* 123, no. 4:564.

45. Stephan, J.L., V. Vlekova, F. Le Deist, G. De Saint Basile, J. Donadieu, A. Durandy, S. Blanche, C. Griscelli, and A. Fischer. 1993. A retrospective single-center study of clinical presentation and outcome in 117 patients with severe combined immunodeficiency. *Immunodeficiency* 4, no. 1-4:87.
46. Shultz, L.D., and C.L. Sidman. 1987. Genetically determined murine models of immunodeficiency. *Annual Review of Immunology* 5:367.
47. Shultz, L.D. 1991. Hematopoiesis and models of immunodeficiency. *Seminars in Immunology* 3, no. 6:397.
48. Harrison, T.R. 1998. *Principles of Internal Medicine*, ed. A.S.e.a. Fauci. McGraw-Hill Co., Inc., New York.
49. Gaulton, G.N., J.V. Scobie, and M. Rosenzweig. 1997. HIV-1 and the thymus. *AIDS* 11, no. 4:403.
50. McCune, J.M. 1997. Thymic function in HIV-1 disease. *Seminars in Immunology* 9, no. 6:397.
51. Muller, J.G., V. Krenn, C. Schindler, S. Czub, C. Stahl-Hennig, C. Coulibaly, G. Hunsmann, C. Kneitz, T. Kerkau, and A. Rethwilm. 1993. Alterations of thymus cortical epithelium and interdigitating dendritic cells but no increase of thymocyte cell death in the early course of simian immunodeficiency virus infection. *American Journal of Pathology* 143, no. 3:699.
52. Kourtis, A.P., C. Ibegbu, A.J. Nahmias, F.K. Lee, W.S. Clark, M.K. Sawyer, and S. Nesheim. 1996. Early progression of disease in HIV-infected infants with thymus dysfunction. [erratum appears in *N Engl J Med* 1997 Feb 20;336(8):595]. *New England Journal of Medicine* 335, no. 19:1431.
53. Haynes, B.F., L.P. Hale, K.J. Weinhold, D.D. Patel, H.X. Liao, P.B. Bressler, D.M. Jones, J.F. Demarest, K. Gebhard-Mitchell, A.T. Haase, and J.A. Bartlett. 1999. Analysis of the adult thymus in reconstitution of T lymphocytes in HIV-1 infection. [erratum appears in *J Clin Invest* 1999 Mar;103(6):921]. *Journal of Clinical Investigation* 103, no. 4:453.
54. Janeway, C.A., Jr., P. Travers, S. Hunt, and M. Walport. 1997. *Immunobiology*. Current Biology, Ltd., New York and London.
55. Haynes, B.F., M.E. Martin, H.H. Kay, and J. Kurtzberg. 1988. Early events in human T cell ontogeny. Phenotypic characterization and immunohistologic localization of T cell precursors in early human fetal tissues. [erratum appears in *J Exp Med* 1989 Feb 1;169(2):603]. *Journal of Experimental Medicine* 168, no. 3:1061.
56. Moore, K.L. 1982. *The Developing Human- Clinically Oriented Embryology*. W.B. Saunders Company, Philadelphia.
57. McVay, L.D., and S.R. Carding. 1996. Extrathymic origin of human gamma delta T cells during fetal development. *Journal of Immunology* 157, no. 7:2873.
58. McVay, L.D., S.S. Jaswal, C. Kennedy, A. Hayday, and S.R. Carding. 1998. The generation of human gammadelta T cell repertoires during fetal development. *Journal of Immunology* 160, no. 12:5851.
59. Fung-Leung, W.P., T.M. Kundig, K. Ngo, J. Panakos, J. De Sousa-Hitzler, E. Wang, P.S. Ohashi, T.W. Mak, and C.Y. Lau. 1994. Reduced thymic maturation but normal effector function of CD8+ T cells in CD8 beta gene-targeted mice. *Journal of Experimental Medicine* 180, no. 3:959.

60. Liu, C.P., R. Ueda, J. She, J. Sancho, B. Wang, G. Weddell, J. Loring, C. Kurahara, E.C. Dudley, and A. Hayday. 1993. Abnormal T cell development in CD3-zeta/- mutant mice and identification of a novel T cell population in the intestine. *EMBO Journal* 12, no. 12:4863.
61. Malissen, M., A. Gillet, B. Rocha, J. Trucy, E. Vivier, C. Boyer, F. Kontgen, N. Brun, G. Mazza, and E. Spanopoulou. 1993. T cell development in mice lacking the CD3-zeta/eta gene. *EMBO Journal* 12, no. 11:4347.
62. Ohno, H., T. Aoe, S. Taki, D. Kitamura, Y. Ishida, K. Rajewsky, and T. Saito. 1993. Developmental and functional impairment of T cells in mice lacking CD3 zeta chains. *EMBO Journal* 12, no. 11:4357.
63. Rocha, B., P. Vassalli, and D. Guy-Grand. 1992. The extrathymic T-cell development pathway. [see comments]. *Immunology Today* 13, no. 11:449.
64. Guy-Grand, D., and P. Vassalli. 1993. Gut intraepithelial T lymphocytes. *Current Opinion in Immunology* 5, no. 2:247.
65. Rocha, B., D. Guy-Grand, and P. Vassalli. 1995. Extrathymic T cell differentiation. *Current Opinion in Immunology* 7, no. 2:235.
66. Makino, Y., N. Yamagata, T. Sasho, Y. Adachi, R. Kanno, H. Koseki, M. Kanno, and M. Taniguchi. 1993. Extrathymic development of V alpha 14-positive T cells. *Journal of Experimental Medicine* 177, no. 5:1399.
67. Rocha, B. 1990. Characterization of V beta-bearing cells in athymic (nu/nu) mice suggests an extrathymic pathway for T cell differentiation. *European Journal of Immunology* 20, no. 4:919.
68. Sato, K., K. Ohtsuka, K. Hasegawa, S. Yamagiwa, H. Watanabe, H. Asakura, and T. Abo. 1995. Evidence for extrathymic generation of intermediate T cell receptor cells in the liver revealed in thymectomized, irradiated mice subjected to bone marrow transplantation. *Journal of Experimental Medicine* 182, no. 3:759.
69. Bendelac, A., M.N. Rivera, S.H. Park, and J.H. Roark. 1997. Mouse CD1-specific NK1 T cells: development, specificity, and function. *Annual Review of Immunology* 15:535.
70. Cepek, K.L., S.K. Shaw, C.M. Parker, G.J. Russell, J.S. Morrow, D.L. Rimm, and M.B. Brenner. 1994. Adhesion between epithelial cells and T lymphocytes mediated by E-cadherin and the alpha E beta 7 integrin. *Nature* 372, no. 6502:190.
71. Guy-Grand, D., N. Cerf-Bensussan, B. Malissen, M. Malassis-Seris, C. Briottet, and P. Vassalli. 1991. Two gut intraepithelial CD8+ lymphocyte populations with different T cell receptors: a role for the gut epithelium in T cell differentiation. *Journal of Experimental Medicine* 173, no. 2:471.
72. Guy-Grand, D., C. Vanden Broecke, C. Briottet, M. Malassis-Seris, F. Selz, and P. Vassalli. 1992. Different expression of the recombination activity gene RAG-1 in various populations of thymocytes, peripheral T cells and gut thymus-independent intraepithelial lymphocytes suggests two pathways of T cell receptor rearrangement. *European Journal of Immunology* 22, no. 2:505.
73. Lynch, S., D. Kelleher, R. McManus, and C. O'Farrelly. 1995. RAG1 and RAG2 expression in human intestinal epithelium: evidence of extrathymic T cell differentiation. *European Journal of Immunology* 25, no. 5:1143.

74. Abo, T., T. Kawamura, and H. Watanabe. 2000. Physiological responses of extrathymic T cells in the liver. *Immunological Reviews* 174:135.
75. Watanabe, H., C. Miyaji, S. Seki, and T. Abo. 1996. c-kit⁺ stem cells and thymocyte precursors in the livers of adult mice. *Journal of Experimental Medicine* 184, no. 2:687.
76. Narita, J., C. Miyaji, H. Watanabe, S. Honda, T. Koya, H. Umezu, T. Ushiki, S. Sugahara, T. Kawamura, M. Arakawa, and T. Abo. 1998. Differentiation of forbidden T cell clones and granulocytes in the parenchymal space of the liver in mice treated with estrogen. *Cellular Immunology* 185, no. 1:1.
77. Yamagiwa, S., S. Sugahara, T. Shimizu, T. Iwanaga, Y. Yoshida, S. Honda, H. Watanabe, K. Suzuki, H. Asakura, and T. Abo. 1998. The primary site of CD4⁺ 8⁺ B220⁺ alphabeta T cells in lpr mice: the appendix in normal mice. *Journal of Immunology* 160, no. 6:2665.
78. Iiai, T., H. Watanabe, S. Seki, K. Sugiura, K. Hirokawa, M. Utsuyama, H. Takahashi-Iwanaga, T. Iwanaga, T. Ohteki, and T. Abo. 1992. Ontogeny and development of extrathymic T cells in mouse liver. *Immunology* 77, no. 4:556.
79. Sato, K., K. Ohtsuka, H. Watanabe, H. Asakura, and T. Abo. 1993. Detailed characterization of gamma delta T cells within the organs in mice: classification into three groups. *Immunology* 80, no. 3:380.
80. Abo, T., T. Ohteki, S. Seki, N. Koyamada, Y. Yoshikai, T. Masuda, H. Rikiishi, and K. Kumagai. 1991. The appearance of T cells bearing self-reactive T cell receptor in the livers of mice injected with bacteria. *Journal of Experimental Medicine* 174, no. 2:417.
81. Ohteki, T., and H.R. MacDonald. 1994. Major histocompatibility complex class I related molecules control the development of CD4⁺8⁺ and CD4⁺8⁺ subsets of natural killer 1.1⁺ T cell receptor-alpha/beta⁺ cells in the liver of mice. *Journal of Experimental Medicine* 180, no. 2:699.
82. Garcia-Ojeda, M.E., S. Dejbakhsh-Jones, I.L. Weissman, and S. Strober. 1998. An alternate pathway for T cell development supported by the bone marrow microenvironment: recapitulation of thymic maturation. *Journal of Experimental Medicine* 187, no. 11:1813.
83. Zeng, D., G. Gazit, S. Dejbakhsh-Jones, S.P. Balk, S. Snapper, M. Taniguchi, and S. Strober. 1999. Heterogeneity of NK1.1⁺ T cells in the bone marrow: divergence from the thymus. *Journal of Immunology* 163, no. 10:5338.
84. Ho, D.D., A.U. Neumann, A.S. Perelson, W. Chen, J.M. Leonard, and M. Markowitz. 1995. Rapid turnover of plasma virions and CD4 lymphocytes in HIV-1 infection. [see comments]. *Nature* 373, no. 6510:123.
85. Wei, X., S.K. Ghosh, M.E. Taylor, V.A. Johnson, E.A. Emini, P. Deutsch, J.D. Lifson, S. Bonhoeffer, M.A. Nowak, and B.H. Hahn. 1995. Viral dynamics in human immunodeficiency virus type 1 infection. [see comments]. *Nature* 373, no. 6510:117.
86. Perelson, A.S., P. Essunger, Y. Cao, M. Vesanen, A. Hurley, K. Saksela, M. Markowitz, and D.D. Ho. 1997. Decay characteristics of HIV-1-infected compartments during combination therapy. [see comments]. *Nature* 387, no. 6629:188.

87. Perelson, A.S., P. Essunger, and D.D. Ho. 1997. Dynamics of HIV-1 and CD4+ lymphocytes in vivo. *AIDS* 11 Suppl A:S17.
88. Perelson, A.S., A.U. Neumann, M. Markowitz, J.M. Leonard, and D.D. Ho. 1996. HIV-1 dynamics in vivo: virion clearance rate, infected cell life-span, and viral generation time. *Science* 271, no. 5255:1582.
89. Pakker, N.G., D.W. Notermans, R.J. de Boer, M.T. Roos, F. de Wolf, A. Hill, J.M. Leonard, S.A. Danner, F. Miedema, and P.T. Schellekens. 1998. Biphasic kinetics of peripheral blood T cells after triple combination therapy in HIV-1 infection: a composite of redistribution and proliferation. [see comments]. *Nature Medicine* 4, no. 2:208.
90. Wolthers, K.C., G. Bea, A. Wisman, S.A. Otto, A.M. de Roda Husman, N. Schaft, F. de Wolf, J. Goudsmit, R.A. Coutinho, A.G. van der Zee, L. Meyaard, and F. Miedema. 1996. T cell telomere length in HIV-1 infection: no evidence for increased CD4+ T cell turnover. *Science* 274, no. 5292:1543.
91. Wolthers, K.C., and F. Miedema. 1998. Telomeres and HIV-1 infection: in search of exhaustion. *Trends in Microbiology* 6, no. 4:144.
92. Sachsenberg, N., A.S. Perelson, S. Yerly, G.A. Schockmel, D. Leduc, B. Hirschel, and L. Perrin. 1998. Turnover of CD4+ and CD8+ T lymphocytes in HIV-1 infection as measured by Ki-67 antigen. *Journal of Experimental Medicine* 187, no. 8:1295.
93. Tenner-Racz, K., H.J. Stellbrink, J. van Lunzen, C. Schneider, J.P. Jacobs, B. Raschdorff, G. Grosschupff, R.M. Steinman, and P. Racz. 1998. The unenlarged lymph nodes of HIV-1-infected, asymptomatic patients with high CD4 T cell counts are sites for virus replication and CD4 T cell proliferation. The impact of highly active antiretroviral therapy. *Journal of Experimental Medicine* 187, no. 6:949.
94. Hellerstein, M., M.B. Hanley, D. Cesar, S. Siler, C. Papageorgopoulos, E. Wieder, D. Schmidt, R. Hoh, R. Neese, D. Macallan, S. Deeks, and J.M. McCune. 1999. Directly measured kinetics of circulating T lymphocytes in normal and HIV-1-infected humans. [see comments]. *Nature Medicine* 5, no. 1:83.
95. Mohri, H., A.S. Perelson, K. Tung, R. Ribeiro, B. Ramratnam, M. Markowitz, R. Kost, A. Hurley, L. Weinberger, D. Cesar, M. Hellerstein, and D.D. Ho. 2001. Increased Turnover of T Lymphocytes in HIV-1 Infection and Its Reduction by Antiretroviral Therapy. in press, *Journal of Experimental Medicine*.
96. Mohri, H., S. Bonhoeffer, S. Monard, A.S. Perelson, and D.D. Ho. 1998. Rapid turnover of T lymphocytes in SIV-infected rhesus macaques. *Science* 279, no. 5354:1223.
97. Rosenzweig, M., M.A. DeMaria, D.M. Harper, S. Friedrich, R.K. Jain, and R.P. Johnson. 1998. Increased rates of CD4(+) and CD8(+) T lymphocyte turnover in simian immunodeficiency virus-infected macaques. *Proceedings of the National Academy of Sciences of the United States of America* 95, no. 11:6388.
98. Bonyhadi, M.L., L. Rabin, S. Salimi, D.A. Brown, J. Kosek, J.M. McCune, and H. Kaneshima. 1993. HIV induces thymus depletion in vivo. *Nature* 363, no. 6431:728.
99. Bertho, J.M., C. Demarquay, N. Moulian, A. Van Der Meeren, S. Berrih-Aknin, and P. Gourmelon. 1997. Phenotypic and immunohistological analyses of the

- human adult thymus: evidence for an active thymus during adult life. *Cellular Immunology* 179, no. 1:30.
100. Braun, J., H. Valentin, M.T. Nugeyre, H. Ohayon, P. Gounon, and F. Barre-Sinoussi. 1996. Productive and persistent infection of human thymic epithelial cells in vitro with HIV-1. *Virology* 225, no. 2:413.
 101. Hays, E.F., C.H. Uittenbogaart, J.C. Brewer, L.W. Vollger, and J.A. Zack. 1992. In vitro studies of HIV-1 expression in thymocytes from infants and children. *AIDS* 6, no. 3:265.
 102. Jenkins, M., M.B. Hanley, M.B. Moreno, E. Wieder, and J.M. McCune. 1998. Human immunodeficiency virus-1 infection interrupts thymopoiesis and multilineage hematopoiesis in vivo. *Blood* 91, no. 8:2672.
 103. Joshi, V.V., J.M. Oleske, S. Saad, C. Gadol, E. Connor, R. Bobila, and A.B. Minnefor. 1986. Thymus biopsy in children with acquired immunodeficiency syndrome. *Archives of Pathology & Laboratory Medicine* 110, no. 9:837.
 104. Koka, P.S., J.K. Fraser, Y. Bryson, G.C. Bristol, G.M. Aldrovandi, E.S. Daar, and J.A. Zack. 1998. Human immunodeficiency virus inhibits multilineage hematopoiesis in vivo. *Journal of Virology* 72, no. 6:5121.
 105. Nahmias, A.J., W.S. Clark, A.P. Kourtis, F.K. Lee, G. Cotsonis, C. Ibegbu, D. Thea, P. Palumbo, P. Vink, R.J. Simonds, and S.R. Nesheim. 1998. Thymic dysfunction and time of infection predict mortality in human immunodeficiency virus-infected infants. CDC Perinatal AIDS Collaborative Transmission Study Group. *Journal of Infectious Diseases* 178, no. 3:680.
 106. Stanley, S.K., J.M. McCune, H. Kaneshima, J.S. Justement, M. Sullivan, E. Boone, M. Baseler, J. Adelsberger, M. Bonyhadi, and J. Orenstein. 1993. Human immunodeficiency virus infection of the human thymus and disruption of the thymic microenvironment in the SCID-hu mouse. *Journal of Experimental Medicine* 178, no. 4:1151.
 107. Vigano, A., S. Vella, N. Principi, D. Bricalli, N. Sala, A. Salvaggio, M. Saresella, A. Vanzulli, and M. Clerici. 1999. Thymus volume correlates with the progression of vertical HIV infection. *AIDS* 13, no. 5:F29.
 108. Schuurman, H.J., W.J. Krone, R. Broekhuizen, and J. Goudsmit. 1988. Expression of RNA and antigens of human immunodeficiency virus type-1 (HIV-1) in lymph nodes from HIV-1 infected individuals. *American Journal of Pathology* 133, no. 3:516.
 109. Schuurman, H.J., W.J. Krone, R. Broekhuizen, J. van Baarlen, P. van Veen, A.L. Golstein, J. Huber, and J. Goudsmit. 1989. The thymus in acquired immune deficiency syndrome. Comparison with other types of immunodeficiency diseases, and presence of components of human immunodeficiency virus type 1. *American Journal of Pathology* 134, no. 6:1329.
 110. Lee, S., H. Goldstein, M. Baseler, J. Adelsberger, and H. Golding. 1997. Human immunodeficiency virus type 1 infection of mature CD3hiCD8+ thymocytes. *Journal of Virology* 71, no. 9:6671.
 111. Rosenzweig, M., D.P. Clark, and G.N. Gaulton. 1993. Selective thymocyte depletion in neonatal HIV-1 thymic infection. *AIDS* 7, no. 12:1601.

112. Tanaka, K.E., W.C. Hatch, Y. Kress, R. Soeiro, T. Calvelli, W.K. Rashbaum, A. Rubinstein, and W.D. Lyman. 1992. HIV-1 infection of human fetal thymocytes. *Journal of Acquired Immune Deficiency Syndromes* 5, no. 1:94.
113. Valentin, H., M.T. Nugeyre, F. Vuillier, L. Boumsell, M. Schmid, F. Barre-Sinoussi, and R.A. Pereira. 1994. Two subpopulations of human triple-negative thymic cells are susceptible to infection by human immunodeficiency virus type 1 in vitro. *Journal of Virology* 68, no. 5:3041.
114. Bonyhadi, M.L., L. Su, J. Auten, J.M. McCune, and H. Kaneshima. 1995. Development of a human thymic organ culture model for the study of HIV pathogenesis. *AIDS Research & Human Retroviruses* 11, no. 9:1073.
115. Aldrovandi, G.M., G. Feuer, L. Gao, B. Jamieson, M. Kristeva, I.S. Chen, and J.A. Zack. 1993. The SCID-hu mouse as a model for HIV-1 infection. *Nature* 363, no. 6431:732.
116. Goldstein, H., M. Pettoello-Mantovani, N.F. Katopodis, A. Kim, S. Yurasov, and T.R. Kollmann. 1996. SCID-hu mice: a model for studying disseminated HIV infection. *Seminars in Immunology* 8, no. 4:223.
117. Jamieson, B.D., G.M. Aldrovandi, and J.A. Zack. 1996. The SCID-hu mouse: an in-vivo model for HIV-1 pathogenesis and stem cell gene therapy for AIDS. *Seminars in Immunology* 8, no. 4:215.
118. Kollmann, T.R., A. Kim, M. Pettoello-Mantovani, M. Hachamovitch, A. Rubinstein, M.M. Goldstein, and H. Goldstein. 1995. Divergent effects of chronic HIV-1 infection on human thymocyte maturation in SCID-hu mice. *Journal of Immunology* 154, no. 2:907.
119. McCune, J., H. Kaneshima, J. Krowka, R. Namikawa, H. Outzen, B. Peault, L. Rabin, C.C. Shih, E. Yee, and M. Lieberman. 1991. The SCID-hu mouse: a small animal model for HIV infection and pathogenesis. *Annual Review of Immunology* 9:399.
120. Autran, B., P. Guet, M. Raphael, M. Grandadam, H. Agut, D. Candotti, P. Grenot, F. Puech, P. Debre, and J.Y. Cesbron. 1996. Thymocyte and thymic microenvironment alterations during a systemic HIV infection in a severe combined immunodeficient mouse model. *AIDS* 10, no. 7:717.
121. Kaneshima, H., C.C. Shih, R. Namikawa, L. Rabin, H. Outzen, S.G. Machado, and J.M. McCune. 1991. Human immunodeficiency virus infection of human lymph nodes in the SCID-hu mouse. *Proceedings of the National Academy of Sciences of the United States of America* 88, no. 10:4523.
122. Kaneshima, H., L. Su, M.L. Bonyhadi, R.I. Connor, D.D. Ho, and J.M. McCune. 1994. Rapid-high, syncytium-inducing isolates of human immunodeficiency virus type 1 induce cytopathicity in the human thymus of the SCID-hu mouse. *Journal of Virology* 68, no. 12:8188.
123. Kollmann, T.R., M. Pettoello-Mantovani, X. Zhuang, A. Kim, M. Hachamovitch, P. Smarnworawong, A. Rubinstein, and H. Goldstein. 1994. Disseminated human immunodeficiency virus 1 (HIV-1) infection in SCID-hu mice after peripheral inoculation with HIV-1. *Journal of Experimental Medicine* 179, no. 2:513.
124. Mosier, D.E., R.J. Gulizia, S.M. Baird, D.B. Wilson, D.H. Spector, and S.A. Spector. 1991. Human immunodeficiency virus infection of human-PBL-SCID mice. *Science* 251, no. 4995:791.

125. Mosier, D.E., R.J. Gulizia, P.D. MacIsaac, B.E. Torbett, and J.A. Levy. 1993. Rapid loss of CD4+ T cells in human-PBL-SCID mice by noncytopathic HIV isolates. *Science* 260, no. 5108:689.
126. Su, L., H. Kaneshima, M. Bonyhadi, S. Salimi, D. Kraft, L. Rabin, and J.M. McCune. 1995. HIV-1-induced thymocyte depletion is associated with indirect cytopathogenicity and infection of progenitor cells in vivo. *Immunity* 2, no. 1:25.
127. Jamieson, B.D., S. Pang, G.M. Aldrovandi, J. Zha, and J.A. Zack. 1995. In vivo pathogenic properties of two clonal human immunodeficiency virus type 1 isolates. *Journal of Virology* 69, no. 10:6259.
128. Baskin, G.B., M. Murphey-Corb, L.N. Martin, B. Davison-Fairburn, F.S. Hu, and D. Kuebler. 1991. Thymus in simian immunodeficiency virus-infected rhesus monkeys. *Laboratory Investigation* 65, no. 4:400.
129. Wykrzykowska, J.J., M. Rosenzweig, R.S. Veazey, M.A. Simon, K. Halvorsen, R.C. Desrosiers, R.P. Johnson, and A.A. Lackner. 1998. Early regeneration of thymic progenitors in rhesus macaques infected with simian immunodeficiency virus. *Journal of Experimental Medicine* 187, no. 11:1767.
130. Muller, J.G., S. Czub, A. Marx, R. Brinkmann, R. Plesker, and H.K. Muller-Hermelink. 1994. Detection of SIV in rhesus monkey thymus stroma cell cultures. *Research in Virology* 145, no. 3-4:239.
131. Li, S.L., E.E. Kaaya, C. Ordonez, M. Ekman, H. Feichtinger, P. Putkonen, D. Bottiger, G. Biberfeld, and P. Biberfeld. 1995. Thymic immunopathology and progression of SIVsm infection in cynomolgus monkeys. *Journal of Acquired Immune Deficiency Syndromes* 9, no. 1:1.
132. Lackner, A.A., P. Vogel, R.A. Ramos, J.D. Kluge, and M. Marthas. 1994. Early events in tissues during infection with pathogenic (SIVmac239) and nonpathogenic (SIVmac1A11) molecular clones of simian immunodeficiency virus. *American Journal of Pathology* 145, no. 2:428.
133. Reimann, K.A., J.T. Li, R. Veazey, M. Halloran, I.W. Park, G.B. Karlsson, J. Sodroski, and N.L. Letvin. 1996. A chimeric simian/human immunodeficiency virus expressing a primary patient human immunodeficiency virus type 1 isolate env causes an AIDS-like disease after in vivo passage in rhesus monkeys. *Journal of Virology* 70, no. 10:6922.
134. Luciw, P.A., E. Pratt-Lowe, K.E. Shaw, J.A. Levy, and C. Cheng-Mayer. 1995. Persistent infection of rhesus macaques with T-cell-line-tropic and macrophage-tropic clones of simian/human immunodeficiency viruses (SHIV). *Proceedings of the National Academy of Sciences of the United States of America* 92, no. 16:7490.
135. Joag, S.V., Z. Li, L. Foresman, E.B. Stephens, L.J. Zhao, I. Adany, D.M. Pinson, H.M. McClure, and O. Narayan. 1996. Chimeric simian/human immunodeficiency virus that causes progressive loss of CD4+ T cells and AIDS in pig-tailed macaques. *Journal of Virology* 70, no. 5:3189.
136. Mackall, C.L., L. Granger, M.A. Sheard, R. Cepeda, and R.E. Gress. 1993. T-cell regeneration after bone marrow transplantation: differential CD45 isoform expression on thymic-derived versus thymic-independent progeny. *Blood* 82, no. 8:2585.

137. Miller, J.F. 1962. Immunological significance of the thymus of the adult mouse. *Nature* 195:1318.
138. Zinkernagel, R.M., A. Althage, G. Callahan, and R.M. Welsh. 1980. On the immunocompetence of H-2 incompatible irradiation bone marrow chimeras. *Journal of Immunology* 124, no. 5:2356.
139. Mackall, C.L., T.A. Fleisher, M.R. Brown, M.P. Andrich, C.C. Chen, I.M. Feuerstein, M.E. Horowitz, I.T. Magrath, A.T. Shad, and S.M. Steinberg. 1995. Age, thymopoiesis, and CD4+ T-lymphocyte regeneration after intensive chemotherapy. [see comments]. *New England Journal of Medicine* 332, no. 3:143.
140. Mackall, C.L., D. Stein, T.A. Fleisher, M.R. Brown, F.T. Hakim, C.V. Bare, S.F. Leitman, E.J. Read, C.S. Carter, L.H. Wexler, and R.E. Gress. 2000. Prolonged CD4 depletion after sequential autologous peripheral blood progenitor cell infusions in children and young adults. *Blood* 96, no. 2:754.
141. Storek, J., R.P. Witherspoon, and R. Storb. 1995. T cell reconstitution after bone marrow transplantation into adult patients does not resemble T cell development in early life. *Bone Marrow Transplantation* 16, no. 3:413.
142. Weinberg, K., G. Annett, A. Kashyap, C. Lenarsky, S.J. Forman, and R. Parkman. 1995. The effect of thymic function on immunocompetence following bone marrow transplantation. *Biology of Blood & Marrow Transplantation* 1, no. 1:18.
143. Fischer, A., P. Landais, W. Friedrich, G. Morgan, B. Gerritsen, A. Fasth, F. Porta, C. Griscelli, S.F. Goldman, and R. Levinsky. 1990. European experience of bone-marrow transplantation for severe combined immunodeficiency. *Lancet* 336, no. 8719:850.
144. Patel, D.D., M.E. Gooding, R.E. Parrott, K.M. Curtis, B.F. Haynes, and R.H. Buckley. 2000. Thymic function after hematopoietic stem-cell transplantation for the treatment of severe combined immunodeficiency. *New England Journal of Medicine* 342, no. 18:1325.
145. Heitger, A., N. Neu, H. Kern, E.R. Panzer-Grumayer, H. Greinix, D. Nachbaur, D. Niederwieser, and F.M. Fink. 1997. Essential role of the thymus to reconstitute naive (CD45RA+) T-helper cells after human allogeneic bone marrow transplantation. *Blood* 90, no. 2:850.
146. Autran, B., G. Carcelain, T.S. Li, C. Blanc, D. Mathez, R. Tubiana, C. Katlama, P. Debre, and J. Leibowitch. 1997. Positive effects of combined antiretroviral therapy on CD4+ T cell homeostasis and function in advanced HIV disease. [see comments]. *Science* 277, no. 5322:112.
147. Connors, M., J.A. Kovacs, S. Krevat, J.C. Gea-Banacloche, M.C. Sneller, M. Flanigan, J.A. Metcalf, R.E. Walker, J. Falloon, M. Baseler, I. Feuerstein, H. Masur, and H.C. Lane. 1997. HIV infection induces changes in CD4+ T-cell phenotype and depletions within the CD4+ T-cell repertoire that are not immediately restored by antiviral or immune-based therapies. [see comments]. *Nature Medicine* 3, no. 5:533.
148. Walker, R.E., C.S. Carter, L. Muul, V. Natarajan, B.R. Herpin, S.F. Leitman, H.G. Klein, C.A. Mullen, J.A. Metcalf, M. Baseler, J. Falloon, R.T. Davey, Jr., J.A. Kovacs, M.A. Polis, H. Masur, R.M. Blaese, and H.C. Lane. 1998. Peripheral

- expansion of pre-existing mature T cells is an important means of CD4+ T-cell regeneration HIV-infected adults. *Nature Medicine* 4, no. 7:852.
149. Ho, D.D. 1997. Perspectives series: host/pathogen interactions. Dynamics of HIV-1 replication in vivo. *Journal of Clinical Investigation* 99, no. 11:2565.
 150. Cohen Stuart, J.W., W.A. Sliker, G.T. Rijkers, A. Noest, C.A. Boucher, M.H. Suur, R. de Boer, S.P. Geelen, H.J. Scherpbier, N.G. Hartwig, H. Hooijkaas, M.T. Roos, B. de Graeff-Meeder, and R. de Groot. 1998. Early recovery of CD4+ T lymphocytes in children on highly active antiretroviral therapy. Dutch study group for children with HIV infections. *AIDS* 12, no. 16:2155.
 151. Vigano, A., S. Vella, M. Saresella, A. Vanzulli, D. Bricalli, S. Di Fabio, P. Ferrante, M. Andreotti, M. Pirillo, L.G. Dally, M. Clerici, and N. Principi. 2000. Early immune reconstitution after potent antiretroviral therapy in HIV-infected children correlates with the increase in thymus volume. *AIDS* 14, no. 3:251.
 152. Gorochov, G., A.U. Neumann, A. Kereveur, C. Parizot, T. Li, C. Katlama, M. Karmochkine, G. Raguin, B. Autran, and P. Debre. 1998. Perturbation of CD4+ and CD8+ T-cell repertoires during progression to AIDS and regulation of the CD4+ repertoire during antiviral therapy. [see comments]. *Nature Medicine* 4, no. 2:215.
 153. McFarland, R.D., D.C. Douek, R.A. Koup, and L.J. Picker. 2000. Identification of a human recent thymic emigrant phenotype. *Proceedings of the National Academy of Sciences of the United States of America* 97, no. 8:4215.
 154. Baron, R.L., J.K. Lee, S.S. Sagel, and R.R. Peterson. 1982. Computed tomography of the normal thymus. *Radiology* 142, no. 1:121.
 155. Erkeller-Yuksel, F.M., V. Deneys, B. Yuksel, I. Hannet, F. Hulstaert, C. Hamilton, H. Mackinnon, L.T. Stokes, V. Munhyeshuli, and F. Vanlangendonck. 1992. Age-related changes in human blood lymphocyte subpopulations. *Journal of Pediatrics* 120, no. 2 Pt 1:216.
 156. Fujii, Y., M. Okumura, K. Inada, K. Nakahara, and H. Matsuda. 1992. CD45 isoform expression during T cell development in the thymus. *European Journal of Immunology* 22, no. 7:1843.
 157. Pilarski, L.M., R. Gillitzer, H. Zola, K. Shortman, and R. Scollay. 1989. Definition of the thymic generative lineage by selective expression of high molecular weight isoforms of CD45 (T200). *European Journal of Immunology* 19, no. 4:589.
 158. Picker, L.J., J.R. Treer, B. Ferguson-Darnell, P.A. Collins, D. Buck, and L.W. Terstappen. 1993. Control of lymphocyte recirculation in man. I. Differential regulation of the peripheral lymph node homing receptor L-selection on T cells during the virgin to memory cell transition. *Journal of Immunology* 150, no. 3:1105.
 159. Michie, C.A., A. McLean, C. Alcock, and P.C. Beverley. 1992. Lifespan of human lymphocyte subsets defined by CD45 isoforms. *Nature* 360, no. 6401:264.
 160. Tough, D.F., and J. Sprent. 1995. Life span of naive and memory T cells. *Stem Cells* 13, no. 3:242.
 161. Bell, E.B., and S.M. Sparshott. 1990. Interconversion of CD45R subsets of CD4 T cells in vivo. [see comments]. *Nature* 348, no. 6297:163.

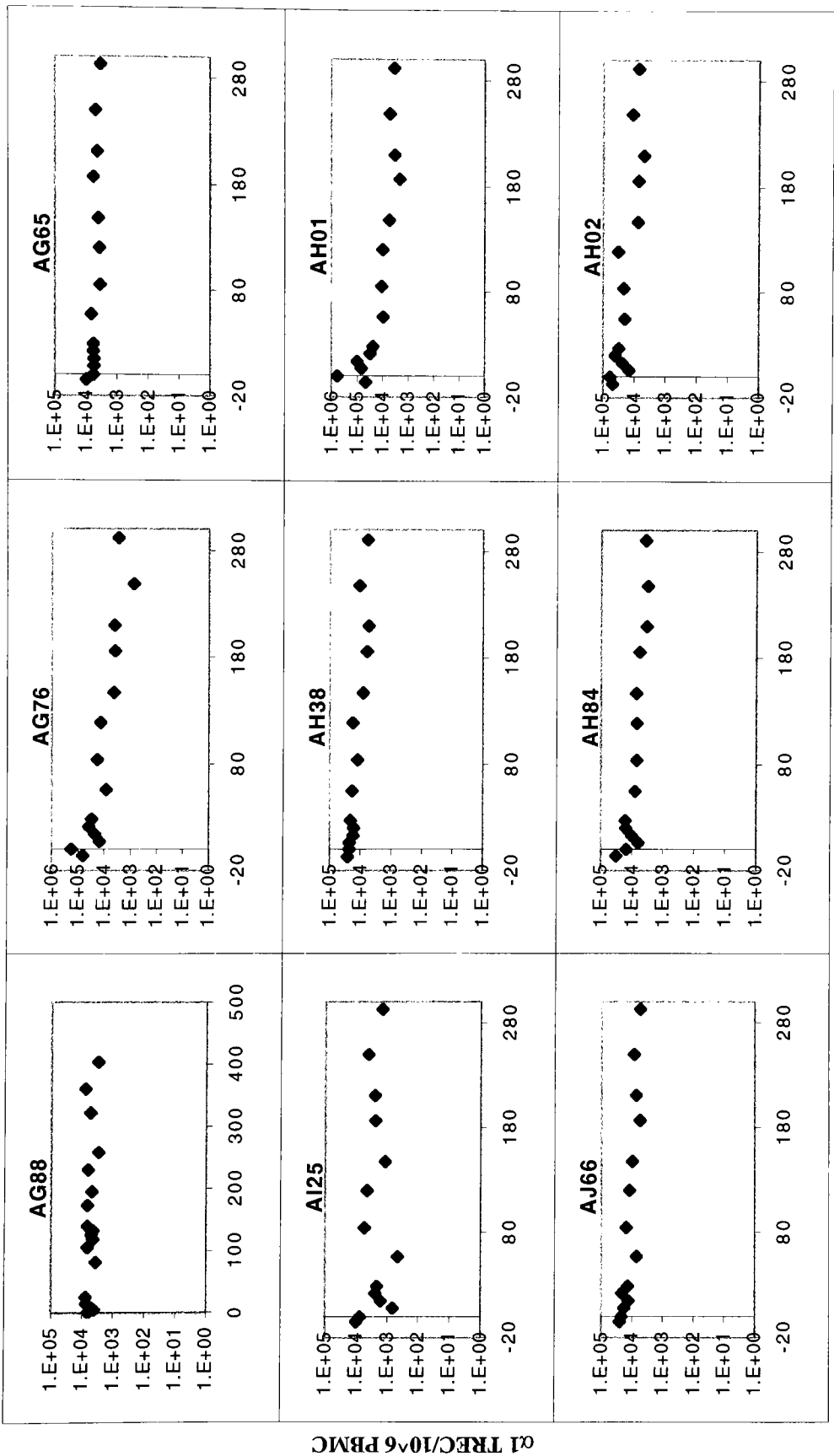
162. Hargreaves, M., and E.B. Bell. 1997. Identical expression of CD45R isoforms by CD45RC+ 'revertant' memory and CD45RC+ naive CD4 T cells. *Immunology* 91, no. 3:323.
163. Kong, F., C.H. Chen, and M.D. Cooper. 1998. Thymic function can be accurately monitored by the level of recent T cell emigrants in the circulation. *Immunity* 8, no. 1:97.
164. Graziano, M., Y. St-Pierre, C. Beauchemin, M. Desrosiers, and E.F. Potworowski. 1998. The fate of thymocytes labeled in vivo with CFSE. *Experimental Cell Research* 240, no. 1:75.
165. Sprent, J., and D.F. Tough. 1994. Lymphocyte life-span and memory. *Science* 265, no. 5177:1395.
166. Penit, C., and F. Vasseur. 1997. Expansion of mature thymocyte subsets before emigration to the periphery. *Journal of Immunology* 159, no. 10:4848.
167. de Villartay, J.P., R.D. Hockett, D. Coran, S.J. Korsmeyer, and D.I. Cohen. 1988. Deletion of the human T-cell receptor delta-gene by a site-specific recombination. *Nature* 335, no. 6186:170.
168. Takeshita, S., M. Toda, and H. Yamagishi. 1989. Excision products of the T cell receptor gene support a progressive rearrangement model of the alpha/delta locus. *EMBO Journal* 8, no. 11:3261.
169. Verschuren, M.C., I.L. Wolvers-Tettero, T.M. Breit, J. Noordzij, E.R. van Wering, and J.J. van Dongen. 1997. Preferential rearrangements of the T cell receptor-delta-deleting elements in human T cells. *Journal of Immunology* 158, no. 3:1208.
170. Kong, F.K., C.L. Chen, A. Six, R.D. Hockett, and M.D. Cooper. 1999. T cell receptor gene deletion circles identify recent thymic emigrants in the peripheral T cell pool. *Proceedings of the National Academy of Sciences of the United States of America* 96, no. 4:1536.
171. Jin, X., D.E. Bauer, S.E. Tuttleton, S. Lewin, A. Gettie, J. Blanchard, C.E. Irwin, J.T. Safrit, J. Mittler, L. Weinberger, L.G. Kostrikis, L. Zhang, A.S. Perelson, and D.D. Ho. 1999. Dramatic rise in plasma viremia after CD8(+) T cell depletion in simian immunodeficiency virus-infected macaques. *Journal of Experimental Medicine* 189, no. 6:991.
172. Kostrikis, L.G., S. Tyagi, M.M. Mhlanga, D.D. Ho, and F.R. Kramer. 1998. Spectral genotyping of human alleles. *Science* 279, no. 5354:1228.
173. Tyagi, S., and F.R. Kramer. 1996. Molecular beacons: probes that fluoresce upon hybridization. *Nature Biotechnology* 14, no. 3:303.
174. Suryanarayana, K., T.A. Wiltout, G.M. Vasquez, V.M. Hirsch, and J.D. Lifson. 1998. Plasma SIV RNA viral load determination by real-time quantification of product generation in reverse transcriptase-polymerase chain reaction. *AIDS Research & Human Retroviruses* 14, no. 2:183.
175. Veazey, R.S., M. Rosenzweig, D.E. Shvetz, D.R. Pauley, M. DeMaria, L.V. Chalifoux, R.P. Johnson, and A.A. Lackner. 1997. Characterization of gut-associated lymphoid tissue (GALT) of normal rhesus macaques. *Clinical Immunology & Immunopathology* 82, no. 3:230.
176. Veazey, R.S., M. DeMaria, L.V. Chalifoux, D.E. Shvetz, D.R. Pauley, H.L. Knight, M. Rosenzweig, R.P. Johnson, R.C. Desrosiers, and A.A. Lackner. 1998.

- Gastrointestinal tract as a major site of CD4+ T cell depletion and viral replication in SIV infection. *Science* 280, no. 5362:427.
177. Heid, C.A., J. Stevens, K.J. Livak, and P.M. Williams. 1996. Real time quantitative PCR. *Genome Research* 6, no. 10:986.
 178. Gibson, U.E., C.A. Heid, and P.M. Williams. 1996. A novel method for real time quantitative RT-PCR. *Genome Research* 6, no. 10:995.
 179. Chen, Z.W., Z.C. Kou, L. Shen, K.A. Reimann, and N.L. Letvin. 1993. Conserved T-cell receptor repertoire in simian immunodeficiency virus-infected rhesus monkeys. *Journal of Immunology* 151, no. 4:2177.
 180. Zhou, D., Y. Shen, L. Chalifoux, D. Lee-Parritz, M. Simon, P.K. Sehgal, L. Zheng, M. Halloran, and Z.W. Chen. 1999. *Mycobacterium bovis* bacille Calmette-Guerin enhances pathogenicity of simian immunodeficiency virus infection and accelerates progression to AIDS in macaques: a role of persistent T cell activation in AIDS pathogenesis. *Journal of Immunology* 162, no. 4:2204.
 181. Hedrick, S.M., and F.J. Eidelman. 1993. T Lymphocyte Antigen Receptors. 3 ed. In *Fundamental Immunology*. W.E. Paul, editor. Raven Press, Ltd., New York. 383.
 182. Fujimoto, S., and H. Yamagishi. 1987. Isolation of an excision product of T-cell receptor alpha-chain gene rearrangements. [erratum appears in *Nature* 1987 Jun 4-10;327(6121):439]. *Nature* 327, no. 6119:242.
 183. Okazaki, K., D.D. Davis, and H. Sakano. 1987. T cell receptor beta gene sequences in the circular DNA of thymocyte nuclei: direct evidence for intramolecular DNA deletion in V-D-J joining. *Cell* 49, no. 4:477.
 184. Okazaki, K., and H. Sakano. 1988. Thymocyte circular DNA excised from T cell receptor alpha-delta gene complex. *EMBO Journal* 7, no. 6:1669.
 185. Mombaerts, P., J. Iacomini, R.S. Johnson, K. Herrup, S. Tonegawa, and V.E. Papaioannou. 1992. RAG-1-deficient mice have no mature B and T lymphocytes. *Cell* 68, no. 5:869.
 186. Oettinger, M.A., D.G. Schatz, C. Gorka, and D. Baltimore. 1990. RAG-1 and RAG-2, adjacent genes that synergistically activate V(D)J recombination. *Science* 248, no. 4962:1517.
 187. Oettinger, M.A., B. Stanger, D.G. Schatz, T. Glaser, K. Call, D. Housman, and D. Baltimore. 1992. The recombination activating genes, RAG 1 and RAG 2, are on chromosome 11p in humans and chromosome 2p in mice. *Immunogenetics* 35, no. 2:97.
 188. Schatz, D.G., and D. Baltimore. 1988. Stable expression of immunoglobulin gene V(D)J recombinase activity by gene transfer into 3T3 fibroblasts. *Cell* 53, no. 1:107.
 189. Shinkai, Y., G. Rathbun, K.P. Lam, E.M. Oltz, V. Stewart, M. Mendelsohn, J. Charron, M. Datta, F. Young, and A.M. Stall. 1992. RAG-2-deficient mice lack mature lymphocytes owing to inability to initiate V(D)J rearrangement. *Cell* 68, no. 5:855.
 190. Wilson, A., W. Held, and H.R. MacDonald. 1994. Two waves of recombinase gene expression in developing thymocytes. *Journal of Experimental Medicine* 179, no. 4:1355.

191. Chakrabarti, L.A., S.R. Lewin, L. Zhang, A. Gettie, A. Luckay, L.N. Martin, E. Skulsky, D.D. Ho, C. Cheng-Mayer, and P.A. Marx. 2000. Normal T-cell turnover in sooty mangabeys harboring active simian immunodeficiency virus infection. *Journal of Virology* 74, no. 3:1209.
192. Chun, T.W., K. Chadwick, J. Margolick, and R.F. Siliciano. 1997. Differential susceptibility of naive and memory CD4+ T cells to the cytopathic effects of infection with human immunodeficiency virus type 1 strain LAI. *Journal of Virology* 71, no. 6:4436.
193. Schnittman, S.M., H.C. Lane, J. Greenhouse, J.S. Justement, M. Baseler, and A.S. Fauci. 1990. Preferential infection of CD4+ memory T cells by human immunodeficiency virus type 1: evidence for a role in the selective T-cell functional defects observed in infected individuals. *Proceedings of the National Academy of Sciences of the United States of America* 87, no. 16:6058.
194. Livak, F., and D.G. Schatz. 1996. T-cell receptor alpha locus V(D)J recombination by-products are abundant in thymocytes and mature T cells. *Molecular & Cellular Biology* 16, no. 2:609.
195. McLean, A.R., and C.A. Michie. 1995. In vivo estimates of division and death rates of human T lymphocytes. *Proceedings of the National Academy of Sciences of the United States of America* 92, no. 9:3707.
196. Haynes, B.F., M.L. Markert, G.D. Sempowski, D.D. Patel, and L.P. Hale. 2000. The role of the thymus in immune reconstitution in aging, bone marrow transplantation, and HIV-1 infection. *Annual Review of Immunology* 18:529.
197. Hazenberg, M.D., J.W. Stuart, S.A. Otto, J.C. Borleffs, C.A. Boucher, R.J. de Boer, F. Miedema, and D. Hamann. 2000. T-cell division in human immunodeficiency virus (HIV)-1 infection is mainly due to immune activation: a longitudinal analysis in patients before and during highly active antiretroviral therapy (HAART). *Blood* 95, no. 1:249.
198. Hazenberg, M.D., S.A. Otto, J.W. Cohen Stuart, M.C. Verschuren, J.C. Borleffs, C.A. Boucher, R.A. Coutinho, J.M. Lange, T.F. Rinke de Wit, A. Tsegaye, J.J. van Dongen, D. Hamann, R.J. de Boer, and F. Miedema. 2000. Increased cell division but not thymic dysfunction rapidly affects the T-cell receptor excision circle content of the naive T cell population in HIV-1 infection. [see comments]. *Nature Medicine* 6, no. 9:1036.
199. Schnittman, S.M., S.M. Denning, J.J. Greenhouse, J.S. Justement, M. Baseler, J. Kurtzberg, B.F. Haynes, and A.S. Fauci. 1990. Evidence for susceptibility of intrathymic T-cell precursors and their progeny carrying T-cell antigen receptor phenotypes TCR alpha beta + and TCR gamma delta + to human immunodeficiency virus infection: a mechanism for CD4+ (T4) lymphocyte depletion. *Proceedings of the National Academy of Sciences of the United States of America* 87, no. 19:7727.
200. Chen, Z.W., Y. Shen, Z. Kou, C. Ibegbu, D. Zhou, L. Shen, P. Morrison, C. Bogle, H.M. McClure, A.J. Nahmias, P.K. Sehgal, and N.L. Letvin. 2000. Prolonged dominance of clonally restricted CD4(+) T cells in macaques infected with simian immunodeficiency viruses. *Journal of Virology* 74, no. 16:7442.
201. Wilson, J.D., M. Cranage, N. Cook, S. Leech, A.J. McMichael, and M.F. Callan. 1998. Evidence for the persistence of monoclonal expansions of CD8+ T cells

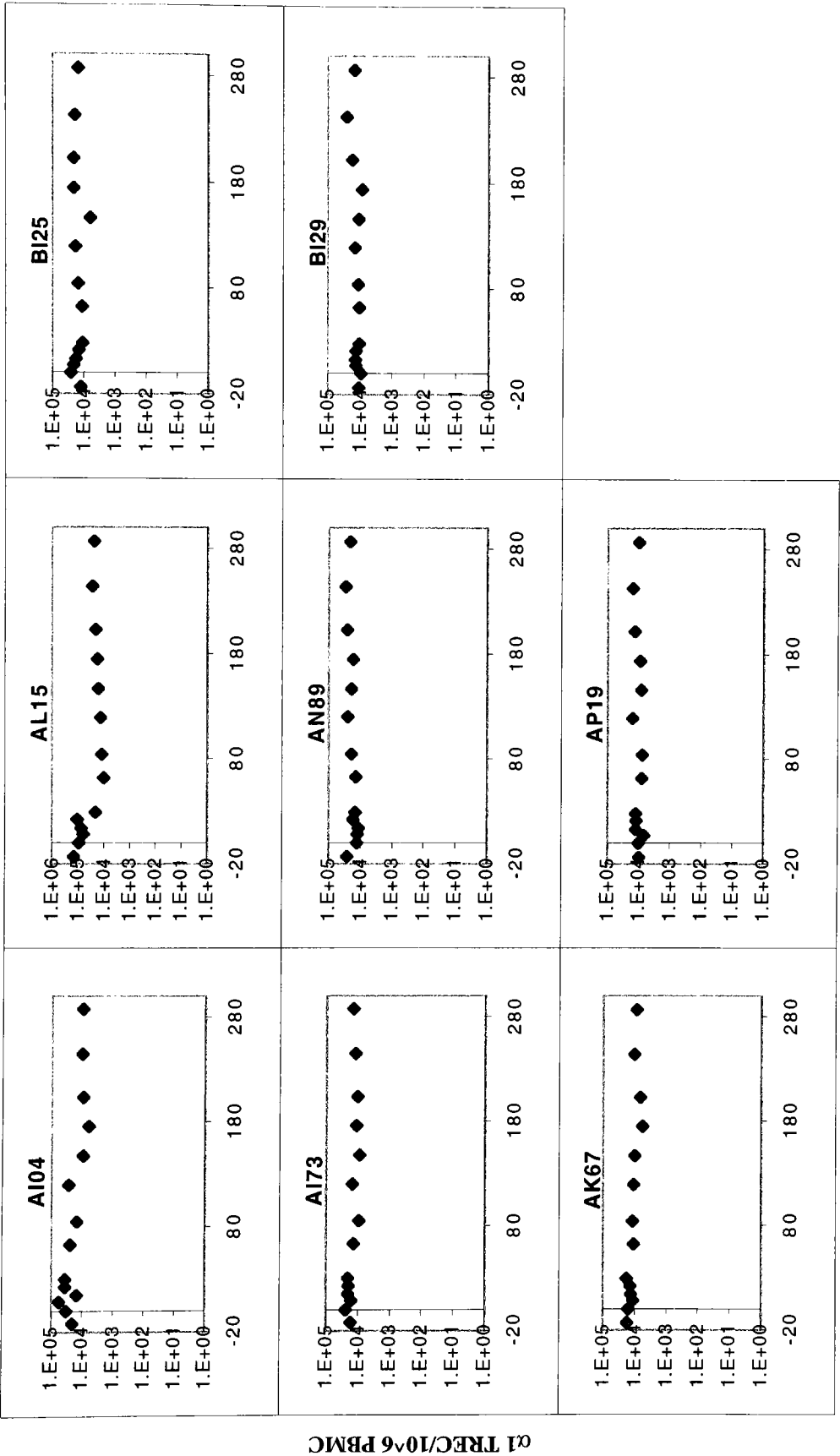
following primary simian immunodeficiency virus infection. *European Journal of Immunology* 28, no. 4:1172.

202. Kou, Z.C., J.S. Pühr, M. Rojas, W.T. McCormack, M.M. Goodenow, and J.W. Sleasman. 2000. T-Cell receptor Vbeta repertoire CDR3 length diversity differs within CD45RA and CD45RO T-cell subsets in healthy and human immunodeficiency virus-infected children. *Clinical & Diagnostic Laboratory Immunology* 7, no. 6:953.

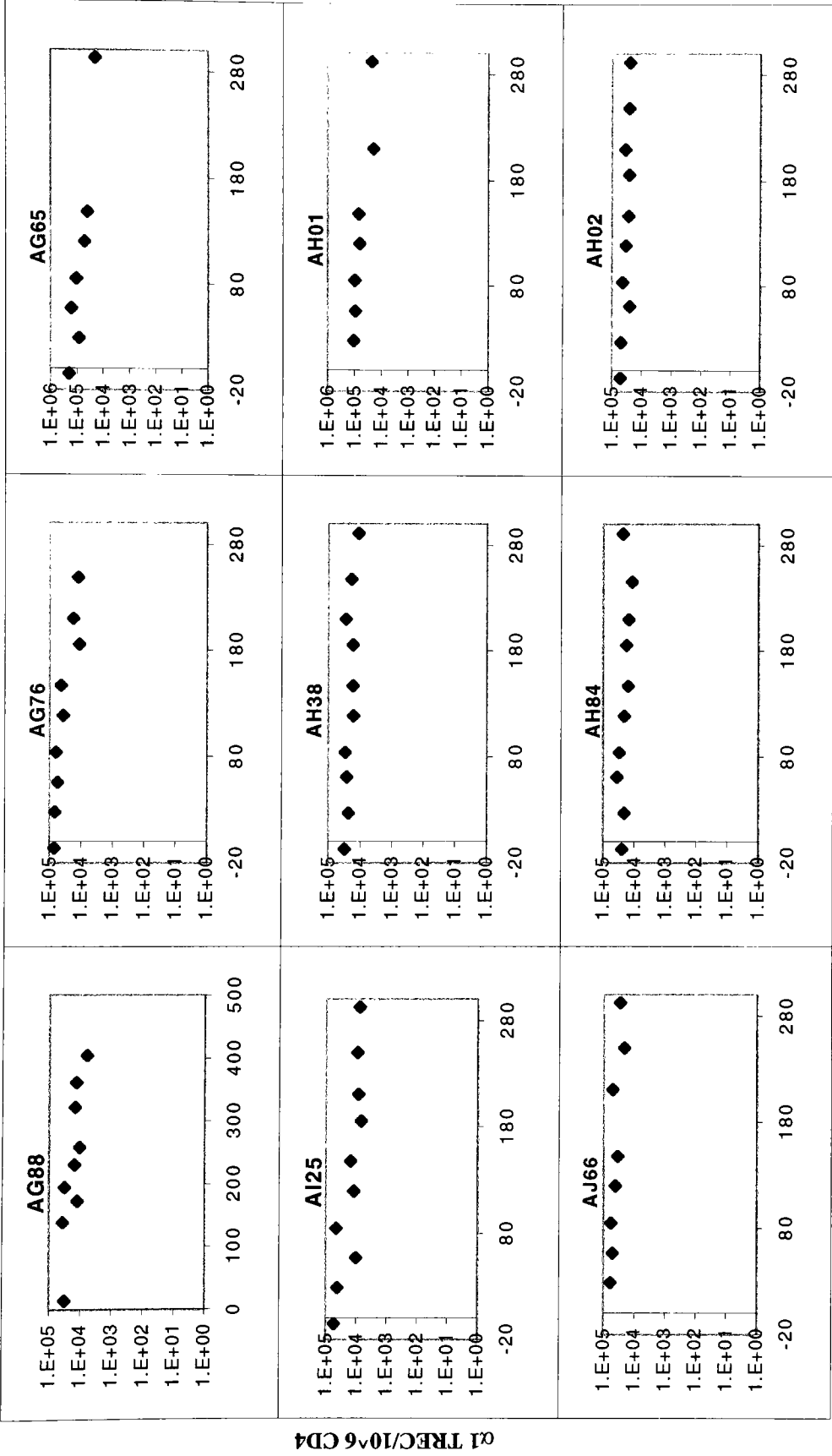


Time Post Surgery (days)

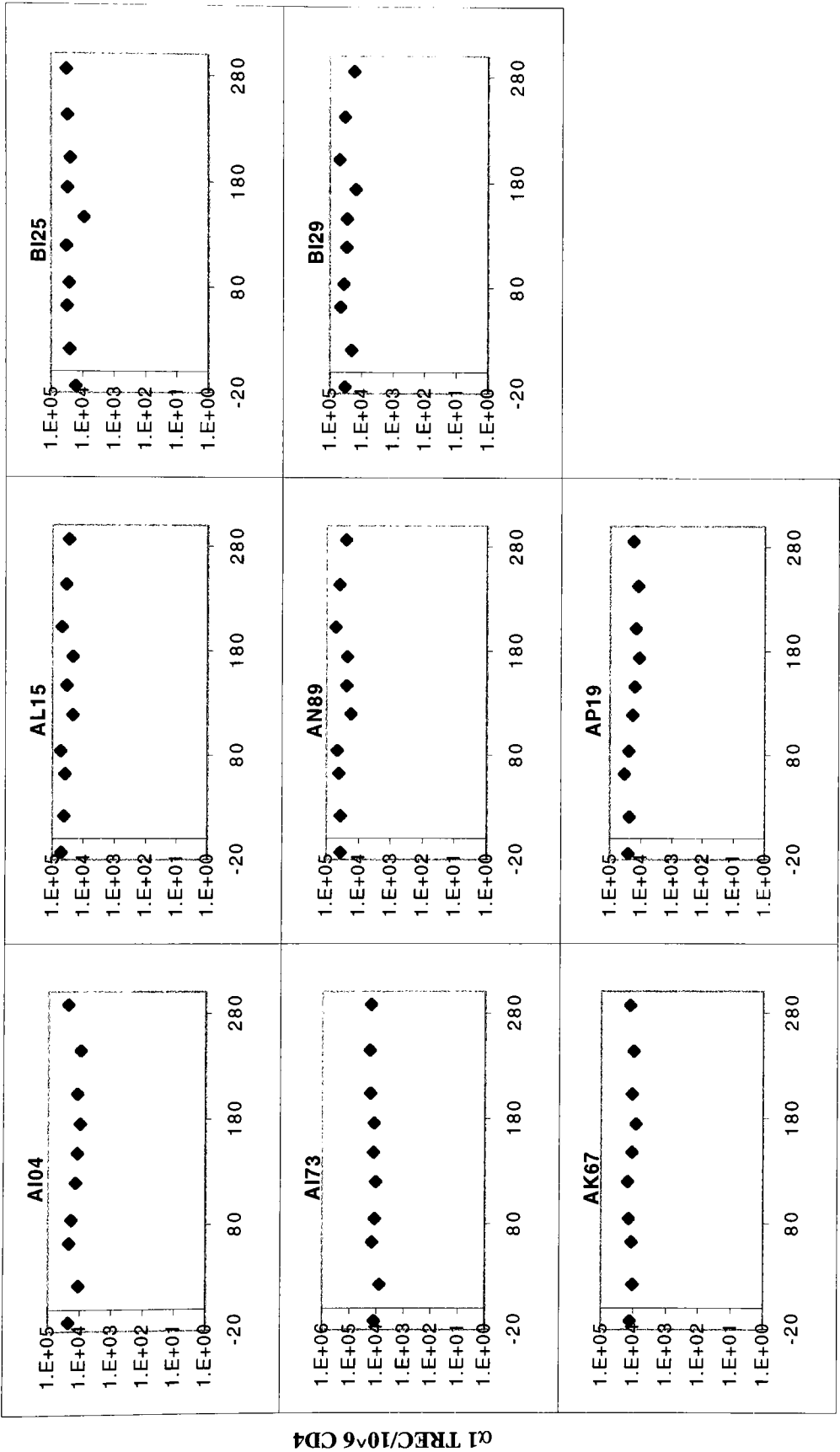
Appendix 1a. $\alpha 1$ TREC per 10^6 PBMC; thymectomized macaques.



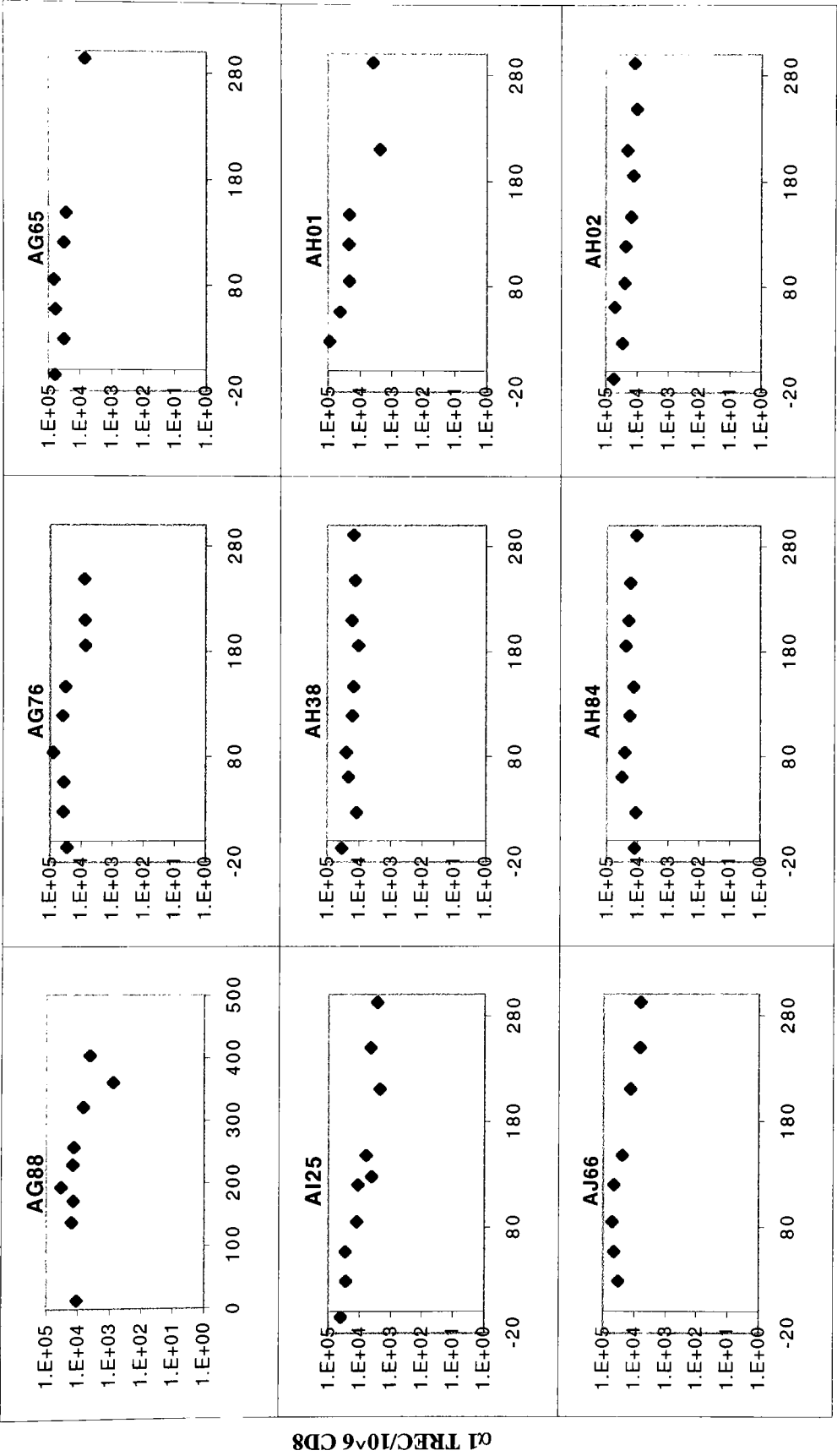
Appendix 1b. $\alpha 1$ TREC per 10^6 PBMC: sham macaques.



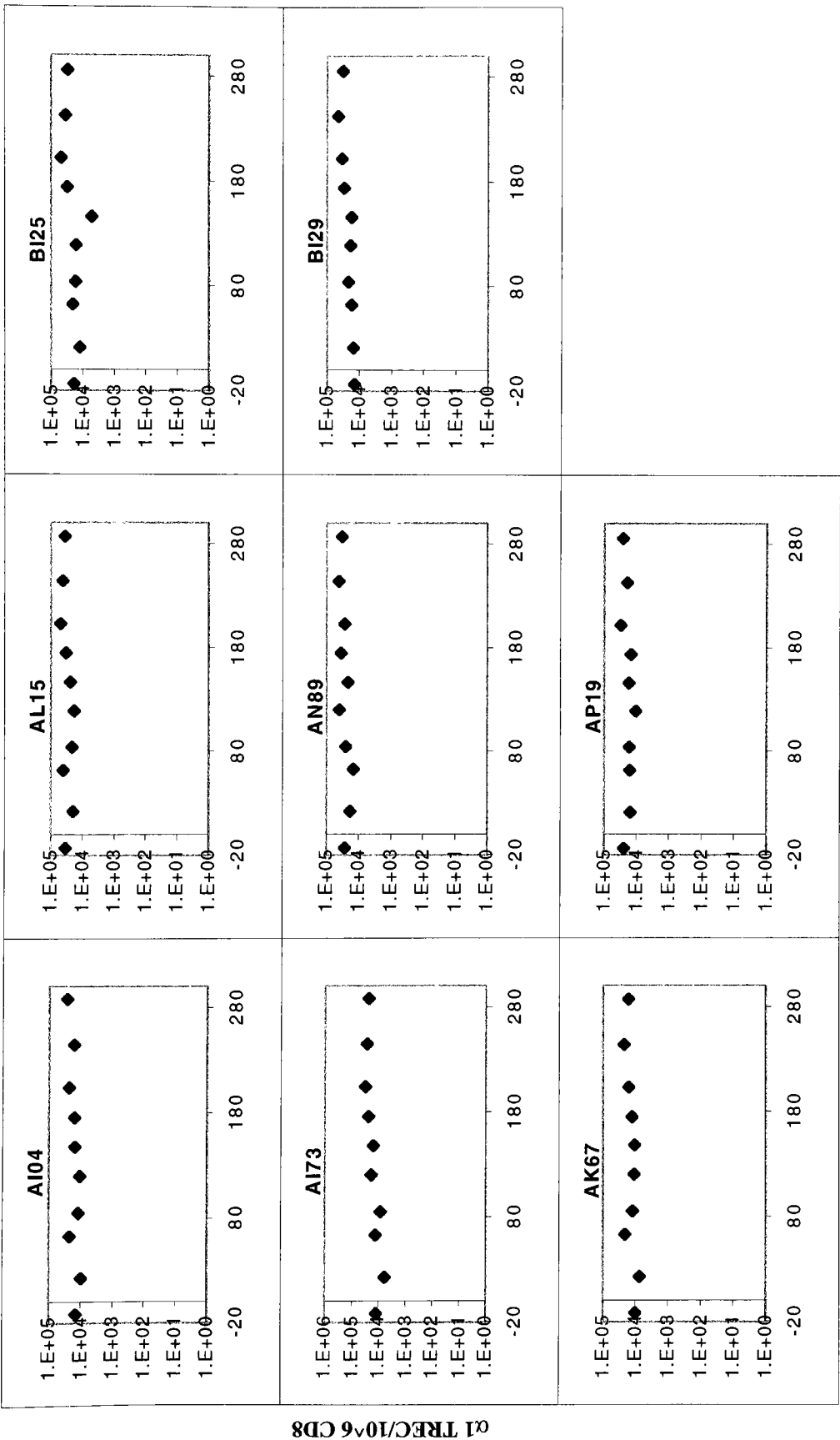
Appendix 1c. $\alpha 1$ TREC per 10^6 CD4: thymectomized macaques.



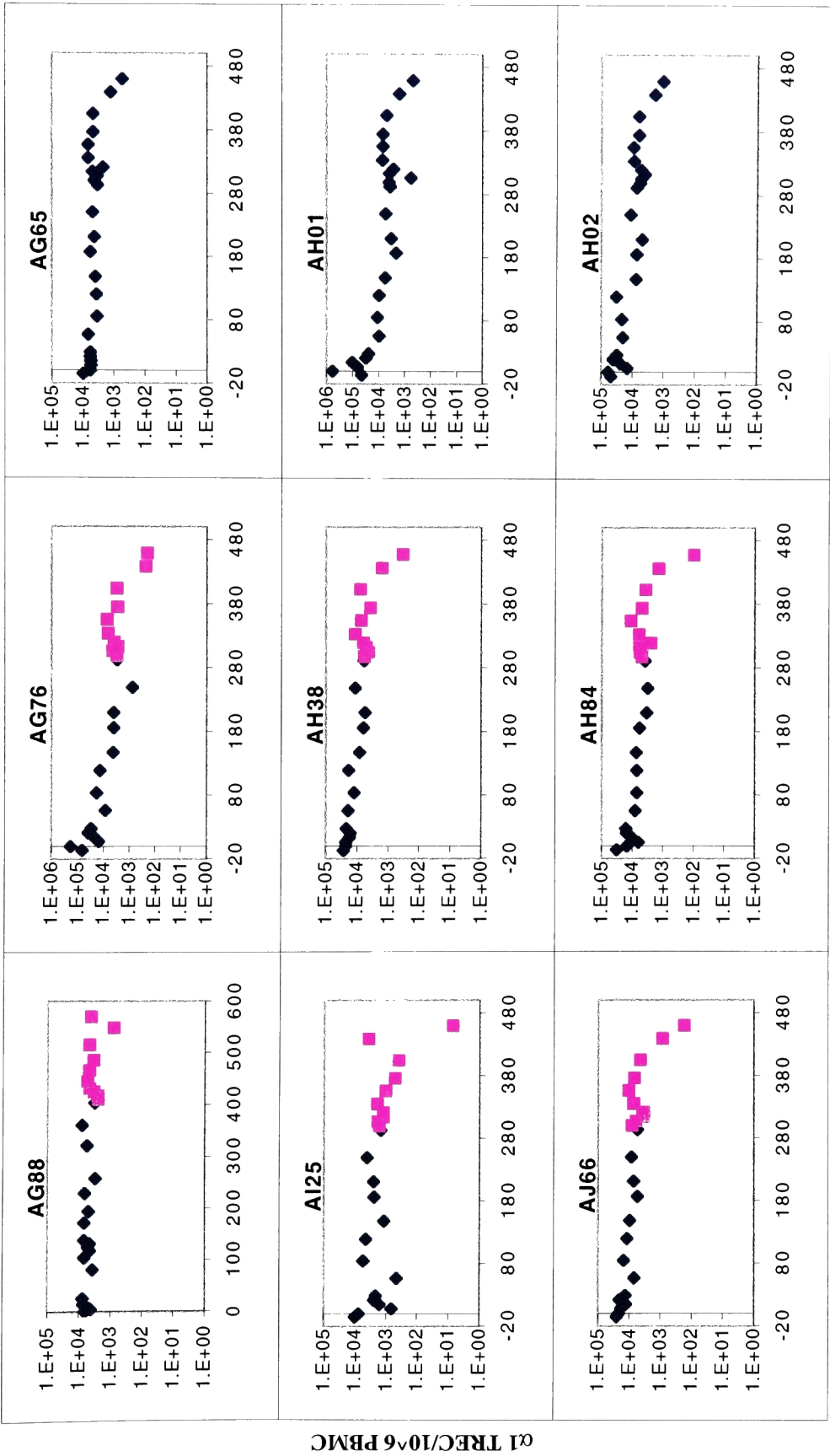
Appendix 1d. $\alpha 1$ TREC per 10^6 CD4: sham macaques.



Appendix 1e. $\alpha 1$ TREC per 10^6 CD8: thymectomized macaques.

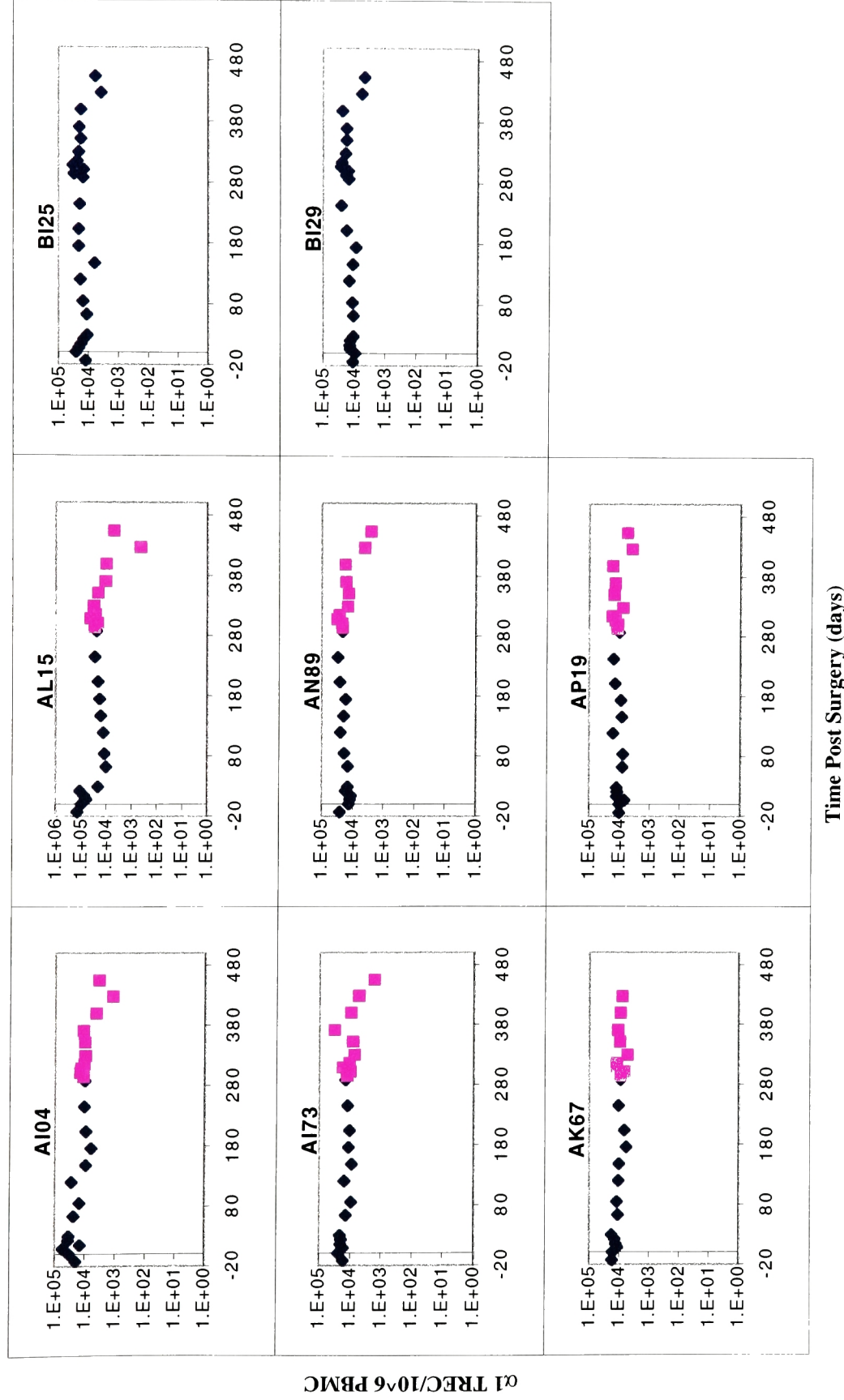


Appendix 1f. $\alpha 1$ TREC per 10^6 CD8: sham macaques.



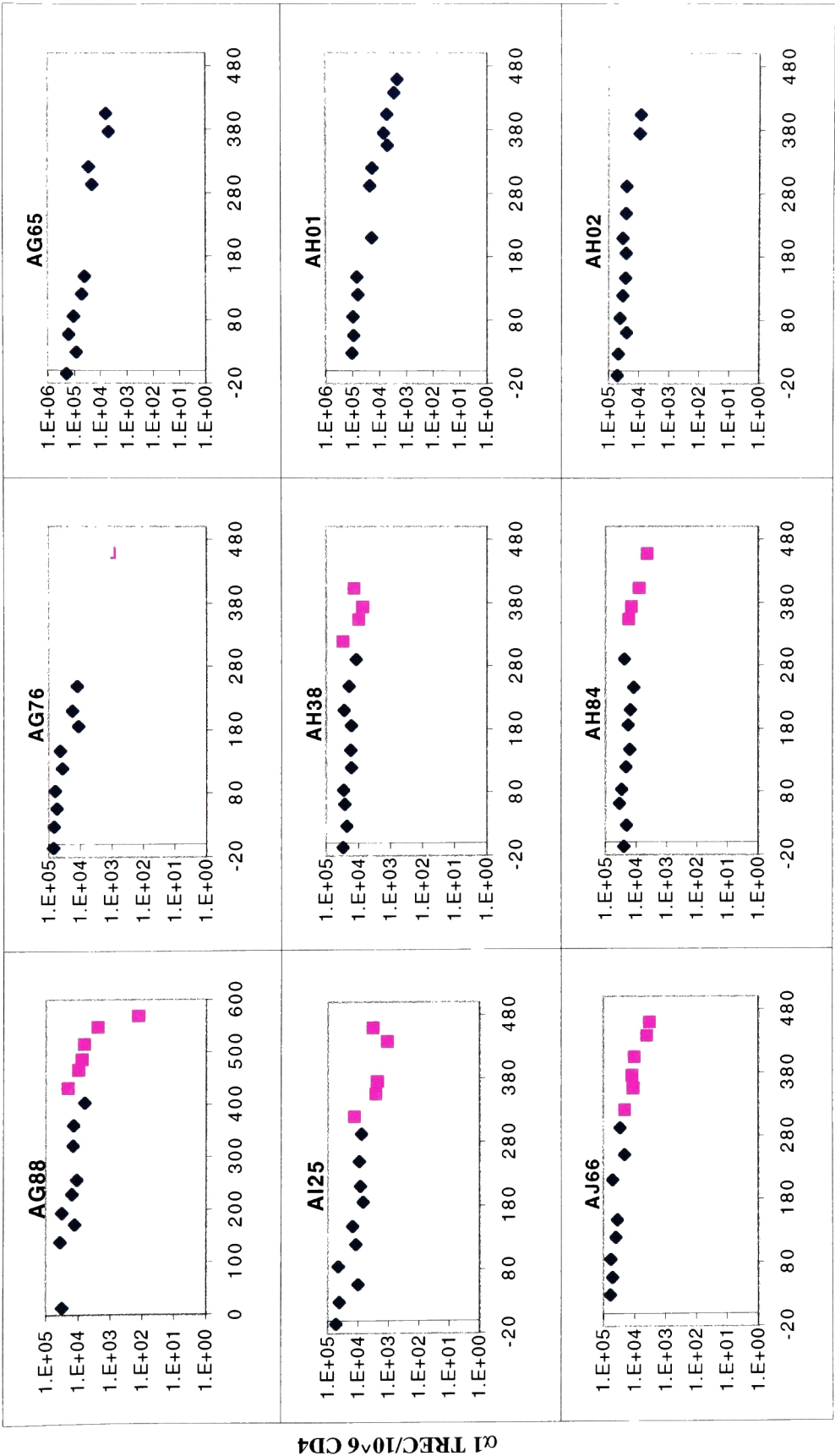
Time Post Surgery (days)

Appendix 2a. $\alpha 1$ TREC per 10^6 PBMC: thymectomized macaques.
Blue diamonds represent preinfection and uninfected time points, purple squares represent postinfection time points.



Appendix 2b. $\alpha 1$ TREC per 10^6 PBMC: sham macaques.

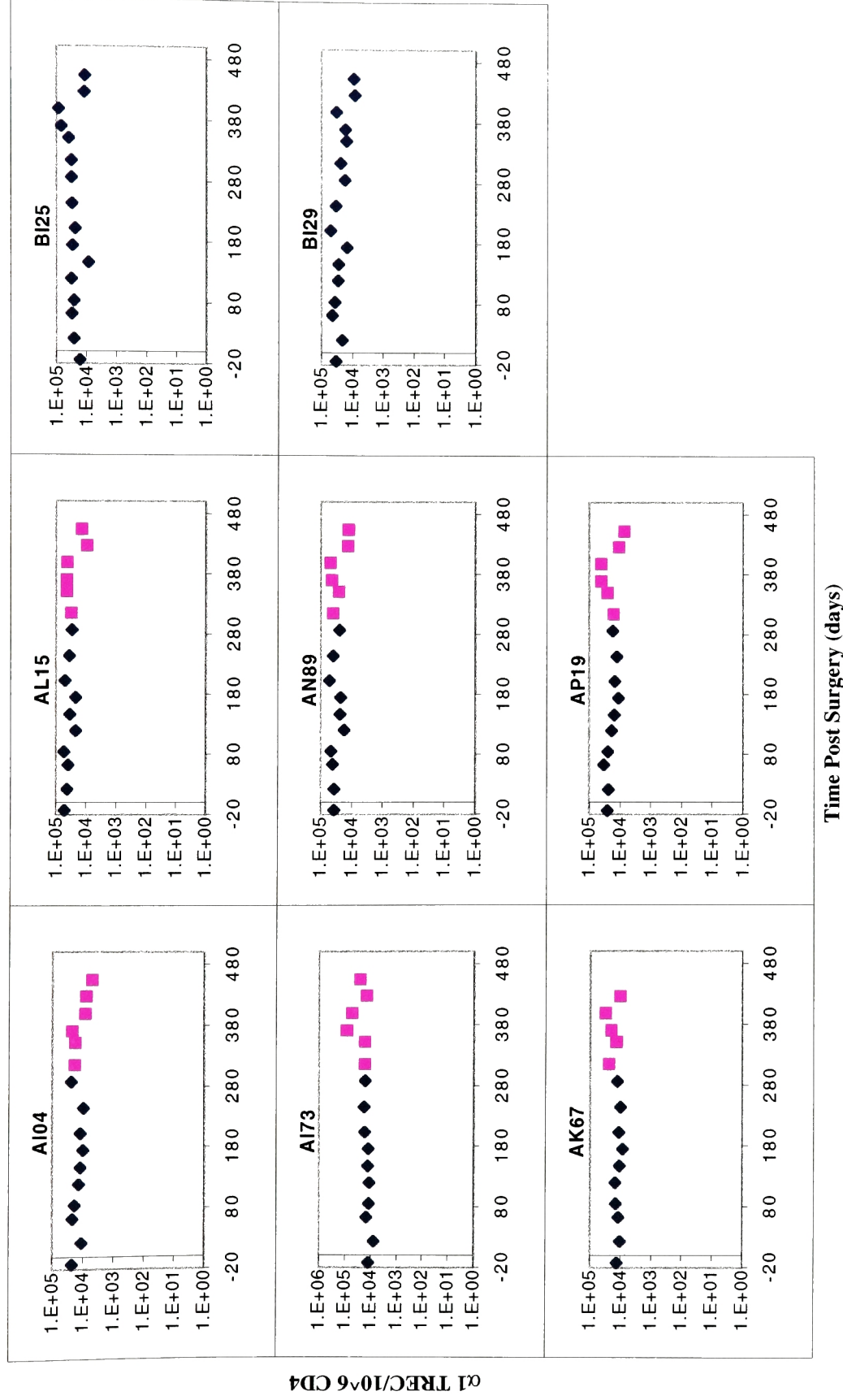
Blue diamonds represent preinfection and uninfected time points, purple squares represent postinfection time points.



Time Post Surgery (days)

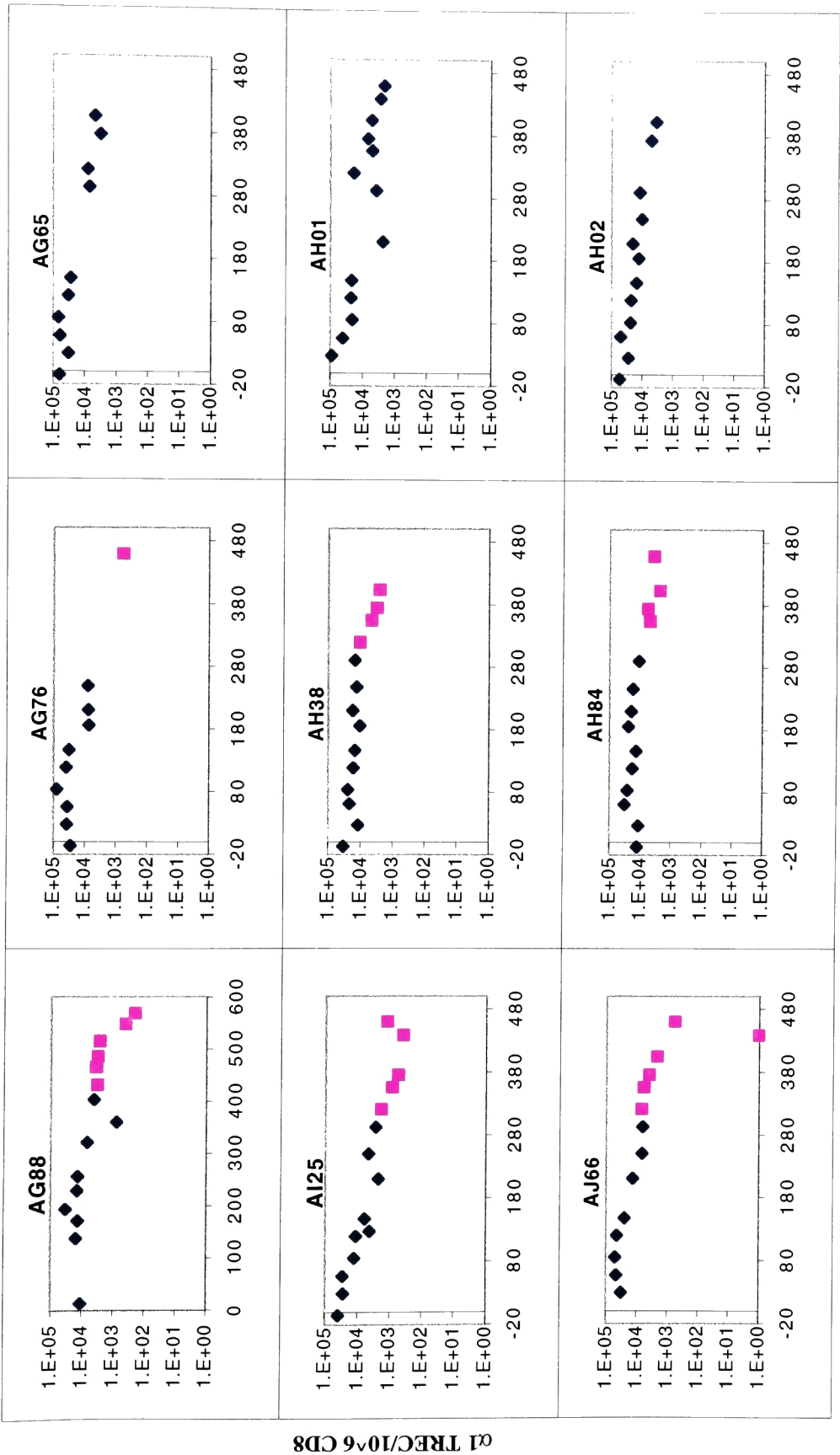
Appendix 2c. $\alpha 1$ TREC per 10^6 CD4: thymectomized macaques.

Blue diamonds represent preinfection and uninfected time points, purple squares represent postinfection time points.

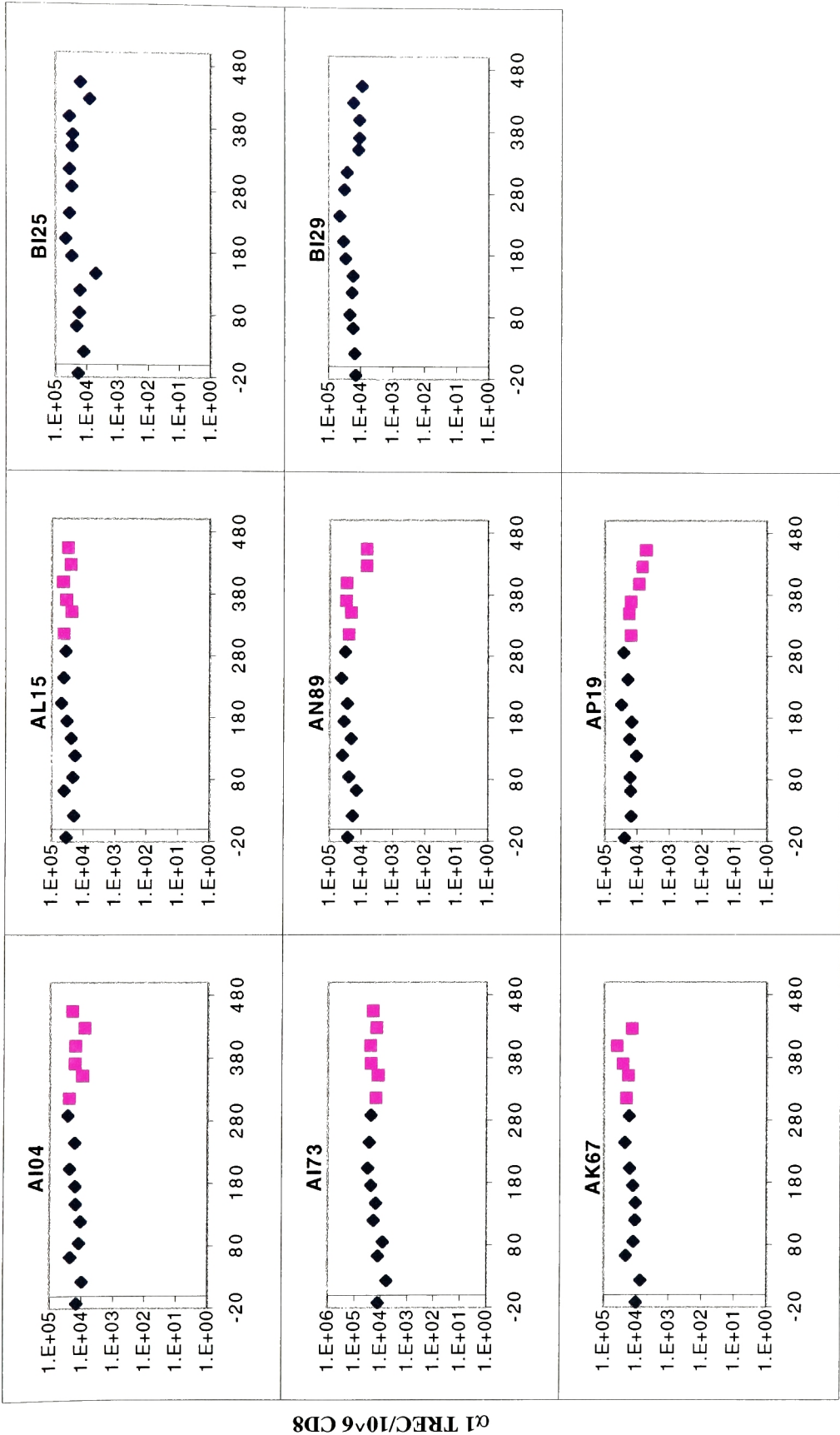


Appendix 2d. $\alpha 1$ TREC per 10^6 CD4: sham macaques.

Blue diamonds represent preinfection and uninfected time points, purple squares represent postinfection time points.



Appendix 2e. $\alpha 1$ TREC per 10^6 CD8: thymectomized macaques.
Blue diamonds represent preinfection and uninfected time points, purple squares represent postinfection time points.



Appendix 2f. $\alpha 1$ TREC per 10^6 CD8: sham macaques.
Blue diamonds represent preinfection and uninfected time points, purple squares represent postinfection time points.

116910A
05-06-02 13220

2
TH





THE LIBRARY



19010000405512

